HIGHWAY RESEARCH RECORD

Number 328

Concrete Durability, Cement Paste, Aggregates, and Sealing Compounds

9 Reports

Subject Areas

32 Cement and Concrete
34 General Materials
35 Mineral Aggregates

HIGHWAY RESEARCH BOARD
DIVISION OF ENGINEERING NATIONAL RESEARCH COUNCIL
NATIONAL ACADEMY OF SCIENCES—NATIONAL ACADEMY OF ENGINEERING
WASHINGTON, D.C. 1970

ISBN 0-309-01827-7

Price: $3.20

Available from

Highway Research Board
National Academy of Sciences
2101 Constitution Avenue
Washington, D.C. 20418

Department of Materials and Construction

R. L. Peyton, Chairman
State Highway Commission of Kansas, Topeka

R. E. Bollen and W. G. Gunderman
Highway Research Board Staff

CONCRETE DIVISION

Bryant Mather, Chairman
Waterways Experiment Station, Jackson, Mississippi

COMMITTEE ON PERFORMANCE OF CONCRETE—PHYSICAL ASPECTS

(As of December 31, 1969)

Thomas D. Larson, Chairman
Pennsylvania State University, University Park

Philip D. Cady, Secretary
Pennsylvania State University, University Park

Howard T. Arni
James E. Backstrom
Cecil H. Best
D. L. Bloem
R. H. Brink
William P. Chamberlin
Herbert K. Cook
Clarence DeYoung
Wade L. Gramling
Paul Klieger
William B. Ledbetter
F. E. Legg, Jr.
John Lemish
Bryant Mather
J. F. McLaughlin
Howard H. Newlon, Jr.
Melville E. Prior
F. A. Renninger
Hollis B. Rushing
V. R. Sturrup
Patrick H. Torrans
R. P. Vellines
Richard D. Walker
E. A. Whitehurst
George H. Zuehlke

COMMITTEE ON MECHANICAL PROPERTIES OF CONCRETE

(As of December 31, 1969)

Thomas W. Reichard, Chairman
National Bureau of Standards, Washington, D.C.

John D. Antrim
James W. Baldwin, Jr.
Irwin A. Benjamin
Eugene Buth
Karl H. Dunn
Richard L. Grey
Frank L. Holman, Jr.
Clyde E. Kesler
D. A. Linger
V. M. Malhotra
Bryant Mather
Leonard J. Mitchell
Richard Alan Meunow
C. C. Oleson
R. E. Philleo
Sandor Popovics
Charles F. Scholer
V. R. Sturrup
H. R. J. Walsh
E. A. Whitehurst

COMMITTEE ON CURING OF CONCRETE

(As of December 31, 1969)

Paul Klieger, Chairman
Portland Cement Association, Skokie, Illinois

E. A. Abdun-Nur
Cecil H. Best
A. W. Eatman
E. A. Finney
Roderick R. Harris
Ronald D. Hughes
John Killian
Kenneth H. McGhee
Harry H. McLean
C. E. Morris
C. K. Preus
M. E. Prior
C. E. Proudley
A. A. Rauchfuss, Jr.
J. C. Reed
Floyd O. Slate
D. L. Spellman
Albert G. Timms
R. A. Tissot

COMMITTEE ON BASIC RESEARCH PERTAINING TO PORTLAND CEMENT AND CONCRETE

(As of December 31, 1969)

W. L. Dolch, Chairman
Purdue University, Lafayette, Indiana

H. A. Berman
Stephen Brunauer
L. E. Copeland
Sidney Diamond
Wilhelm Eitel
G. J. C. Frohnsdorff
Kenneth T. Greene
P. E. Halstead
R. L. Handy
W. C. Hansen
G. M. Idorn
George L. Kalousek
Clyde E. Kesler
Alexander Klein
Kenneth R. Lauer
Katharine Mather
Richard C. Mielenz
R. E. Philleo
T. C. Powers
Della M. Roy
Peter J. Sereda
H. F. W. Taylor
Rudolph C. Valore
R. P. Vellines
George J. Verbeck
Julie C. Yang

COMMITTEE ON EFFECT OF ICE CONTROL

(As of December 31, 1969)

W. M. Stingley, Chairman
State Highway Commission of Kansas, Topeka

H. Bobbitt Aikin
Cecil H. Best
Roland L. Booth
F. C. Brownridge
S. M. Cardone
D. L. Hawkins
Paul Klieger
C. E. MacKinnon
E. W. McGovern
J. C. Reed
P. H. Schultz
W. L. Shearer
John S. Wait
R. J. Walsh
Alden L. West

GENERAL MATERIALS DIVISION

John L. Beaton, Chairman
California Division of Highways, Sacramento

COMMITTEE ON MINERAL AGGREGATES

(As of December 31, 1969)

F. E. Legg, Jr., Chairman
University of Michigan, Ann Arbor

William P. Chamberlin
John C. Cook
J. T. Corkill
Karl H. Dunn
R. D. Gaynor
Joseph E. Gray
Hans I. Hansen
Eugene Y. Huang
Donald R. Lamb
Thomas D. Larson
W. B. Ledbetter
D. W. Lewis
J. F. McLaughlin
Kenneth A. Nelson
Robert G. Pike
F. A. Renninger
R. D. Shumway
Norman G. Smith
Travis W. Smith
G. W. Steele
Richard D. Walker
E. A. Whitehurst
Milton H. Wills, Jr.
D. O. Woolf

COMMITTEE ON METALS IN HIGHWAY STRUCTURES

(As of December 31, 1969)

Arthur W. Moon, Chairman
New York State Department of Transportation, Albany

Philip A. Barnes, Secretary
New York State Department of Transportation, Utica

W. C. Anderson
Gordon Cape
S. K. Coburn
Frank Couch
John R. Daesen
T. D. Dismuke
Eric L. Erickson
Edward A. Fenton
E. Ferrence
LaMotte Grover
Richard L. Hartzell
James H. Havens
Gerald J. Hill
Ray I. Lindberg
Thomas A. Lowe
Robert A. Manson
Theodore A. Mowatt
Eric F. Nordlin
Robert A. Norton
J. C. Oliver
Thomas W. Oliver
Robert A. Pege
Robert G. Pike
Joseph W. Pitts
Harry D. Richardson
Melvin Romanoff
Richard K. Sager
W. W. Sanders, Jr.
E. P. Segner, Jr.
Clyde F. Silvus
James E. Stallmeyer
R. F. Stratfull
George J. Verbeck
Frank O. Wood
L. E. Wood

Foreword

This group of 9 papers, sponsored by 7 committees, represents in part the most significant activity of what has been the Concrete Division and the General Materials Division, Department of Materials and Construction, Highway Research Board. The papers deal with structural lightweight concrete, shrinkage-compensating concrete, concrete bridge decks, sealing compounds for concrete, corrosion of steel in concrete, frost susceptibility of concrete aggregates, hardened cement paste, and temperature control of concrete. They include discussions of field experience, laboratory investigations, and interpretation of results of fundamental research.

All persons concerned with the use of portland cement concrete in transportation facilities will find several or all of these contributions of interest and value. Those concerned with the performance of concrete in bridge decks may refer to these papers in the following sequence:

1. Freyermuth, Klieger, Stark, and Wenke, for a review of cooperative studies of bridge deck durability;
2. Spellman and Stratfull, for the role of chlorides in bridge deck deterioration;
3. Craig and Wood, for comments on admixtures to reduce corrosion;
4. Ryell and Chojnacki, for comments on sealing compounds;
5. Buth and Ledbetter, for information on frost resistance of structural concrete;
6. Harman, Cady, and Bolling, for a discussion on tests for frost susceptibility of aggregates;
7. Yanagida, for a discussion of temperature control to reduce cracking in mass concrete;
8. Epps and Polivka, for information on shrinkage-compensating concrete; and
9. Brunauer, Oder, and Yudenfreund, for a discussion of the fundamental characteristics of cement paste.

Those concerned with fundamental research may well be concerned also with all of these papers but may consult them in the reverse order to that indicated. It will be noted that, based on the amount of discussion received, the paper by Brunauer and associates, which discusses the interpretation of fundamental research results, created the greatest response. Readers of this paper will wish to go back to HRB Special Report 90 (1966), "Symposium on Structure of Portland Cement Paste and Concrete," and review many of the papers contained there.

The authors of these papers have included references in each of them. A total of more than 100 previous works are cited. The reader who finds any or all of these papers stimulating and valuable is urged to pursue the topic through the references provided by the authors.

With the reorganization of the technical committee structure of the Highway Research Board that has taken place in the interim between the preparation and presentation of these papers and their publication here, it seems appropriate to thank not only the authors and those who prepared the discussions but also the chairmen of the 6 committees and the members of these committees who served as reviewers and critic readers.

—Bryant Mather

Contents

Influence of the Degree of Saturation of Coarse Aggregate on the Resistance of Structural Lightweight Concrete to Freezing and Thawing

EUGENE BUTH and W. B. LEDBETTER,
Texas Transportation Institute, Texas A&M University

Six selected commercially produced and 7 TTI kiln-produced lightweight coarse aggregates were used in 69 batches of lightweight concrete. These batches of concrete, containing these coarse aggregates, air entrainment, Type 1 cement, and natural sand, were mixed and subjected to freezing and thawing in accordance with ASTM C 290. Absorption characteristics and porosity values were determined for each of the aggregates. Various degrees of saturation of the coarse aggregate at the time of mixing were obtained by immersing the aggregates in water for periods ranging up to 180 days prior to mixing. The results indicate a failure envelope exists between the number of freeze-thaw cycles to failure and the degree of saturation of the coarse aggregate. The "critical" degree of saturation by volume was found to be 0.25 (or 25 percent), below which the concrete will generally withstand 300 cycles of freeze-thaw. It was also determined that some of these aggregates reached this initial saturation after only 30 minutes of immersion, while other aggregates had to be immersed for several days before becoming critically saturated. The practical implications of the test results are discussed.

•INTERNAL STRESSING OF CONCRETE due to the repeated action of internal water freezing and thawing has long been recognized as a detrimental influence on the performance of concrete. This water is present both in the aggregate voids and in the cement paste matrix. Improvements in mix designs and the use of entrained air have significantly reduced the detrimental effects of water in the paste matrix. However, the problem of handling the water in the aggregate voids has not been solved, especially when lightweight aggregates are used that have a relatively large void volume. The research program reported here was concerned with the effects of water in lightweight aggregate used in concrete and subjected to freezing and thawing.

Six selected commercially produced and 7 TTI produced lightweight coarse aggregates were used in the program. The TTI research kiln, which was used to produce the TTI aggregate, is a 25-ft long by 2-ft inside diameter rotary kiln that allows the processing of synthetic aggregates to be closely controlled. The kiln is located at Texas A&M University. A total of 69 batches of concrete using these coarse aggregates and natural sand were mixed and tested in accordance with ASTM C 290. Absorption characteristics and porosity values were determined for each of the aggregates. Various degrees of saturation of the coarse aggregates at the time of mixing were obtained by immersing them in water for periods ranging from 6 hours to 180 days.

Paper sponsored by Committee on Performance of Concrete—Physical Aspects.

BACKGROUND

Deterioration of concrete caused by freezing and thawing is a result of excessive stresses created by the expansion of water being frozen in the void system of the concrete. This void system may exist in the cement paste or in the aggregate. As water expands some 9 percent upon freezing, this expansion is accommodated either by water expansion into pores and capillaries or by elastic dilation of the concrete, or the concrete is ruptured. The factors influencing the amount of stress created are many. Porosity, permeability, void size distribution, degree of saturation of the aggregate and the paste, freezing rate, and the ability of the paste to accommodate water being expelled from the aggregate all combine to influence the stresses created during freezing temperatures.

The effects of the more influential aggregate parameters involved in the durability of concrete may be briefly summarized as follows. For an aggregate to be potentially nondurable in a freezing and thawing environment, it must have sufficiently large porosity and must have been saturated to a degree that is greater than some critical value. If these conditions exist, the expansion of the water during freezing may create excessive stresses and, in turn, cause deterioration of the concrete. Theoretically, the critical degree of saturation is 0.917. However, experiments have failed to verify this value. Reasons for the lack of experimental verification given by Powers (1) are nonuniform distribution of water in particle, pore size distribution (macropores that protect saturated capillaries), and nonhomogeneity of particles. A lower limit of critical saturation exists, above which excessive stresses will be created.

Two types of deterioration may be caused by nondurable aggregates. Combinations of pore size distribution or permeability and freezing rate exist for which excessive stresses may be created if the aggregates were frozen, even if they were unconfined. The other possibility that exists in this respect is that of a high permeability that will allow the expanding water to escape the aggregate particle during freezing. In this instance excessive stresses may be created in the surrounding cement paste if its air content is such that it cannot accommodate the excess water (2). Dolch (3) has summarized as follows: "Therefore, while the type of failure one gets depends on the permeability, whether or not one gets failure will depend on the several factors that determine the degree of saturation of the aggregate."

An aggregate may be saturated beyond the critical value at the time it is mixed and placed or may become critically saturated in the hardened concrete if placed where free drainage is not provided. The major factors that appear to influence the time required for an aggregate to become critically saturated in concrete after being placed are the absorption characteristics of the aggregate and the permeability and thickness of the paste cover separating the aggregate from the external supply of water (2). In any case, the important point is whether the aggregate is critically saturated at the time freezing occurs.

The objective of the investigation reported here was to provide information on the resistance of structural lightweight concrete to freezing and thawing as a function of the degree of aggregate saturation.

COARSE AGGREGATES

Sources

Structural lightweight concrete coarse aggregates from 6 commercial sources and 7 aggregates produced with the TTI kiln were investigated in this program. All commercial sources of aggregate were produced in rotary kilns. The properties of weight and specific gravity for the various aggregates are given in Table 1. The properties of absorption, porosity, and degree of saturation are discussed in the following sections.

Absorption

The Bryant method (4) was used to determine the absorption-time relationships of the various coarse aggregates (Appendix A). Curves of the first 24-hour absorption-time relationships are shown in Figures 1 and 2; curves for periods of up to 40 days

TABLE 1

PROPERTIES OF LIGHTWEIGHT COARSE AGGREGATES

Aggregate and Lot No.	Unit Weight	Dry Bulk Specific Gravity	Apparent Specific Gravity[a]	Production
R1	46.8	1.39	2.11	Commercial
R2	48.1	1.43	2.17	Commercial
C2	38.5	1.40	2.02	Commercial
C3	38.1	1.27	1.99	Commercial
C5A1	37.4	1.19	1.98	TTI[b]
S3	42.0	1.41	2.32	Commercial
E4	45.3	1.36	2.11	Commercial
E6	44.9	1.40	2.06	Commercial
D2	35.8	1.18	2.20	Commercial
D3	39.4	1.24	2.16	Commercial
W3	40.8	1.48	2.24	Commercial
W6D1	40.6	1.11	2.14	TTI[c]
W7B1	47.8	1.31	1.74	TTI[c]
M2B2	42.5	1.20	2.07	TTI
M2C2	37.6	1.12	2.07	TTI
M3C2	33.9	1.09	2.02	TTI
M3D2	37.9	1.21	2.04	TTI

[a]Obtained by using the pressure pycnometer.
[b]From same raw material as aggregate C.
[c]From same raw material as aggregate W.

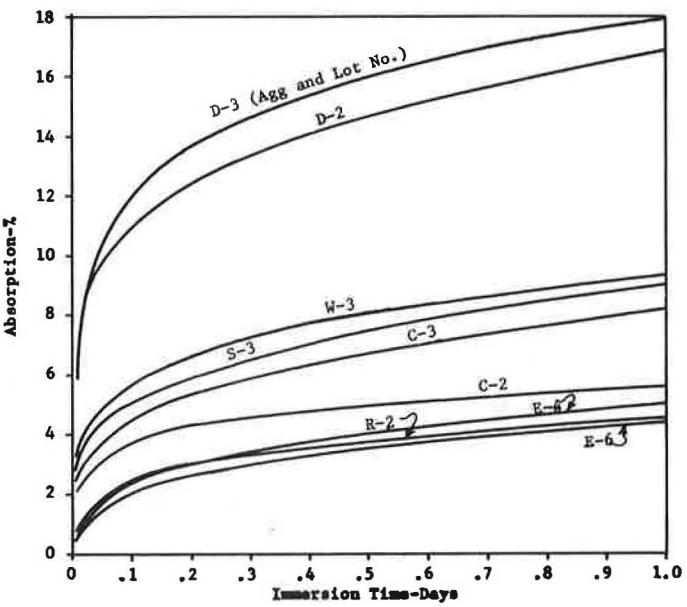

Figure 1. Absorption-time relationships for commercially produced coarse aggregates for first 24 hours.

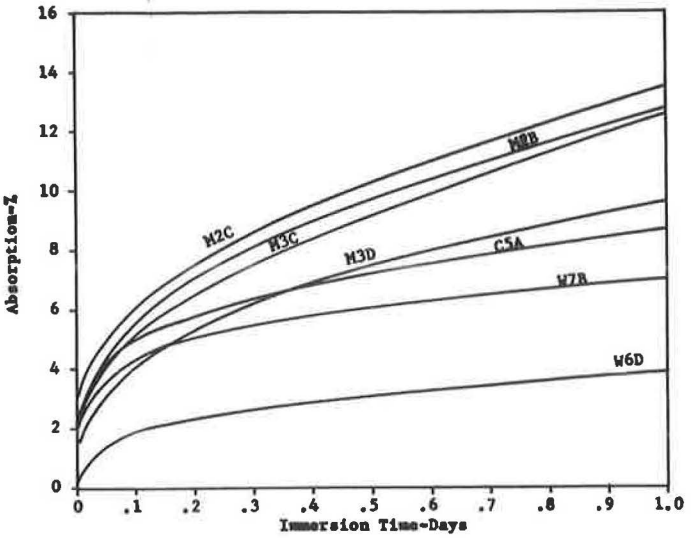

Figure 2. Absorption-time relationships for TTI produced coarse aggregates for first 24 hours.

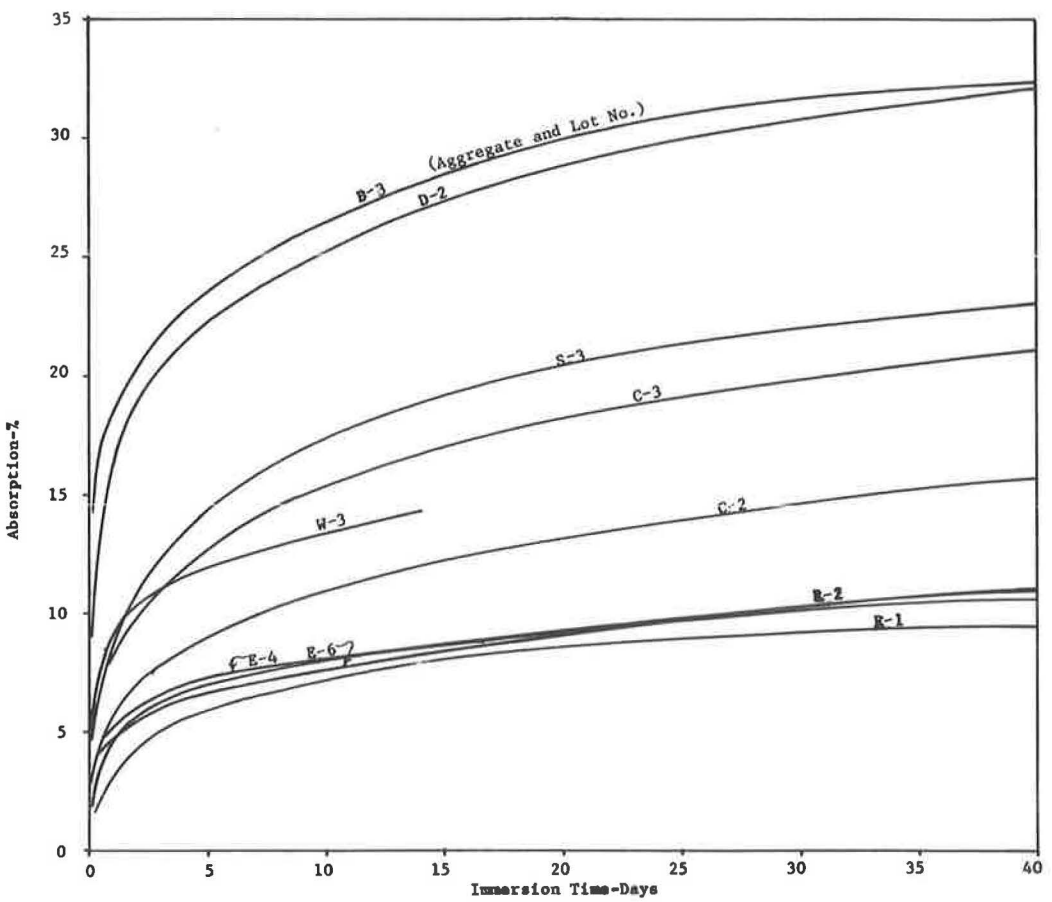

Figure 3. Absorption-time relationships for commercially produced coarse aggregates for 40 hours.

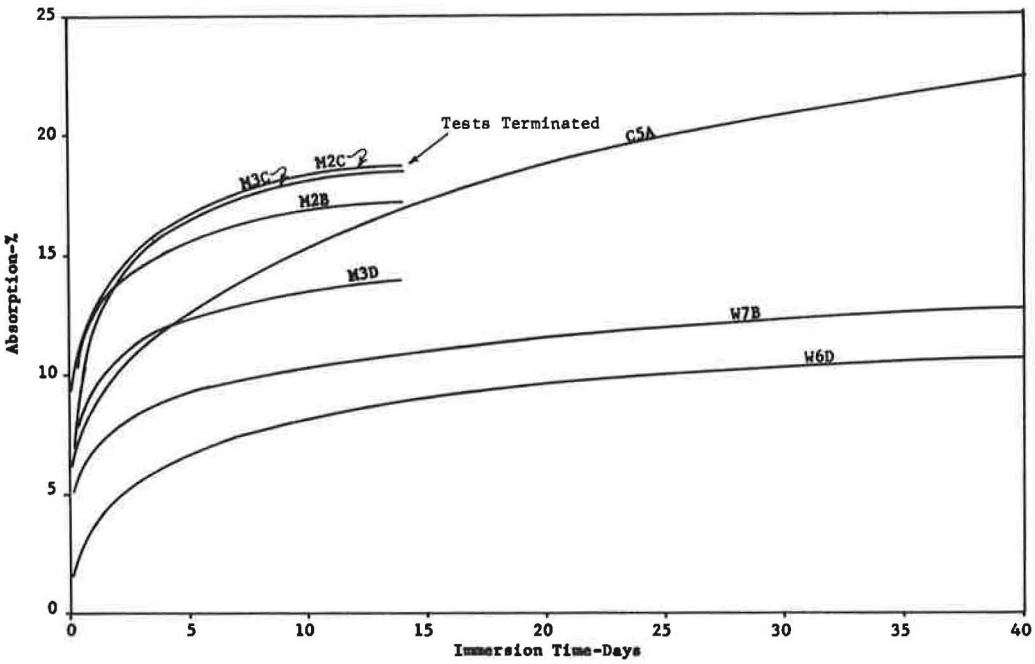

Figure 4. Absorption-time relationships for TTI produced coarse aggregates for 40 hours.

are shown in Figures 3 and 4. The wide range in absorption values is one of the most obvious differences noticed among the lightweight aggregates. Most of these aggregates continue to absorb water for long periods of time, and their final absorption values may be many times their 24-hour values. However, in terms of freeze-thaw durability, the important difference among the aggregates is not a particular value of absorption, but rather the rate at which the aggregates absorb water and become saturated. Thus, the slope of the absorption-time curve, a value that changes with time or degree of saturation, is the more influential parameter as it is a measure of the rate at which the aggregate is "soaking up" water, which in turn influences the ease with which an aggregate may become critically saturated.

Porosity

The porosity of each of the aggregates was calculated by using the dry bulk and apparent specific gravities.

The dry bulk specific gravity used to determine the porosity by this method is that obtained from the Bryant absorption and specific gravity test (Appendix A). The apparent specific gravity was determined by using a pressure pycnometer, which is capable of rapidly saturating an aggregate under 1,200-psi pressure. The porosity was determined by the equation

$$N = 1 - \frac{G_B}{Gpp}$$

where

G_B = dry bulk specific gravity,
Gpp = apparent specific gravity (using pressure pycnometer), and
N = porosity.

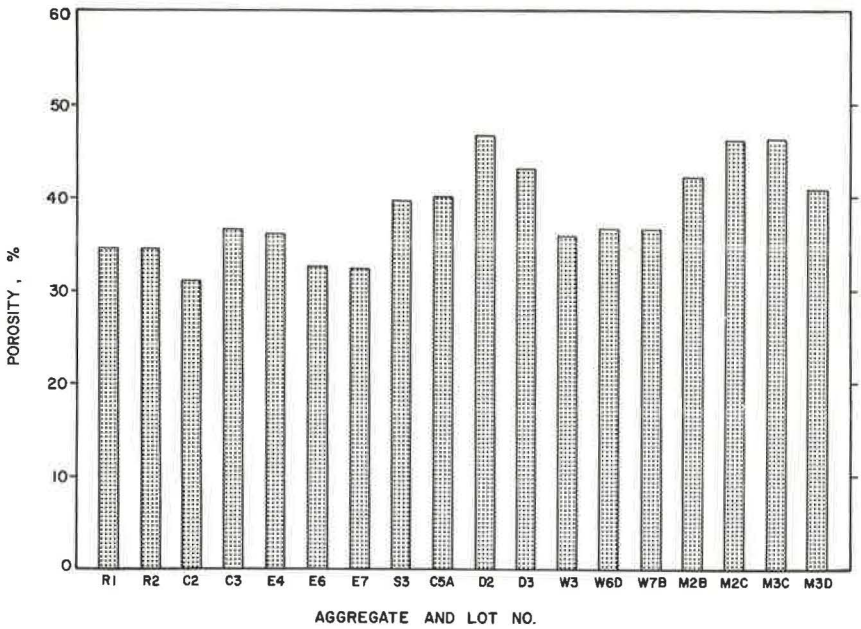

Figure 5. Porosity of aggregates.

The values of porosity are shown in Figure 5. These aggregates are very definitely porous enough (in all cases, over 30 percent) to accommodate sufficient water to cause disruption when frozen. However, as shown by the foregoing absorption-time curves, some of the voids contained in these aggregates apparently are isolated and not subject to saturation under atmospheric pressure, even after long periods of wetting.

Degree of Saturation

Absorption-time relationships and porosities can be combined and presented in the form of degree of saturation-time relationships. Curves illustrating such relationships are shown in Figures 6 through 9. Obviously, the degree of saturation obtained after a given immersion time is much greater for some aggregates than for others. This is in agreement with the following statement by Powers (1): "Various observations... suggest that a principal difference among different kinds of rock particles is the rate at which they become saturated when given free access to water."

CONCRETE

Mixtures

Sixty-nine batches of concrete were mixed and cast using the 6 selected lightweight coarse aggregates produced commercially and the 7 produced in the TTI kiln. Various degrees of prewetting of the coarse aggregates were obtained by immersing the aggregates in water for periods ranging from 6 hours to 180 days prior to mixing. All concrete mixtures had a nominal cement factor of 5 sacks/cu yd, a 3- to 4-in. slump, and 5 to 6 percent entrained air. A natural sand was used in all mixtures. The proportions of coarse and fine aggregate did not vary significantly. The various coarse aggregates and the amount of prewetting they received were the only parameters varied. Mixture proportions and properties of the concrete are given in Appendix B[1]. Three

[1]The original manuscript of the paper included Appendix B, which is available in Xerox form at cost of reproduction and handling from the Highway Research Board. When ordering, refer to XS-32, Highway Research Record 328.

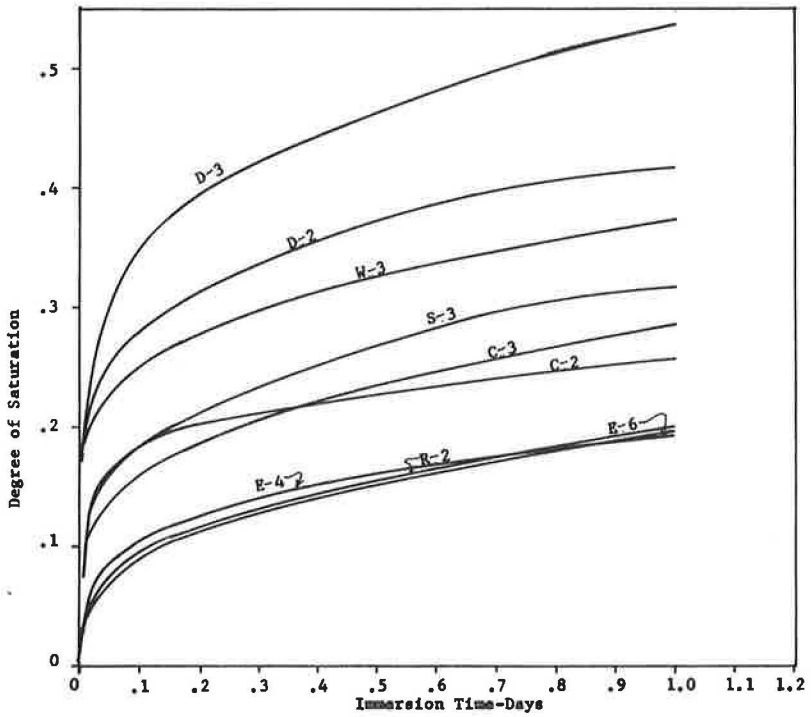

Figure 6. Relationship between degree of saturation and immersion time for commercially produced coarse aggregates for first 24 hours.

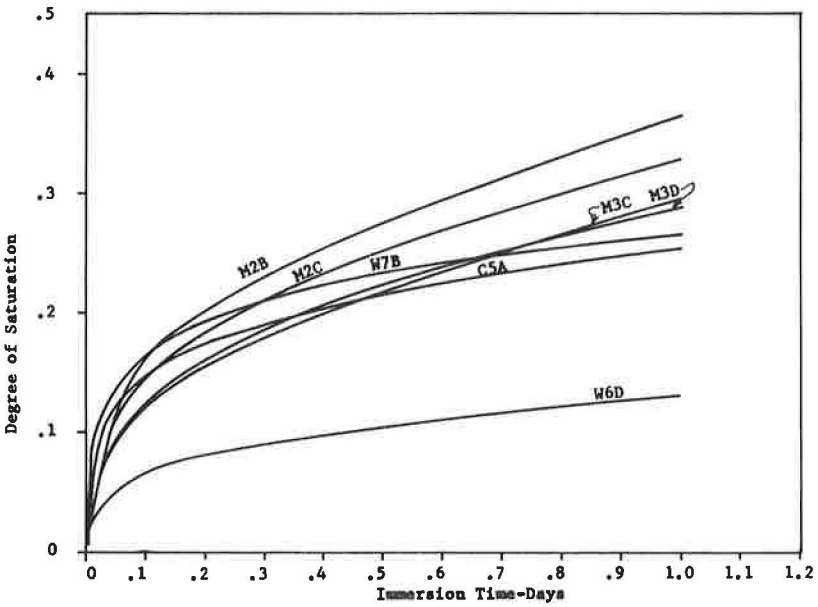

Figure 7. Relationship between degree of saturation and immersion time for TTI produced coarse aggregates for first 24 hours.

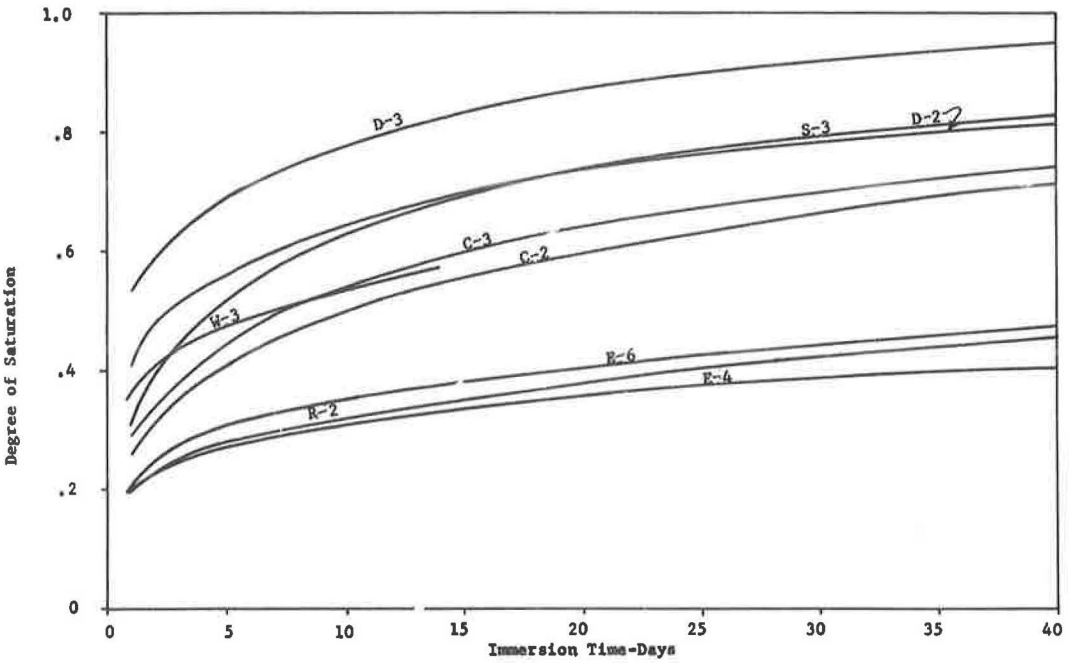

Figure 8. Relationship between degree of saturation and immersion time for commercially produced coarse aggregates for 40 days.

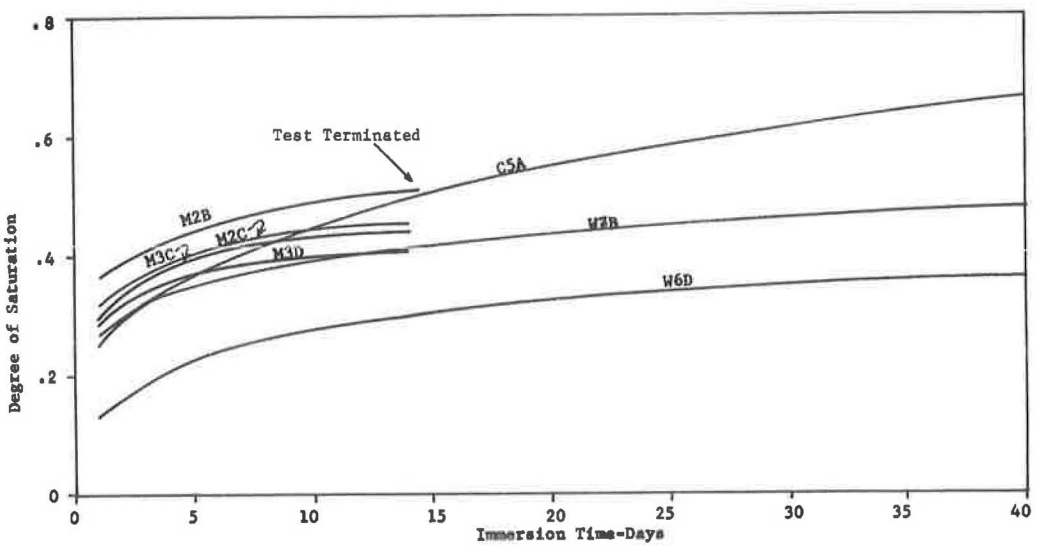

Figure 9. Relationship between degree of saturation and immersion time for TTI produced coarse aggregates for 40 days.

3-in. by 3-in. by 16-in. specimens for freeze-thaw testing were cast from each batch. These specimens were moist-cured until 14 days of age at which time they were subjected to cycles of freezing and thawing in water in accordance with ASTM C 290. Automatic cabinets with a capacity of 17 specimens and a capability of approximately 8 cycles per day were used in conducting these tests. Standard cylinders were cast and moist-cured for compressive strength determination at 14 and 28 days of age (strength values are given in Appendix B[1]).

Freezing and Thawing

The number of cycles to failure of the concrete specimens subjected to freezing and thawing is defined here as the number of cycles at which the square of the fundamental transverse frequency of vibration of the specimen decreased to 60 percent of its original value. This is substantially in accordance with ASTM C 215. Data obtained from these tests compared with degree of saturation of the coarse aggregate at the time of mixing are shown in Figure 10; a failure envelope is suggested. As each point (without an arrow attached) represents a failure, a failure envelope was drawn indicating the safe-unsafe areas. For example, according to the failure envelope, a concrete containing a coarse lightweight aggregate with a degree of saturation of 0.4 would withstand at least 80 cycles of freezing and thawing before failure. A concrete containing a coarse lightweight aggregate with a degree of saturation of 0.25 would withstand at least 300 cycles of freezing and thawing before failure. Four batches failed to the left of the failure envelope. One batch of aggregate E concrete failed at 44

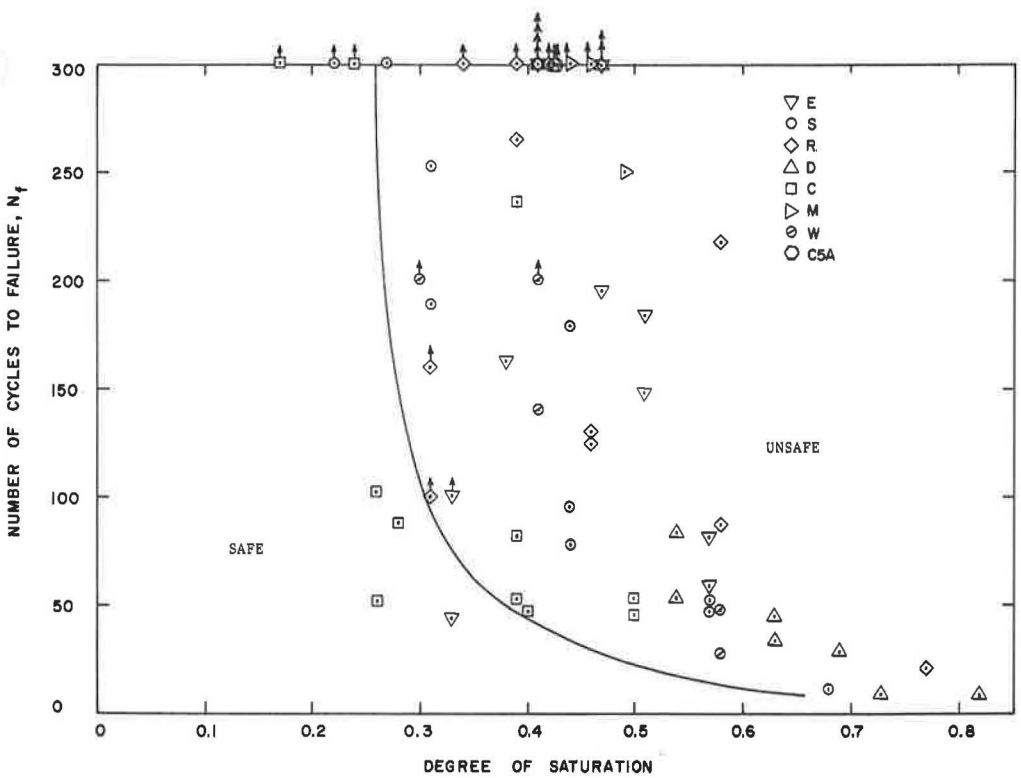

Figure 10. Relationship between number of cycles to failure (ASTM C 290) and degree of saturation of the coarse aggregate at the time of mixing.

cycles but, as it was the only one to fail prematurely, it was not considered representative and thus was ignored. The other 3 batches were made with aggregate C. Aggregate C, which is commercially produced, is made up of small particles partially fused together (Fig. 11) and has always been somewhat of a maverick in experimental work (4, 5). Aggregate C5A (Fig. 11), TTI produced from the same raw material as commercial aggregate C, yielded aggregate properties similar to aggregate C but behaved in the manner predicted by the failure envelope. For this reason, it was believed that the results from aggregate C concrete should also be disregarded when constructing the failure envelope. However, the fact remains that a commercially produced aggregate (aggregate C) did not behave as predicted. Even though this can be at least partially explained, the disparity, or maverick behavior of 1 out of 13 aggregates serves as a warning that the freezing-thawing mechanisms at work are extremely complex and experimental results must be interpreted in the light of the best available engineering judgment.

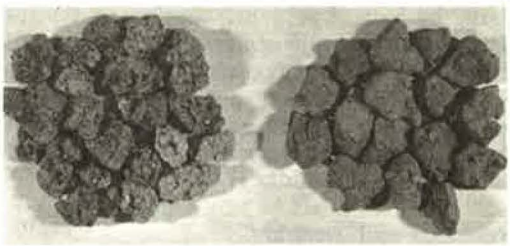

Figure 11. Aggregate C (left) and aggregate C5A (right).

If the failure envelope suggested by the data shown in Figure 10 is accepted, then judgment indicates that a lightweight aggregate with less than a 0.25 degree of satura-

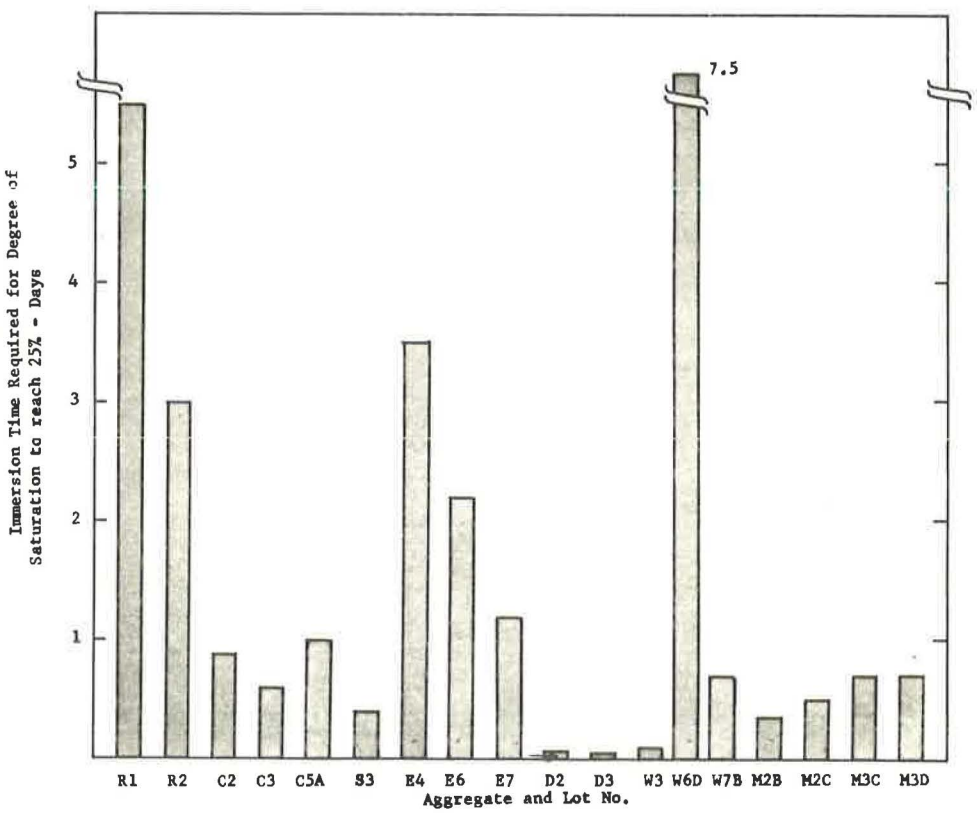

Figure 12. Immersion time required for degree of saturation of the coarse aggregates to reach 25 percent.

tion should produce a durable concrete. What does this mean in terms of the ease with which a given aggregate will reach this "critical" saturation? For the aggregates investigated, this question is answered by the data shown in Figure 12. When immersed in water, aggregate D will reach this critical value almost immediately (actually about 30 minutes), while aggregate W6D will not reach a critical saturation for over 7 days. The conclusion is obvious. Although almost any aggregate will produce durable concrete, extreme care must be exercised with some because of their rapid rate of water absorption.

CONCLUSIONS

Based on the experimental program reported here, the following conclusions are drawn:

1. Lightweight aggregates, when immersed, continue to absorb water for long periods of time (far in excess of 24 hours).
2. A failure envelope has been established between the number of lightweight concrete freeze-thaw cycles to failure and degree of saturation of the coarse aggregate. Lightweight concrete containing lightweight coarse aggregate with a degree of saturation less than 0.25 will generally withstand 300 cycles of freezing and thawing. Conversely, if the aggregate has a degree of saturation in excess of 0.25, the concrete may or may not fail in 300 cycles of freezing and thawing.
3. The time required for some lightweight aggregates to reach the critical degree of saturation of 0.25 can be extremely short (30 minutes immersion in one case), and thus the engineer should fully explore this property with any aggregates he has under consideration.

PRACTICAL IMPLICATION OF TEST RESULTS

Durability in a given environment such as ASTM C 290 can be reasonably predicted. owever, the infinite number of environments encountered in the field make accurate predictions an impossibility. The best one can do is to assume that the most severe environment expected will occur and to design accordingly.

A lightweight concrete may be made potentially nondurable (when tested by ASTM C 290 after 14 days of moist-curing) if the coarse aggregate is more than about 25 percent saturated at the time of mixing. As always, it is very difficult to interpret the meaning of these results for field use. The quantitative effect of a drying period prior to freezing temperatures has not been determined. If drying will reduce the degree of saturation of the aggregate sufficiently below 25 percent prior to the occurrence of freezing temperatures, the concrete would be expected to be durable. Also, if the aggregate is less than 25 percent saturated at the time of mixing, it appears reasonable that the aggregate would not reach a critical degree of saturation after being cast in any location where free drainage is provided.

If concrete should not be mixed and placed with the aggregate above critical saturation (a degree of saturation of about 25 percent for the aggregates studied), a field test method for determining the degree of aggregate saturation at the time of mixing must be developed. Consideration should be given to the expected environment and the effect of drying period in establishing any limits on the degree of saturation. Additional information is needed on this subject.

REFERENCES

1. Powers, T. C. Basic Considerations Pertaining to Freezing and Thawing Tests. Proc. ASTM, Vol. 55, 1955, p. 1132.
2. Verbeck, G., and Landgren, R. Influence of Physical Characteristics of Aggregates on Frost Resistance of Concrete. Proc. ASTM, Vol. 60, 1960, pp. 1063-1079.
3. Dolch, W. L. Porosity. In Significance of Test and Properties of Concrete Aggregate, ASTM, Spec. Publication 169, 1956, pp. 443-461.

4. Ledbetter, W. B., and Buth, E. Aggregate Absorption Factor as an Indicator of the Freeze-Thaw Durability of Structural Lightweight Concrete. Texas Transportation Institute, Texas A&M Univ., Research Rept. 81-3, Feb. 1967.
5. Ledbetter, W. B. Correlation Studies of Fundamental Aggregate Properties With Freeze-Thaw Durability of Structural Lightweight Concrete. Texas Transportation Institute, Texas A&M Univ., Research Rept. 81-1, Aug. 1965.
6. Bryant, J. S. The Determination of the Moisture Absorption Characteristics of Lightweight Concrete Aggregates. Texas A&M Univ., Thesis, Jan. 1959.

Appendix A

ABSORPTION-TIME TEST (BRYANT METHOD)

The purpose of this research (4, 6) was to devise a simple, reliable method of test that would determine values of absorption, rate of absorption, and specific gravities for both fine and coarse fractions of lightweight aggregates.

The Theory

It was necessary to devise a method of test that did not require handling of the sample or obtaining a saturated, surface-dry condition physically in the sample, and also one which would determine the rate of absorption. The approach was to devise a method that would give the saturated weight of the sample and the surface-dry volume without actually obtaining this condition at the same time.

If the sample is immersed in water in a container of known volume and the water is maintained at a constant level by adding water as the sample absorbs it, then the rate of absorption can be measured by weighing the container at specific time intervals during the test. Then if a rate curve can be established and extrapolated to include zero time, the total amount of absorption can be obtained. Also, the surface-dry volume of the sample can be obtained by subtracting the volume of water at zero time from the volume of the container.

The Test

Scope—This method of test is intended for use in determining the bulk specific gravity, both dry and saturated surface-dry, apparent specific gravity, absorption, and rate of absorption of both the coarse and the fine lightweight concrete aggregates. The specific gravity values are as defined in ASTM Designation E 12.

Apparatus—The apparatus shall consist of the following:

1. A balance having a capacity of 3 kg or more and a sensitivity of 0.1 gram or less, and
2. A glass mason jar fitted with a conical brass cap with a hole ¼ in. in diameter in the top.

Sample—Approximately 400 grams of the aggregate shall be selected by the method of quartering from the sample to be tested.

Procedure—The procedure shall be as follows:

1. The jar and cap shall be weighed to the nearest 0.1 gram. The jar shall then be filled completely with distilled water and weighed to the nearest 0.1 gram and the temperature of the water recorded. The test shall be conducted in an environment temperature of 72 ± 5 F.
2. The sample shall be dried in an oven at a temperature of 105 C for 24 hours. It shall then be allowed to cool to room temperature in a desiccator and the weight determined to the nearest 0.1 gram.

3. After it is weighed, the sample shall be placed in the mason jar and the jar filled with distilled water. The cap shall then be placed on the jar and water added to fill the jar and cap completely. The jar with sample and water shall then be weighed to the nearest 0.1 gram and the temperature recorded. With a little practice, this first weighing can be accomplished 2 minutes after the water is first introduced into the container. Weighings shall then be made at intervals of 2, 4, 6, 8, 10, 20, 30, 60, 90, and 120 minutes from the beginning of the test and for each 24 hours thereafter, taking care to agitate the sample by rolling and shaking the jar to remove any air trapped between the particles and refilling the jar so that a constant volume is maintained before each weighing is made.

Calculations—The weight of total water in the container at any time can be obtained by subtracting the weight of the container and the oven-dry weight of the sample from the total weight of the sample, container, and water at that time. The weight of total water for each of the time intervals shall be calculated. Then, if the time intervals are represented by t_1, t_2, t_3, ..., t_t and the weights of total water corresponding to those intervals are represented by w_1, w_2, w_3, ..., w_t, a curve can be plotted with time as the abscissa and total water as the ordinate. This curve should be extended to a minimum time of 10 minutes. The total water at zero time shall be referred to as the free water. The curve shall be extended to time zero to determine the amount of free water. For purposes of this test, free water is defined as all water in the container that is not absorbed by the sample. Assuming that the volume of the sample remains constant, then the amount of free water is constant through the test. The volume of free water can then be calculated by dividing the weight of free water by the specific gravity of water at the temperature recorded when the test began. The bulk volume of the sample shall be calculated by subtracting the volume of free water from the volume of the container. The volume of total water at any time, t, shall be calculated by dividing the weight of total water at time, t, by the specific gravity of water at the temperature recorded when the test began. The apparent volume of the sample at any time, t, can then be calculated by subtracting the volume of total water at time, t, from the volume of the container. The absorbed water at any time can be calculated by subtracting the free water from the total water at that time.

Absorption—The percentage of absorption shall be calculated for each time interval by dividing the weight of absorbed water at each time interval by the oven-dry weight of the sample. The percentage of absorption versus time shall be plotted on rectangular coordinate graph paper and a smooth curve drawn through these points to establish the rate of absorption.

Bulk Specific Gravity (Dry)—The bulk specific gravity shall be calculated by dividing the oven-dry weight of the sample by the bulk volume of the sample.

Bulk Specific Gravity (Saturated Surface-Dry)—The bulk specific gravity on a saturated, surface-dry basis at any time, t, shall be calculated by dividing the sum of the oven-dry weight of the sample and the weight of adsorbed water at time, t, by the bulk volume of the sample.

Apparent Specific Gravity—The apparent specific gravity at any time, t, shall be calculated by dividing the oven-dry weight of the sample by the apparent volume at that time.

Discussion

W. P. CHAMBERLIN, New York State Department of Transportation—The authors conclude that 0.25 is the level of saturation prior to mixing below which a lightweight aggregate will not attain its critical degree of saturation when mixed in concrete and subjected to 300 cycles of ASTM C 290 after 14 days of immersion. Further, they suggest that a field acceptance test based on this value be developed.

It is interesting to look at their data also from the point of view of what can be learned about the water sorption of lightweight aggregate in concrete. For instance, if the number of freeze-thaw cycles to failure is looked upon as a measure of the time required for the aggregates to attain critical saturation in "wet" concrete, then the authors' data may be organized in such a way as to yield a similar but more generalized interpretation. Specifically, if the aggregates (Fig. 10) for which there are sufficient data are plotted separately, they appear to reflect a common trend (Fig. 13a and 13b) that can be stated as follows: The length of time required for any particular lightweight aggregate to attain its critical degree of saturation in concrete decreases at a decreasing rate as the level of saturation prior to mixing is increased above some minimum value. This minimum value is different for different lightweight aggregates. These minimum values for the exposure cited are approximately the following:

Aggregate	Value
C	0.24
D	0.46
E	0.47
R	0.40
S	0.27

In this sense, lightweight aggregates perform as do other aggregates; only the numbers are different.

The curves shown in Figure 13 also help to illustrate the fact that 0.25 is a conservative value (3 of the minimum values cited above exceed 0.25 by 60 to 80 percent) and, perhaps, very conservative for most uses of structural lightweight concrete, considering the severity of the ASTM C 290 exposure.

A second point that may be worth exploring is the feasibility of using degree of aggregate saturation under some standard conditions as a method of prejudging (that is, prior to mixing and testing in concrete) potential performance. Such a test could be useful in identifying at least (a) those lightweight aggregates with a very high probability of acceptable performance under any exposure, and (b) those with a high proba-

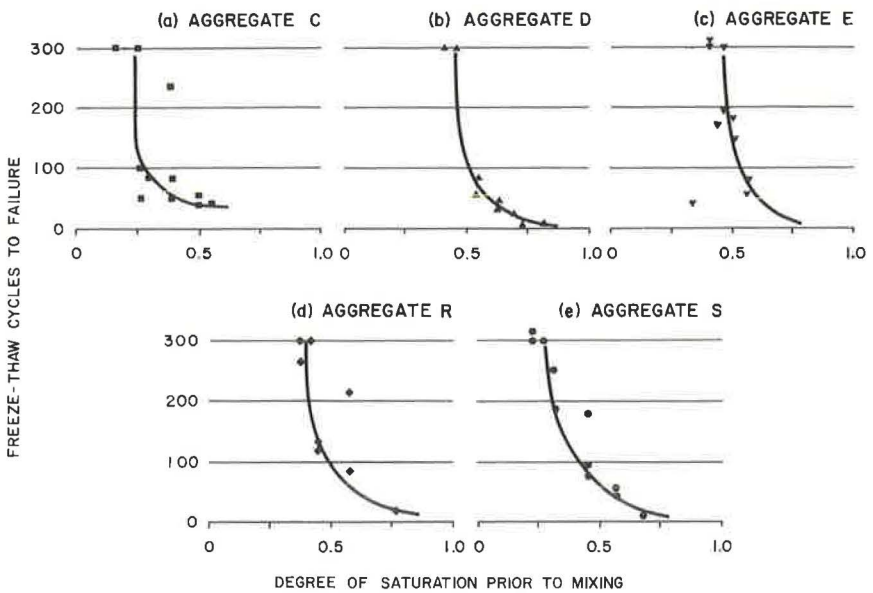

Figure 13. Experimental results for individual aggregates.

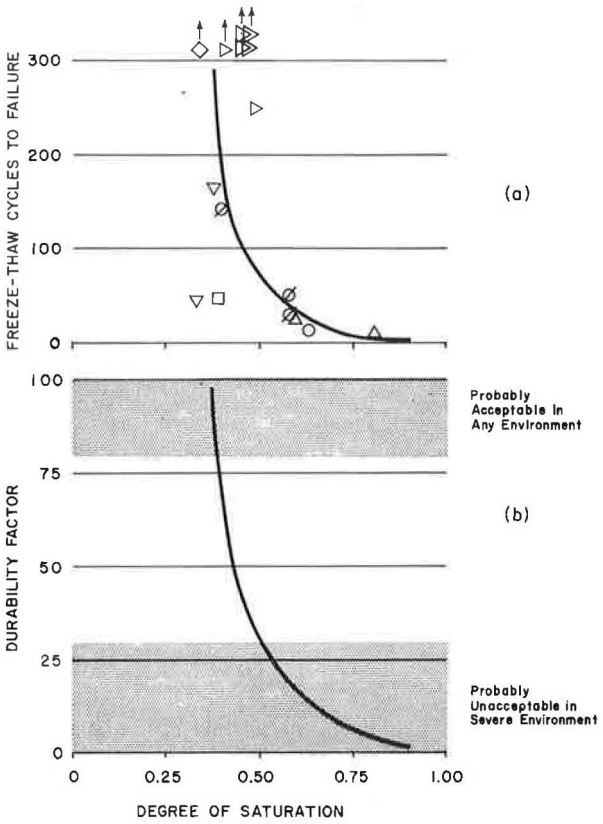

Figure 14. All aggregates after 14 days of immersion.

bility of failure under severe exposure. This is shown in Figure 14 in which the authors' data for 14 days of aggregate immersion are plotted.

If the apparent relationship described by the solid line in Figure 14a is valid (and this could be explored through a carefully designed experiment) and the ordinate were expressed in terms of durability factor (DF) as defined by ASTM C 290, there would then be a basis for making some absolute judgments about quality. For instance, Walker et al. (7) have suggested a DF ≥ 80 as indicating condition a, and a DF ≤ 30 as indicating condition b. Accordingly, it could be reasoned that a lightweight aggregate with a 14-day degree of saturation less than some particular value (about 0.38 in the schematic example of Figure 14b) would probably perform acceptably in any environment and one with a 14-day degree of saturation in excess of some other particular value (0.50 in the example) would probably fail in a severe environment.

Reference

7. Walker, R. D., et al. One Cycle Slow-Freeze Test for Evaluating Aggregate Performance in Frozen Concrete. NCHRP Rept. 65, 1969.

EUGENE BUTH and W. B. LEDBETTER, Closure—Mr. Chamberlin raises 2 points in his discussion. In considering the first point, the authors agree that the limiting value

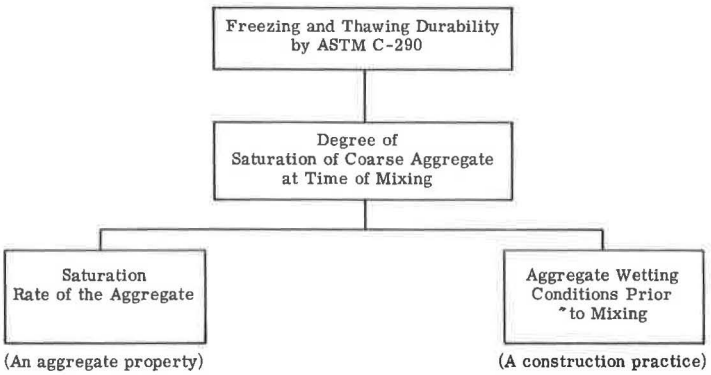

Figure 15. Parameters affecting degree of saturation of aggregates.

of degree of saturation of 0.25 is conservative for aggregates R, E, and D but not conservative for aggregates C and S. The value of 0.25 was chosen as a number applicable to all lightweight aggregates tested and must therefore be conservative for some.

Mr. Chamberlin's second point, concerning the feasibility of using aggregate degree of saturation under some standard conditions as a method of prejudging potential performance, warrants additional discussion. The test results indicate the minimum values of degree of saturation that Mr. Chamberlin states and correctly interprets. However, these values, which can be used to predict performance as determined by freezing and thawing durability, are a function of 2 parameters: the saturation rate of the aggregate (an aggregate property) and the length of time that water is available (a construction practice) to the aggregate (Fig. 15). By controlling the amount of pr wetting time, any of the aggregates studied (and perhaps all lightweight aggregates) can be conditioned to have a degree of saturation that is less than the minimum values stated. The test results show that, when the degrees of saturation are below these minimum values, the concrete proved to be durable even in the severe exposure of ASTM C 290.

The authors are therefore forced to conclude that the use of degree of saturation under standard conditions as a method of prejudging performance is a slight oversimplification in that it does not account for the influence of amount of prewetting that will take place on the job.

Effect of Aggregate Type on the Properties of Shrinkage-Compensating Concrete

JON A. EPPS, Department of Civil Engineering, Texas A&M University; and
MILOS POLIVKA, University of California, Berkeley

Expansive cement concretes, if adequately restrained by reinforcing steel, can minimize or prevent the development of cracks due to drying shrinkage. Such concretes are referred to as shrinkage-compensating. Reported are results of an investigation undertaken to determine the effect of aggregate type on the properties of shrinkage-compensating concretes. Included in this study were 3 types of natural aggregates and one lightweight aggregate. Two types of cement were used. One was the shrinkage-compensating cement that was a blend of 15 percent by weight of calcium sulfoaluminate expansive component and 85 percent of type V portland cement. The second cement used in the control concretes was 100 percent type V portland cement. The expansion and shrinkage characteristics of the shrinkage-compensating concretes were determined for both restrained and unrestrained prisms. Compressive strength and modulus of elasticity were determined for unrestrained cylindrical specimens. All concretes had a cement content of 5.5 scy and a water-cement ratio of 0.58 by weight. With these fixed mix proportions, the slump of the concretes with the 4 different types of aggregate varied from 2 to 4 in. From the results of this investigation it is concluded that the aggregate type is an important factor in the properties of a shrinkage-compensating concrete. Shrinkage-compensating concrete mixes must be so designed that their restrained expansion is of sufficient magnitude to compensate for the potential shrinkage of the concrete containing a certain type of aggregate. The expansion and shrinkage behavior of a shrinkage-compensating concrete is related to its modulus of elasticity. Concretes of high elastic modulus exhibit a larger expansion than do concretes of lower modulus of elasticity.

•SHRINKAGE-COMPENSATING CEMENTS, now being produced by several manufacturers in the United States, are used in various types of concrete construction. California, Connecticut, Ohio, and Wisconsin have constructed concrete pavement sections with shrinkage-compensating cement (1). Other uses of concrete utilizing shrinkage-compensating cement included, for example, a folded-plate roof in Yuba City, California (2), floors of several large commerical buildings, a motel, and a municipal pumping station (3). The expansive cement developed by Alexander Klein (4), of the University of California at Berkeley, is designated by ACI Committee 223 as type K. A number of review papers and reports covering the properties and uses of expansive cement concretes have been published (5, 6, 7). ACI Committee 223 is currently preparing a comprehensive report on expansive cement concretes (8) that will be published by the American Concrete Institute.

The benefits obtained from the use of shrinkage-compensating cements are derived from the expansion of the concrete. If this expansion, which takes place during the early ages of curing, is restrained by reinforcing steel, the steel goes into tension and

Paper sponsored by Committee on Performance of Concrete—Physical Aspects.

the concrete into compression. On drying the concrete shrinks causing a relief of the precompression rather than the development of tensile stresses as is the case in conventional concrete. When the drying shrinkage is essentially complete, a properly designed shrinkage-compensating concrete will remain under a slight compression thus reducing cracking.

The rate and magnitude of expansion are influenced by several factors including the chemical composition and fineness of the expansive cement, richness of mix, conditions of curing, and degree and type of restraint. These and other factors have been investigated and reported (9). One of the most important factors affecting not only the expansion characteristics of the concrete but also its drying shrinkage is the aggregate. Carlson (10) has shown that the drying shrinkage of concrete, which is but a fraction of that of neat cement paste, is greatly influenced by the compressibility of the aggregate and the volume change of aggregate due to drying. The maximum size, grading, shape, and surface texture of the aggregate also have an effect on the shrinkage of the concrete. Pickett (11) has developed an equation for shrinkage of concrete as a function of the shrinkage of the cement paste, volume of aggregate in the mix, and the elastic constants of the aggregate and of the concrete mix. Hansen and Nielsen (12) have extended this theory by including the effect of shrinkage of aggregate and modulus of elasticity of cement paste and aggregate.

SCOPE OF INVESTIGATION

The objective of this investivation was to evaluate the influence of the nature of aggregate used on the physical and mechanical properties of shrinkage-compensating concrete. Three types of natural aggregates and one lightweight aggregate were employed. To permit a direct evaluation of the effect of type of aggregate, all concretes employed contained the same volume of aggregate per unit volume of concrete. The expansion of the concrete during its 14-day curing period and the drying shrinkage during storage at 50 percent relative humidity and 70 F was determined for restrained as well as unrestrained concrete prisms. Compressive strength and modulus of elasticity were det mined for each concrete at ages of 3, 7, 14, and 28 days. As a control mix for each type of aggregate a type V portland cement was used. The strength and drying shrinkage of the concrete made using this cement were determined and used as a reference.

Although only a single concrete mixture (identical cement factor, w/c ratio, and aggregate volume) was employed, similar trends as those reported in this study should be expected for other mixes.

MATERIALS AND TEST SPECIMENS

Cements

Two types of cement were used. One was the shrinkage-compensating cement that was a blend of 15 percent by weight of calcium sulfoaluminate expansive component, made at the University of California (4, 13), and 85 percent of type V portland cement of the following compound composition: C3S = 55 percent, C2S = 25 percent, C3A = 3.4 percent, and C4AF = 8.9 percent. A portland cement low in C3A content was selected, as previous research (9) has established that the lower the C3A content of the portland cement (15) the greater the expansion of the expansive cement. Furthermore, the composition and expansion of the shrinkage-compensating cement used in this study are similar to the commercially produced shrinkage-compensating cement.

The second cement, which was used for the control concrete mixes, was 100 percent type V portland cement of the same composition as that used in the shrinkage-compensating cement.

Aggregates

Three natural coarse aggregates of $^{3}/_{4}$-in. maximum size and a lightweight aggregate of $^{5}/_{8}$-in. maximum size were used. The natural coarse aggregates were selected on the basis of their influence on the shrinkage characteristics of concrete. One of thes coarse aggregates was crushed granite, which produces concretes of low shrinka

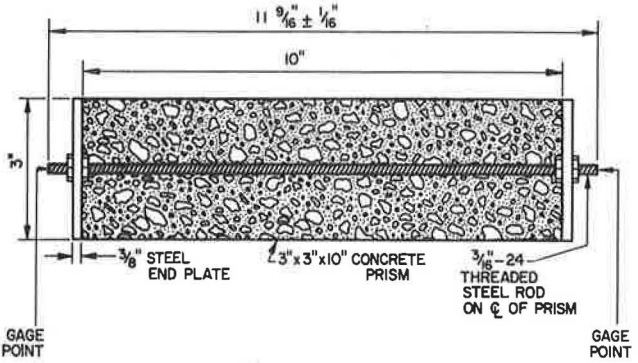

Figure 1. Restrained concrete prism.

characteristics. Its specific gravity was 2.87 and its absorption was 0.9 percent. The second coarse aggregate, also producing concretes of low shrinkage characteristics, was a river gravel of relatively smooth rounded shape. Its specific gravity was 2.80 and absorption was 0.7 percent. The main rock types present in this aggregate were basalt, andesite, dacite, and quartz. The fine aggregate used with these 2 coarse aggregates was a well-graded quartz sand with an F. M. of 2.76, specific gravity 2.60, and absorption of 1.3 percent. The third natural aggregate, both coarse and fine (F. M. 2.60), was a partially crushed river aggregate, primarily sandstone and graywacke, which produces concretes of relatively high shrinkage characteristics. Its specific gravity was 2.67, and its absorption was 1.4 percent. These 3 natural aggregates are hereinafter designated as granite, river gravel, and sandstone aggregate.

The lightweight aggregate, both coarse and fine, was an expanded shale produced by calcining crushed shale in a rotary kiln, resulting in a rounded hard-coated product. The $\frac{5}{8}$-in. maximum size coarse aggregate had a specific gravity of 1.28 and absorption of 14.5 percent; and the fine expanded shale aggregate (F. M. 2.18) had a specific gravity of 2.12 and absorption of 10.5 percent. This expanded shale aggregate is hereinafter designated as lightweight aggregate.

Concretes

In designing the concrete mixes for the 4 different types of aggregates, it was essential to select proportions resulting in a fixed volume of aggregate per unit volume of concrete to permit a direct comparison of the effect of type of aggregate on properties of shrinkage-compensating concrete. The final mix selected had a cement content of 5.5 scy and water-cement ratio of 0.58 by weight. With the fixed volumes of aggregate, cement, and water, the slump was allowed to vary from 2 to 4 in. (3.0 ± 1 in.). The nominal unit weight of the concretes containing the natural aggregates was 152 pcf and of the lightweight aggregate concretes 105 pcf.

Test Specimens

The expansion and the drying shrinkage characteristics of the concrete were determined on both restrained and unrestrained 3- by 3- by 10-in. prisms. The restrained prisms, as shown in Figure 1, had an embedded $\frac{3}{16}$-in. threaded rod (24 threads per in.) with end plates providing 0.30 percent of steel in the longitudinal direction.

The ends of the threaded rod were furnished with a gage point for length measurements. The unrestrained prisms had only a gage plug in each end for length measurements. After casting, the prisms were stored in a fog room, the sides of the prism molds were removed at age 8 hours, an initial length measurement was taken, and the prisms on their base plates (to prevent damage to the weak concrete) were stored in

lime-saturated water. The base plates were removed after 24 hours. All prisms were water-cured for 14 days and then transferred to a low humidity room maintained at 70 F and 50 percent relative humidity. Measurements of expansion during water-curing and shrinkage during storage in the low humidity room were taken at frequent intervals.

Compressive strength and modulus of elasticity were determined on unrestrained 3- by 6-in. cylindrical specimens at ages of 3, 7, 14, and 28 days. After casting, these specimens were stored in a fog room, molds removed after 24 hours, and the specimens then stored in lime-saturated water up to age of test.

TEST RESULTS

Summarized herein are the test results obtained for shrinkage-compensating concretes made with 4 different aggregates and for corresponding control mixes containing type V portland cement. Included are compressive strength, modulus of elasticity, and the expansion and shrinkage behavior of the shrinkage-compensating concretes. A minimum of 3 specimens was used to determine the relationships presented for any one mixture. The cement content of all concretes was 5.5 scy, the water-cement ratio was 0.58 by weight, and their slump was 3 ±1 in.

Compressive Strength

Results of compressive strength tests on the concretes up to age 28 days are shown in the upper 2 diagrams of Figure 2. The diagram on the right gives results for the

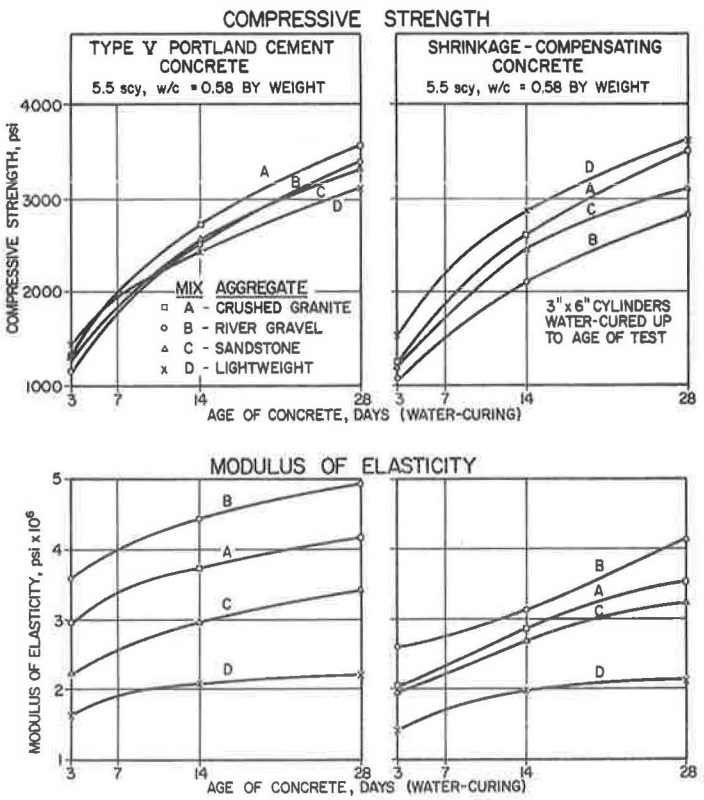

Figure 2. Compressive strength and modulus of elasticity of concretes.

shrinkage-compensating concrete mixes and the one on the left for the corresponding control mixes made with type V portland cement. The nominal 28-day compressive strength of these concretes was 3,000 to 3,500 psi. Compressive strength was determined on 3- by 6-in. unrestrained specimens cured in lime-saturated water up to the age of test.

In making comparisons of data obtained on the shrinkage-compensating concretes and the type V cement concretes, it should be recognized that the type of aggregate has a marked influence on the expansion behavior of the shrinkage-compensating concretes, and this influences their compressive strengths. The greater the expansion of the concrete is, the lower should be its strength. Unrestrained expansion data for these shrinkage-compensating concretes are shown in Figure 3. Note that the expansion of the concrete is almost completed within 14 days of curing and that about 85 to 90 percent of this expansion occurs during the first 7 days.

Referring to Figures 2 and 3, the lightweight aggregate shrinkage-compensating concrete (curves D), which had the lowest expansion, had the highest strength, whereas the river gravel concrete (curves B), which exhibited the largest expansion, had the lowest strength.

The surface texture and angularity of an aggregate may have a more important influence on the strength of shrinkage-compensating concretes than the magnitude of expansion. The rougher the surface texture is, the better the bond between paste and aggregate, thus resulting in higher strength. The crushed granite (curve A) not only produced a concrete of relatively high expansion (Fig. 3) but also a concrete of high strength (Fig. 2). Even after expansion has taken place, its rough textured angular shaped particles will provide better bond than a smooth textured rounded aggregate. This is clearly demonstrated when comparing the results obtained with the river gravel and crushed granite concretes. Inasmuch as the expansion (Fig. 3) of the crushed granite concrete (curve A) was only slightly lower (7 percent) than that of the river gravel concrete (curve B), it might be expected to have a somewhat higher strength. However, the rough textured angular shape of the granite aggregate produced a concrete of much higher strength (25 percent) than the river gravel. It may therefore be concluded that the compressive strength of shrinkage-compensating concrete is influenced by 2 factors: (a) the

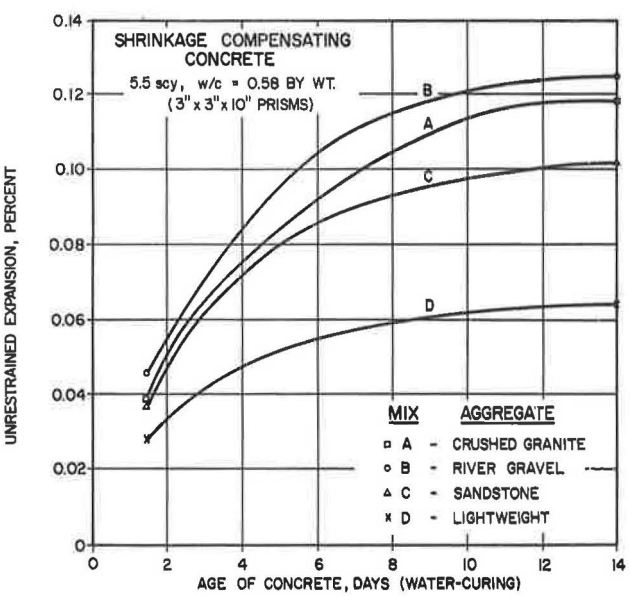

Figure 3. Unrestrained expansion of concretes.

surface texture and shape of the aggregate that influences the bond between paste and aggregate, and (b) the magnitude of expansion.

The small difference in strength observed for the control concretes made with type V cement (Fig. 2) can be attributed primarily to the surface texture and angularity of the aggregate. The lower 28-day strength of the lightweight aggregate concrete is to some degree due to the lower strength of the aggregate itself. The slightly higher 3-day strength of this concrete is probably due to the internal curing, at an early age, provided by the water held in the pores of the lightweight aggregate.

Modulus of Elasticity

Modulus of elasticity was determined at ages of 3, 7, and 28 days on 3- by 6-in. concrete specimens cured in lime-saturated water up to the age of test. Results obtained on the shrinkage-compensating concretes and on the control concretes made with type V cement are shown in the lower 2 diagrams of Figure 2.

For all ages and aggregates investigated, the shrinkage-compensating concretes had a lower modulus of elasticity than the corresponding concrete containing type V cement. This difference in modulus of the concrete is primarily due to the difference in the modulus of the paste, the structure of which is altered during expansion. The higher the expansion is, the lower the modulus. The lightweight aggregate shrinkage-compensating concrete, which had the lowest expansion (curve D, Fig. 3), had a 28-day modulus of elasticity (Fig. 2) only 4 percent lower than that of the corresponding type V cement control mix, whereas for the river-gravel concrete (curve B), which exhibited the largest expansion, the loss in modulus of elasticity was 16 percent.

Referring to the lower diagrams of Figure 2, it can be seen that the type of aggregate has a significant influence on the modulus of elasticity of the type V cement concretes, ranging from 2.2×10^6 psi for the lightweight aggregate mix to 4.9×10^6 psi for the river gravel mix. A much smaller difference in modulus can be observed for the shrinkage-compensating concretes that ranged from 2.1×10^6 psi for the lightweight aggregate mix to 4.1×10 psi for the river gravel mix. This smaller effect of type of aggregate on modulus of elasticity is due to the different expansion characteristics of these concretes. A low modulus concrete has a lower expansion and thus a smaller reduction of modulus than does a high modulus concrete that has a much larger expansion. Thus the effect of aggregate type on modulus of elasticity of the concrete is being masked by the expansion of the paste that reduces its modulus.

Expansion-Shrinkage Characteristics

A shrinkage-compensating concrete is subject to as much drying shrinkage as a portland cement concrete. However, if its expansion is restrained by reinforcing steel, a slight compression is developed in the concrete. On drying the shrinkage of this concrete will reduce the magnitude of the precompression. A properly designed shrinkage-compensating concrete mix will remain under a slight compression even after long periods of drying. By preventing development of tensile stresses during drying, the formation of drying-shrinkage cracks can be avoided. As shown by test results herein reported, the aggregate has a significant effect on expansion as well as on drying shrinkage and is therefore a major factor in the mix design of a shrinkage-compensating concrete.

The expansion characteristics up to 14 days of water-curing and subsequent drying shrinkage up to age of one year of the shrinkage-compensating concretes made with the 4 different types of aggregates are shown in Figure 4. These volume changes were determined on 3- by 3- by 10-in. prisms. Data for unrestrained prisms are shown in the upper diagram of Figure 4, and data for the prisms restrained with reinforcement ($p = 0.3$ percent) are shown in the lower diagram. It should again be pointed out that a shrinkage-compensating concrete can only be effective if restrained. The tests on unrestrained prisms were made for comparison purposes only.

To evaluate the effect of type of aggregate used in this investigation on the shrinkage of concrete, drying shrinkage was determined for the control concrete mixes employing the type V portland cement. Results of these tests, for both restrained ($p = 0.3$ percent)

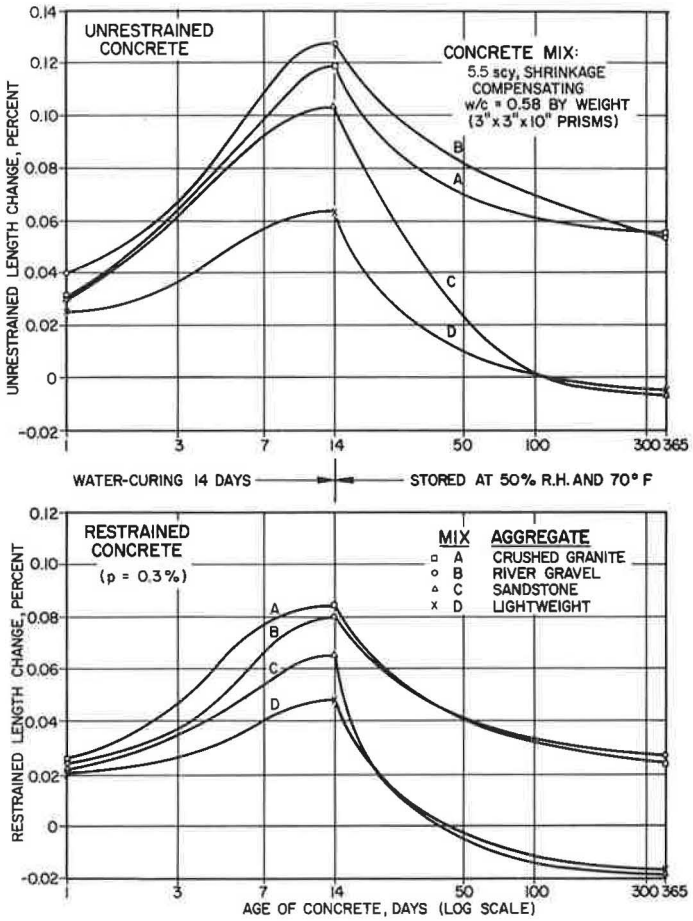

Figure 4. Effect of aggregate type on length change of shrinkage-compensating concrete.

and unrestrained 3- by 3- by 10-in. prisms are shown in the 2 diagrams of Figure 5. These concretes were water-cured for 14 days prior to storage in a room at 50 percent relative humidity and 70 F. These data clearly demonstrate the significant influence of the type of aggregate on drying shrinkage of concrete. For the unrestrained concretes the one-year shrinkage ranged from 0.058 percent for the river gravel mix to 0.108 for the sandstone aggregate. The crushed granite mix had about the same shrinkage characteristics as the river-gravel mix. The one-year unrestrained shrinkage of the lightweight aggregate concrete was 0.065 percent. As is to be expected the drying shrinkage of prisms restrained with reinforcing steel is lower than that of unrestrained prisms. As shown in Figure 5, the one-year shrinkage of the restrained concretes ranged from 0.044 percent for the river-gravel mix to 0.075 percent for the sandstone aggregate concrete. This is about a 30 percent reduction as compared to the shrinkage of the unrestrained concretes.

Referring to Figure 4, the 14-day expansion of the shrinkage-compensating concretes ranged from 0.064 to 0.128 percent for the unrestrained prisms and from 0.048 to 0.084 percent for the restrained prisms. The low expansion values were for the lightweight aggregate and sandstone aggregate concretes and the large expansions for the river-gravel and crushed-granite concrete mixes. Unrestrained concrete made with the river

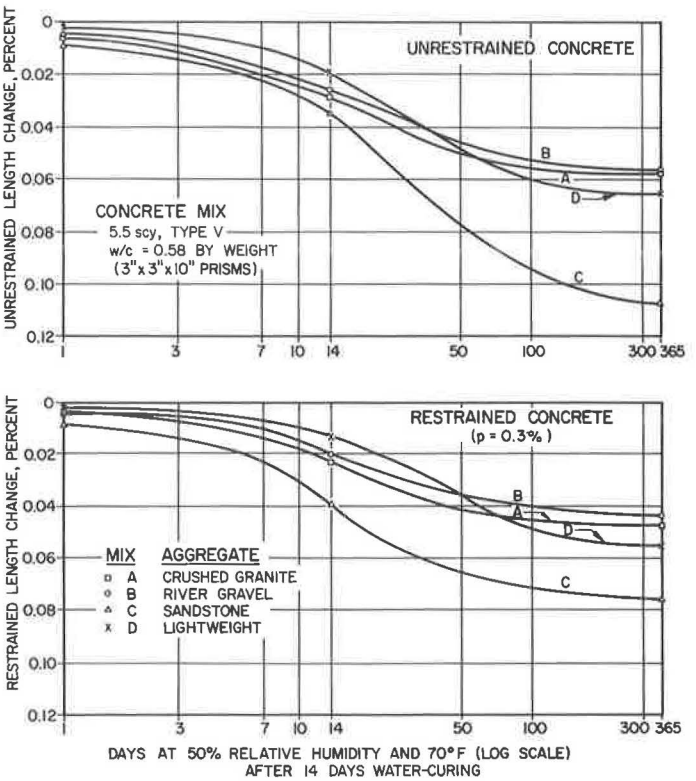

Figure 5. Effect of aggregate type on shrinkage of type V portland cement concrete.

gravel had a somewhat higher expansion than the concrete made with crushed granite; however, the reverse is true for the restrained prisms. No reason other than testing variation can be given for this small discrepancy between restrained and unrestrained prisms. In general, however, the higher the elastic modulus of the concrete is, the larger its expansion.

Data for the restrained prisms (lower diagram of Fig. 4) clearly show that the river-gravel and crushed granite mixes have some residual compression even after one year of drying. This is not true for the sandstone aggregate or lightweight aggregate concretes, which lost all of the precompression after about 40 days of drying. To produce a true shrinkage-compensating concrete with these 2 types of aggregate, a different mix design would need to be employed that would increase the expansion characteristics of the concrete. This could be accomplished either by increasing the expansive cement content of the concrete or by using a cement of higher expansion characteristics. It is therefore essential that in evaluating the behavior of a shrinkage-compensating concrete the same type of aggregate be employed as that which will be used in the structure.

Discussion of Results

Results of this investigation demonstrate that aggregate type is an important variable in the properties of shrinkage-compensating concretes. For a concrete mix of a given cement content and water-cement ratio, the aggregate type controls its strength, elastic modulus, and its expansion and shrinkage behavior. Concretes made with aggregate types producing a high elastic modulus expand more than those of lower modulus. For

the normal weight concrete mixes investigated, the magnitude of shrinkage was inversely proportional to the elastic modulus of the concrete (Figs. 2 and 5). Thus the expansion and shrinkage characteristics of the normal weight concrete are related to the modulus of elasticity of the aggregate. A low modulus aggregate that is easily compressed under load will produce a mix of low expansion and high shrinkage, whereas the reverse will be true for a high modulus aggregate.

Compressive strength is lowered by expansion of the concrete, but not by an amount directly proportional to the expansion of the concrete. Aggregate shape and surface texture play a part in determining how much strength is lost because of expansion.

Modulus of elasticity of the shrinkage-compensating concrete was always lower than that of the corresponding concrete made with the type V portland cement. The higher the expansion of a concrete is, the lower its modulus.

From the results of this study it is evident that in the design of a shrinkage-compensating concrete mix the selection of aggregate type must be carefully considered. Aggregates that produce low shrinkage in conventional concretes are more suitable for use in shrinkage-compensating concretes than are aggregates responsible for high shrinkage of concretes. In general, aggregates producing low shrinkage concretes include quartz, limestone, dolomite, granite, and some basalts, whereas those producing high shrinkage concretes include sandstone, slate, and some basalts or other aggregates of low rigidity or which shrink considerably by themselves. Should an aggregate be selected that is known to produce concretes of high shrinkage characteristics, an increase in expansive cement content, or the use of a cement of higher expansion potential, needs to be considered. It should be recognized, however, that an increase in expansion will tend to reduce the strength and modulus of elasticity of the concrete. It is therefore essential that the properties of a shrinkage-compensating concrete be fully evaluated employing the aggregate type selected for use in a particular structure or project.

REFERENCES

1. Pegram, R. R. Expansive Cement. 7th Annual Concrete Conf., Utah State Univ., Logan, 1965.
2. Expanding Cement Prevents Roof Cracks. Engineering News-Record, Jan. 16, 1964.
3. Bell, J. N. Expansive Concrete: Concrete's Bright New Star. Concrete Products, June 1964, pp. 28-33.
4. Klein, A., and Troxell, G. E. Studies of Calcium Sulfoaluminate Admixtures for Expansive Cements. Proc. ASTM, Vol. 58, 1958, pp. 986-1008.
5. Mather, B. Investigation of Expanding Cements—Summary of Information Available as of 1 July 1963. U.S. Army Engineer Waterways Experiment Station, Corps of Engineers, Vicksburg, Miss., Tech. Rept. 6-691, Sept. 1965, 59 pp.
6. Li, Shu-T'ien. Expansive Cement Concretes—A Review. Proc. American Concrete Institute, Vol. 62, June 1965, pp. 689-706.
7. Aroni, S., Polivka, M., and Bresler, B. Expansive Cements and Expanding Concrete. Dept. of Civil Eng., Univ. of California, Berkeley, SESM Report 66-7, July 1966, 74 pp.
8. Expansive Cement Concrete—Present State of Knowledge. Being prepared by ACI Committee 223 and to be published by the American Concrete Institute.
9. Polivka, M., and Bertero, V. Factors Affecting Properties of Expanding Concrete. Proc. Internat. Conf. on the Structure of Concrete and Its Behavior Under Load, London, Sept. 1965, Cement and Concrete Assn., London, 1968, pp. 479-492.
10. Carlson, R. W. Drying Shrinkage of Concrete as Affected by Many Factors. Proc. ASTM, Vol. 38, Pt. 11, 1938, pp. 419-437.
11. Pickett, G. Effect of Aggregate on Shrinkage of Concrete and a Hypothesis Concerning Shrinkage. Proc. American Concrete Institute, Vol. 52, Jan. 1966, pp. 581-590.
12. Hansen, T. C., and Nielsen, K. E. C. Influence of Aggregate Properties on Concrete Shrinkage. Proc. American Concrete Institute, Vol. 62, July 1965, pp. 781-794.
13. Mehta, P. K., and Pirtz, D. The Expansive-Cement Component. Proc. Internat. Conf. on the Structure of Concrete and Its Behavior Under Load, London, Sept. 1965, Cement and Concrete Assn., London, 1968, pp. 473-478.

Slow-Cooling Tests for Frost Susceptibility of Pennsylvania Aggregates

JOHN W. HARMAN, JR., PHILIP D. CADY, and NANNA B. BOLLING,
Department of Civil Engineering, Pennsylvania State University

The results of a 2-year study of frost susceptibility of Pennsylvania concrete aggregates by slow cooling are presented. The investigation studied 60 aggregate fractions from 20 sources. Petrographic fractionation and examination, a modification of Powers' slow cooling test, and various "quick" methods were compared. Glacial gravels and gravels of suspected glacial origin had a high incidence of deleterious fractions. Grain size was found to have a very important influence on frost susceptibility. Based on test comparisons, the use of the sodium sulfate soundness test (ASTM C 88) is not recommended. A new method, based on a regime plot of bulk vacuum-saturated specific gravity and vacuum-saturated absorption, is presented.

•MUCH OF THE PROBLEM of frost destruction of concrete was alleviated with the gradual introduction of air entrainment, which provides frost protection for the paste portion of the concrete. However, frost-susceptible aggregates can still cause destruction of concrete. Therefore, considerable research has been carried out in recent years to develop test methods for evaluation of frost susceptibility of concrete aggregates.

Previous work at the Pennsylvania State University (1, 2) included investigation of slow-cooling tests, rapid tests, and basic frost-damage mechanism studies. The test aggregates used in those studies came from all over the United States and were chosen for their known frost-sensitive characteristics and lithology.

The latest studies, sponsored by the Pennsylvania Department of Transportation and the U.S. Bureau of Public Roads, entailed investigation of Pennsylvania aggregates, further evaluation of the slow-cooling test, determination of the frost susceptibility of a wide range of aggregates, investigation of more rapid methods for determination of frost susceptibility, and further study of the basic mechanisms of frost destruction.

BACKGROUND

Powers' Freeze-Thaw Method

In 1955, Powers (3) proposed a test method to evaluate more rationally the effect of frost action on concrete. He reasoned that the rapid freeze-thaw tests (ASTM C 290 and C 291) would overestimate the susceptibility of concrete to frost destruction because high cooling rates would produce excessive hydraulic pressures and because the absence of an extended period of low temperature would cause frost damage from the growth of ice lenses to be underestimated.

The new freeze-thaw method proposed by Powers would cool the specimens from room temperature to 0 F at approximately 5 F per hour, would hold this temperature for an extended time period to permit growth of ice bodies, and would thaw the specimens in water at room temperature. The specimens were to be stored in water at room temperature for 2 weeks between cooling cycles. Dilation (expansion during cooling) would be measured continuously with a suitable strain-measuring apparatus, and the

Paper sponsored by Committee on Mineral Aggregates and presented at the 49th Annual Meeting.

cycles would be repeated until dilation (expansion during cooling) appeared in a specimen. Entrained air would be used to inhibit deleterious action of frost in the paste phase of the concrete.

Previous Applications

Tremper and Spellman (4) used the Powers test in 1961 with only minor modifications. The test was used to select aggregates for 70 miles of concrete pavement. Some of the aggregates would have been rejected by rapid freeze-thaw tests, but have performed satisfactorily in service. The California Division of Highways then adopted a slightly modified Powers test as a standard test procedure.

Wills et al. (5), in 1963, reported a second application of the Powers method, with slight variations.

Larson et al. (1, 2), in a program sponsored by the National Cooperative Highway Research Program, found no evidence of the growth of ice bodies during extended periods of subfreezing temperatures. Concrete made with aggregates having exhibited extremely poor service records were found to perform satisfactorily if a 2-week drying period at 50 percent relative humidity was interposed before the first freezing cycle.

Although Powers had indicated that the number of days of soaking before attainment of a measurable dilation is the period of frost immunity, dilations were observed to occur in all soaked concrete specimens during the first freezing cycle. The dilations in succeeding freezing cycles increased linearly up to a point beyond which they increased exponentially. It was hypothesized that this point was the end of frost resistance, and the point at which the dilation first exceeded the elastic limit of the paste; this hypothesis was supported by the dilation data for 124 specimens.

An ASTM test method based on this work is currently being considered by subcommittee III-o of Committee C-9 of the American Society for Testing Materials. This paper describes the work carried out on the most recent project at The Pennsylvania State University.

SAMPLING AND FRACTIONATION

The aggregate sources were selected after conferences with the district materials engineers of the Pennsylvania Department of Transportation and after review of existing information of that department and of the U.S. Army Corps of Engineers. Slow-cooling tests were run on fractions from 20 sources.

Sources tested in slow cooling included 10 gravels, 6 limestones, and 4 sandstones. Figure 1 shows the geographic locations of the various sources.

Samples were first separated into 2 size groups, $\frac{3}{4}$ to 1 in. and $\frac{1}{2}$ to $\frac{3}{4}$ in., by means of a screen shaker. All materials greater than 1 in. and less than $\frac{1}{2}$ in. in size were discarded. The remaining size groups were then separated by heavy media at a specific gravity of 2.50, after which each of the 4 size and specific gravity units was hand-sorted into rock fractions. Because the gravels were comprised of many varieties of rock, each hand-sorted rock fraction often contained several related (by lithology or estimated deleterious characteristics) rock types. However, fractions from quarries were generally monolithologic.

Slow-Cooling Test Fractions

Each hand-sorted rock fraction of $\frac{3}{4}$ to 1 in. size and its corresponding hand-sorted rock fraction of $\frac{1}{2}$ to $\frac{3}{4}$ in. size were recombined in a 50-50 proportion by weight to make up a single slow-cooling test fraction. A flow diagram explaining the fractionation and recombination procedure is shown in Figure 2.

PETROGRAPHIC ANALYSIS

Immediately after the hand-sorting of the aggregate samples, work began on the petrographic analysis of each of the 60 test fractions. Aggregates were described by using techniques and equipment usually employed in the field, such as rock hammer, hydrochloric acid, and binocular microscope. Properties noted were color, shape,

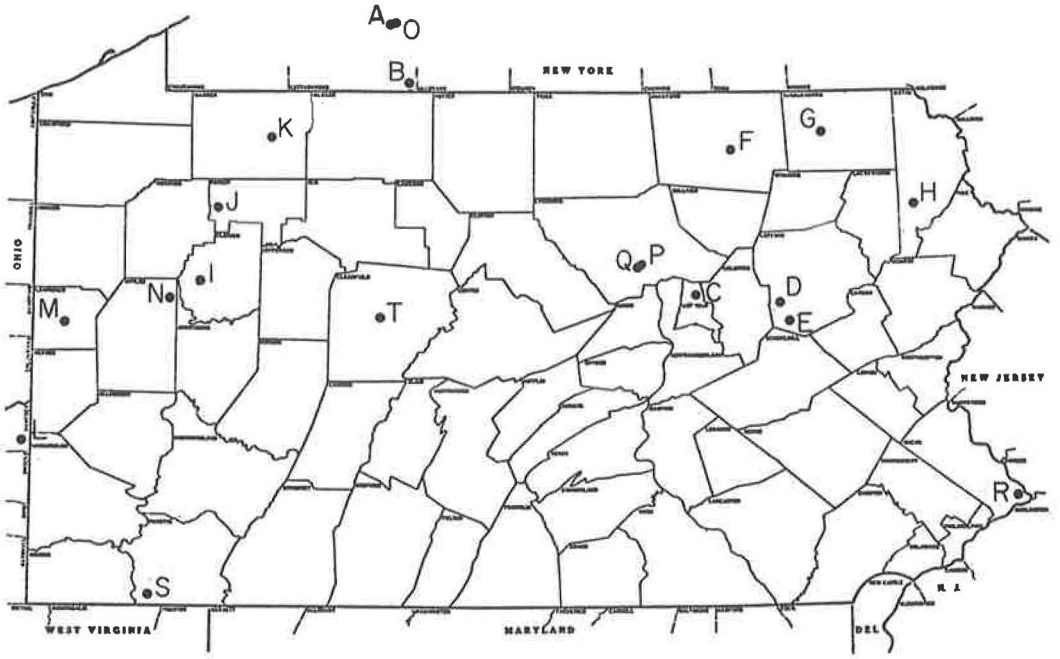

Figure 1. Location of sample sites in Pennsylvania and vicinity.

roundness, condition, surface texture, staining or coating, porosity, toughness, internal texture, and predominant crystal or grain size. The procedure described by Mather and Mather (6) was used as a guide in these descriptions.

Subsequent to the hand specimen study, particles with fine grains or structures and indistinct compositions, or either of these, were thin-sectioned for detailed analysis under the higher power of the petrographic microscope. These transparent sections representing about 75 percent of the fractions were studied with plain and polarized light by using procedures suggested in ASTM C 295-65.

The results of these petrographic studies are too voluminous to present here, but the detailed rock descriptions are given by Larson et al. (7, Appendix A).

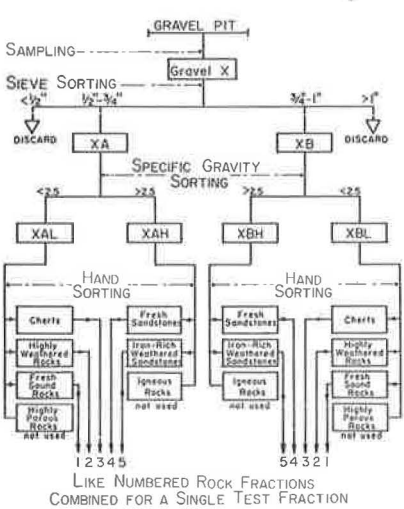

Figure 2. Schematic diagram for sample fractionation.

SPECIMEN PREPARATION

Sampling and fractionation into test fractions of coarse aggregate have previously been described. Each test fraction was the larger half, by weight, of the coarse aggregate phase of its test mixture. The smaller half consisted of equal parts by weight of a No. 4 to $\frac{3}{8}$-in. size and a $\frac{3}{8}$- to $\frac{1}{2}$-in. size of a quartz gravel of known high frost resistance. Thus the test variable was the $\frac{1}{2}$- to 1-in. size of coarse aggregate. According to the critical size concept (8), these larger sizes are the most susceptible to frost action.

A quartz sand of the same source as the quartz gravel was used as fine aggregate. The cement was a Type 1 low-alkali (less than 0.6 percent Na_2O equivalent) cement, all from a single batch. Neutralized vinsol resin was used as an air-entrain' agent.

Mix designs were made for a 6-cylinder batch for each test fraction. Fixed criteria were cement factor, 5½ sacks/cu yd; slump, 3 ± ½ in.; and air content, 6 ± 1 percent.

In order to obtain mixtures as close to job mixtures as possible, ACI 613-54 was the method of design for all mixtures.

The coarse aggregate was vacuum saturated, then brought to a saturated surface-dry condition immediately before mixing, while both mixing water and fine aggregate were compensated for moisture in the fine aggregate. Air content was checked with a Chace meter because of the small batch quantities involved.

For each test fraction, 6 cylinders, 3 in. in diameter by 6 in. long, were cast by placing the concrete in lightly oiled molds in 2 layers, each rodded 25 times with a rounded ¼-in. tamping rod. Stainless steel gage studs with rounded ends were cast in both ends of the cylinders.

After they were cast, the specimens were immediately placed in a moist-curing room at 70 F for 24 hours, molds were removed, and the specimens were placed in a lime-water bath at 70 F for 13 days. They were then conditioned in a 35 F constant temperature clear-water bath for 21 days. This low temperature virtually stopped cement hydration at the 14-day point.

TEST METHOD

Two general test methods were used: Half of the specimens (three from each test fraction) were fully instrumented for dilation, or length change measurement on each slow-cooling cycle, while the other half (the remaining three from each fraction) were instrumented only on the last cycle. Although the first procedure has the advantage of providing enough data for the prediction of the period of frost immunity, it cannot accommodate as many specimens. The second procedure only tells what the dilation is at the end of the testing period, but many more test specimens can be accommodated.

The Test Cycle

During each test cycle, the specimens were cooled from 35 to 15 F over a period of 4 hours, at a rate of 5 F per hour. They were then immediately placed in the 35 F constant temperature bath, where they were stored until the next cycle 14 days later. This procedure was repeated for 12 cooling cycles.

Measured Variables

Recording equipment continuously monitored the length changes of 6 test specimens (3 specimens from each of 2 test fractions) during each cooling cycle. A second recorder monitored the cooling bath temperature. The time scales of the 2 recorders were identical, and the records were matched to relate length changes with temperatures. Figure 3 shows the typical recorder outputs, together with the techniques for measuring length change and temperature.

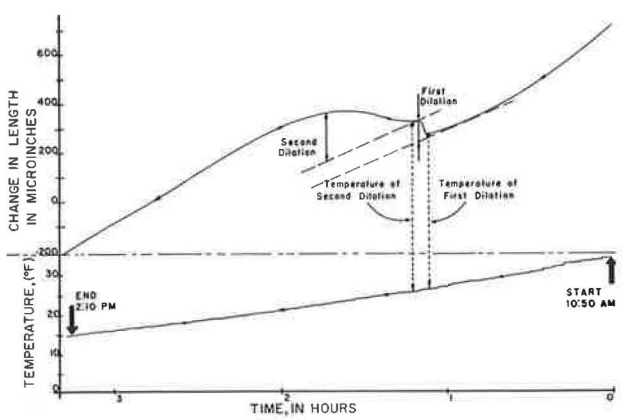

Figure 3. Typical recorder outputs for length and temperature measurement.

EQUIPMENT

Conditioning and Storing

The 35 F constant temperature bath, in which the specimens were conditioned prior to the first cycle and in which they were stored between subsequent cycles, is shown in Figure 4. A

Figure 4. Constant temperature bath.

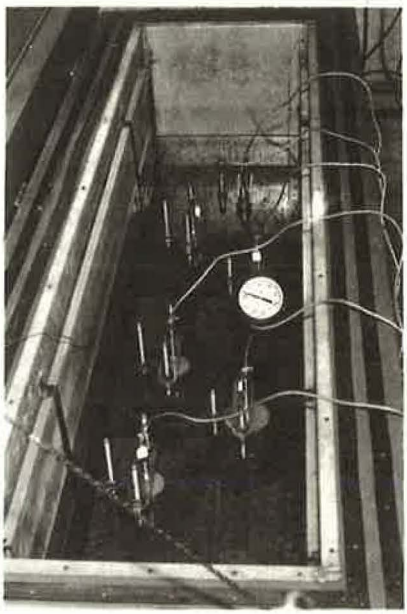

Figure 5. Slow-cooling bath.

thermostatic system working through a solenoid valve in the refrigerant line controlled temperature within ±2 F, and the bath temperature was monitored by means of a gas bulb-type thermometer.

Slow Cooling

Slow-cooling cycles were carried out in a refrigerated kerosene bath with thermostatic equipment similar to that of the constant temperature bath. Kerosene was used because of its relative immiscibility with water, its heat conductance, and its economy. Brine-filled plates at the sides of the tank cooled the kerosene, and propellor-type mixers circulated the fluid. During the first year's testing, temperature was controlled by means of a valve on the refrigerant return line. However, electric immersion heaters and a temperature controller and programmer were installed before the second year's testing. In this manner, constant refrigeration was used, and gradual temperature reduction was achieved by diminishing the heat input to the heating elements at a uniform rate. Figure 5 shows the slow-cooling bath.

Measuring and Recording

A copper-constantan thermocouple, placed in the bath and connected to a recording potentiometer, provided a constant record of bath temperature.

Each test specimen was placed in a strain frame, composed of a brass bottom plate and yoke and Invar steel rods. This mounting method is shown in Figure 6. Length change during cooling was measured by means of a linear variable differential transformer (LVDT), commonly called a transducer, mounted in the yoke of the strain frame. Although not shown in Figure 6, a short piece of $^{3}/_{8}$-in. plastic tubing was inserted between the top of the cylinder and its brass centering strip to keep the specimen from rotating.

As shown in the schematic function diagram in Figure 7, the 6 transducers signaled output (length) to a switching mechanism, which in turn transmitted these signals one at a time to the amplifier indicator. The length was then recorded by a 6-channel recorder, also controlled by the switching mechanism. An interval timer permitted 2 recording cycles every 5 minutes. The mounting of all of this equipment is shown in Figure 8.

EXPERIMENTAL RESULTS

Twelve freezing cycles were run on the 60 test fractions. Although only half of the specimens were instrumented during the first 11 cycles, all of the specimens were instrumented during the final twelfth cycle. Treatment of all specimens was exactly the same during testing and storage.

Table 1 gives a summary of the available information on the test aggregates that existed before this investigation and includes specific gravity and absorption from records of the Pennsylvania Department of Transportation and the U.S. Army Corps of Engineers, petrographic estimates of frost susceptibility, magnesium sulfate soundness, Los Angeles abrasion, and rapid freeze-thaw durability factor from the Corps of Engineers.

The results of the slow-cooling tests are given in Table 2. During the second year's testing, the Pennsylvania Department of Transportation cooperated by testing 51 of the 60 fractions in the sodium sulfate soundness test (ASTM C 88). The results of these tests are given in Table 3 along with summaries of the slow-cooling test results, vacuum-saturated surface-dry specific gravity, and vacuum-saturated absorption information for all fractions.

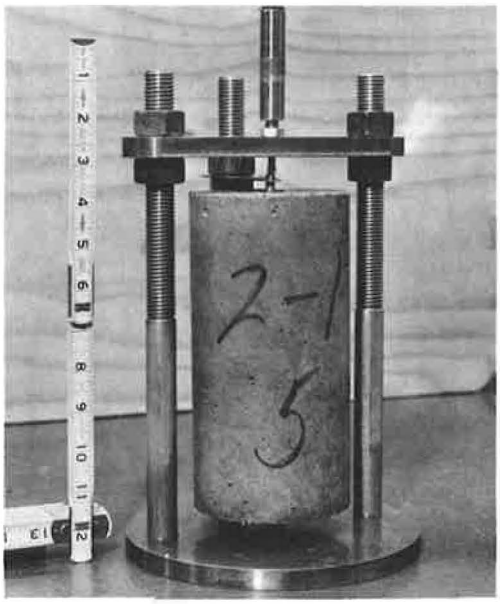

Figure 6. Specimen and LVDT mounted in strain frame.

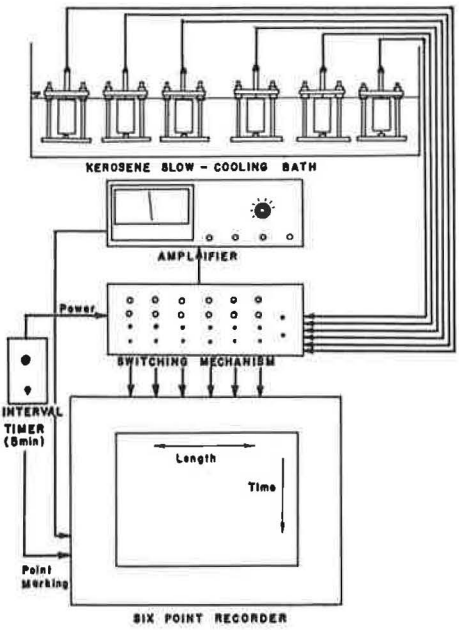

Figure 7. Functioning of dilation recording instrumentation.

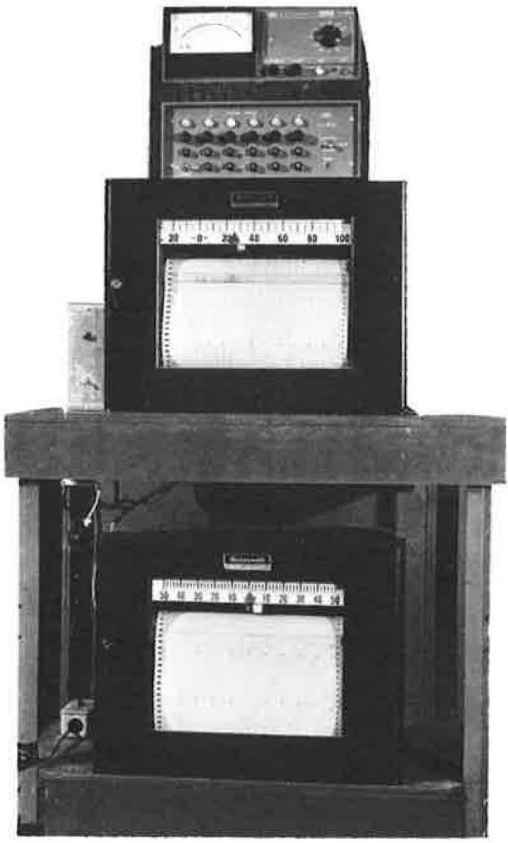

Figure 8. Length change and temperature instrumentation.

Comparisons

Sodium sulfate soundness loss for each of the 2 size ranges of each test fraction are plotted against mean twelfth cycle dilations and are shown in Figure 9. There is no correlation: Twenty-seven fractions would have been accepted by the sodium sulfate test and failed in slow cooling; 3 fractions passing in slow cooling would have been rejected by the sodium sulfate test.

Both vacuum-saturated surface-dry specific gravity versus mean twelfth cycle dilation and vacuum-saturated absorption versus dilation were compared in an attempt to find a "quick" test for frost susceptibility. Correlation coefficients were -0.254 and +0.540 respectively, and their plots are shown in Figures 10 and 11. Neither parameter was considered to be acceptable as a quick test for control purposes, but a combination of the 2 parameters into a regime plot, as shown in Figure 12, shows considerable promise as a rapid test procedure for control purposes. Although 2 anomalies appear in

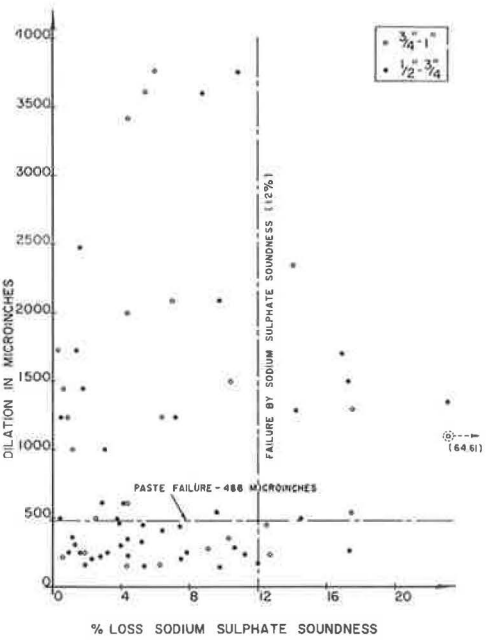

Figure 9. Comparison of slow-cooling dilation and sodium sulfate soundness.

TABLE 1

SUMMARY OF EXISTING LABORATORY TEST DATA REGARDING THE AGGREGATE SOURCES

Pennsylvania Department of Transportation			U.S. Army Corps of Engineers					
Site	Specific Gravity	Absorption	Petrographic Estimate	Specific Gravity	Absorption	Magnesium Sulfate Soundness	Los Angeles Abrasion	Durability Factor DFE/300
A	2.61	1.15	20 percent fair 1 percent poor	2.61	1.8	1.0	4.0	62
B	2.52	2.42						
C	2.68	0.76		2.69	0.8	1.9	26.0	57
				2.68	0.9	2.9	22.3	85
D	2.65	0.90						
E								
F	2.63	1.18						
	2.61	1.69						
G	2.68	1.25						
H	2.70	0.51		2.67	1.1	2.9	22.8	85
I	2.69	0.52	16 percent fair 0 percent poor	2.69	0.5	0.9	24.0	75
J	2.56	1.96	3 percent fair	2.54	2.8	7.3	28.1	52
	2.59	1.44	10 percent poor					
K	2.58	1.58	13.5 percent fair 13.2 percent poor 26 percent <2.5 sp gr	2.55	2.6	5.2	28.4	76
L	2.57	1.48	36 percent poor	2.53	2.6	3.0	37.4	76
M	2.70	0.18		2.70	0.6	3.3	23.0	79
N	2.69	0.32						
O	2.51	2.58						
P								
Q								
R	2.62	0.98	88 percent good 4 percent fair 8 percent poor	2.18 2.61	6.0 1.0	0.6	32.0	83
S	2.67	0.37	3 percent soft Shaley SS	2.69	0.8	13.5	21.0	72
T								

TABLE 2

SLOW-COOLING TEST RESULTS

Fraction	Cycles to Failure[a]			Twelfth Cycle Dilation[b]						Mean Dilation (μin.)	Best Estimate of Standard Deviation
				Instrumented on Each Cycle[c]			Instrumented on Last Cycle Only				
A-1	9	NF	NF	530	220	330	340	190	180	298	121
B-1	1	2	3	4,210	2,960	2,320	4,320	3,500	1,940	3,208	893
C-1	10	10	10	310	340	320	660	460	880	495	210
C-2	NF	NF	NF	220	120	200	250	100	260	192	67
D-1	12	12	12	820	700	550	680	460	440	608	137
D-2	NF	NF	NF	240	130	180	220	200	260	205	42
D-3	4	3	3	1,080	770	5,760	1,200	1,570	2,120	2,083	1,698
E-1	12	NF	NF	530	290	390	210	330	370	353	98
E-2	NF	NF	NF	320	160	440	130	250	180	247	107
E-3	NF	NF	NF	430	200	260	220	210	170	248	85
F-1	3	3	4	1,270	1,570	1,500	2,320	1,550	2,280	1,748	402
F-2	3	6	3	1,600	640	1,820	1,220	1,130	2,000	1,401	458
F-3	NF	NF	NF	170	240	400	200	170	160	223	91
F-4	NF	NF	NF	240	340	410	150	90	240	245	118
G-1	NF	NF	NF	140	350	230	170	260	360	251	83
H-1	NF	NF	NF	180	110	170	130	210	140	157	33
H-2	10	NF	NF	750	270	310	260	550	140	380	206
H-3	NF	NF	NF	250	260	240	340	210	200	250	45
H-4	NF	12	NF	180	500	380	0	240	160	243	176
I-1	NF	NF	NF	230	350	240	140	130	360	215	90
I-2	NF	11	NF	130	480	170	300	710	310	350	196
I-3	NF	NF	NF	240	400	220	170	130	200	227	85
I-4	NF	NF	NF	320	150	140	100	140	140	165	71
I-5	12	12	NF	660	500	230	520	380	950	540	226
I-6	NF	NF	NF	330	300	180	680	870	330	448	243
J-1	10	8	11	EP	EP	EP	1,560	2,060	1,400	1,673	344
J-2	6	6	4	EP	EP	EP	750	1,240	1,760	1,250	505
J-3	3	2	3	2,000	2,800	1,340	330	1,420	960	1,475	778
K-1	3	3	3	1,400	1,940	4,380	1,270	1,460	1,540	1,995	1,099
K-2	4	6	5	1,320	820	1,480	2,160	1,620	1,350	1,458	399
K-3	3	1	2	1,400	4,180	2,960	1,960	2,040	1,480	2,337	1,061
K-4	7	7	7	400	380	400	640	500	420	457	99
L-1	NF	NF	NF	390	360	360	410	370	640	422	109
L-2	3	1	2	1,920	3,200	2,260	1,900	3,880	1,720	2,480	867
L-3	3	2	2	870	1,920	2,900	1,060	2,000	1,450	1,700	740
M-1	NF	NF	NF	300	260	130	140	120	160	185	76
M-2	NF	NF	NF	220	130	120	140	300	100	168	76
N-1	NF	NF	NF	80	170	230	80	150	320	171	84
N-2	NF	NF	NF	300	210	300	190	340	460	300	89
N-3	NF	11	11	360	330	240	510	360	210	335	97
O-1	11	NF	11	430	260	370	200	220	370	308	86
O-2	11	10	11	430	330	200	150	380	220	285	101
O-3	3	2	4	3,410	2,260	4,600	EP	EP	EP	3,423	955
O-4	9	6	5	1,010	1,820	1,760	860	730	EP	1,236	461
O-5	2	4	2	3,880	2,760	5,320	3,200	3,150	4,330	3,773	862
P-1	9	10	9	660	550	530	1,050	1,320	1,440	925	366
P-2	9	6	10	540	760	540	1,250	1,680	1,250	1,003	422
P-3	5	6	8	1,370	1,560	990	EP	EP	EP	1,307	237
P-4	4	4	3	1,290	1,760	1,460	EP	EP	EP	1,510	193
P-5	5	11	4	760	610	4,230	980	970	520	1,345	1,301
P-6	1	2	2	2,060	3,980	2,870	4,980	4,290	3,500	3,613	952
Q-1	NF	NF	NF	160	120	220	90	650	100	223	196
Q-2	12	12	NF	500	540	430	520	480	470	490	36
R-1	10	10	10	600	720	530	670	250	910	613	201
R-2	9	10	11	450	EP	550	200	940	330	494	252
R-3	7	5	7	1,880	1,780	1,880	770	320	750	1,230	635
S-1	NF	NF	NF	140	190	240	160	160	120	168	38
S-2	NF	11	NF	340	640	230	120	320	170	303	169
T-1	5	7	7	980	240	1,530	1,080	920	1,820	1,095	498
T-2	7	7	7	220	1,330	1,600	880	1,340	1,010	1,063	486

[a]Cylinders instrumented on each cycle; NF = no failure during the 12 cycles. [b]All 6 cylinders. [c]EP = equipment problem.

TABLE 3

SLOW-COOLING TEST RESULTS COMPARED TO VACUUM-SATURATED SURFACE-DRY SPECIFIC GRAVITY, VACUUM-SATURATED ABSORPTION, AND SODIUM SULFATE SOUNDNESS TEST RESULTS

Fraction	Bulk-Saturated Surface-Dry Specific Gravity Group	Weight Percent Total	Vacuum-Saturated Surface-Dry Specific Gravity		Vacuum-Saturated Absorption		Mean Dilation (μin.)	Best Estimate of Standard Deviation	Sodium Sulfate Soundness	
		½ to 1 in.	¾ to 1 in.	½ to ¾ in.	¾ to 1 in.	½ to ¾ in.			¾ to 1 in.	½ to ¾ in.
A-1	>2.5	23.5	2.65	2.66	0.49	0.44	298	121		1.37
B-1	<2.5	17.9	2.42	2.55	2.63	2.81	3,208	893		
C-1	>2.5	34.8	2.49	2.60	0.00	0.16	495	210		3.86
C-2	>2.5	19.8	2.83	2.74	0.80	1.44	192	67		2.31
D-1	>2.5	20.2	2.67	2.62	0.40	0.91	608	137	5.56	2.99
D-2	>2.5	13.0	2.71	2.70	0.46	0.44	205	42		
D-3	<2.5	22.4	2.54	2.55	0.96	1.52	2,083	1,698	7.00	9.81
E-1	>2.5	27.7	2.69	2.71	0.54	0.49	353	98		1.25
E-2	>2.5	24.4	2.74	2.74	0.38	0.64	247	107		3.24
E-3	>2.5	18.7	2.76	2.75	1.10	1.00	248	85		17.46
F-1	<2.5	8.9	2.48	2.52	1.97	3.40	1,748	402	0.40	1.50
F-2	<2.5	10.1	2.56	2.50	3.60	4.31	1,401	458		
F-3	>2.5	12.3	2.67	2.67	0.99	1.01	223	91	0.63	2.87
F-4	>2.5	8.3	None	2.68	None	0.85	245	118		1.61
G-1	>2.5	42.1	2.65	2.66	2.02	1.53	251	83		7.87
H-1	>2.5	38.9	2.67	2.64	0.40	1.03	157	33		
H-2	>2.5	11.3	2.74	2.67	0.75	2.23	380	206		
H-3	>2.5	32.1	2.66	2.61	0.97	0.55	250	45	2.05	1.05
H-4	>2.5	14.0	2.74	2.74	0.67	0.85	243	176		11.47
I-1	>2.5	8.9	2.70	2.66	0.32	0.66	215	90		7.71
I-2	>2.5	10.8	2.69	2.69	0.60	0.79	350	196	10.43	4.85
I-3	>2.5	14.1	2.70	2.71	0.50	0.46	227	85		4.48
I-4	>2.5	10.6	2.65	2.71	0.52	0.43	165	71		9.70
I-5	>2.5	8.3	2.66	2.69	0.85	1.34	540	226	17.57	9.66
I-6	>2.5	8.1	2.71	2.69	0.49	0.57	448	243	12.50	7.53
J-1	<2.5	21.4	2.58	2.58	2.61	2.66	1,673	344		5.22
J-2	<2.5	34.9	2.55	2.56	3.13	3.20	1,250	505		7.33
J-3	<2.5	10.4	2.59	2.47	2.03	5.06	1,475	778		3.95
K-1	<2.5	24.1	2.57	2.58	3.11	2.61	1,995	1,099	4.42	
K-2	<2.5	31.8	2.54	2.55	3.40	3.30	1,458	399	0.71	1.85
K-3	<2.5	15.8	2.46	2.47	5.86	5.31	2,337	1,061	14.81	
K-4	>2.5	14.3	2.64	2.69	0.71	0.90	457	99		5.30
L-1	<2.5	16.2	2.58	2.56	1.96	2.54	422	109		6.46
L-2	<2.5	15.8	2.60	2.69	1.25	0.90	2,480	867		1.72
L-3	<2.5	18.5	2.54	2.51	3.34	4.18	1,700	740		17.02
M-1	>2.5	24.3	2.70	2.71	0.52	0.46	185	76		12.00
M-2	>2.5	26.7	2.71	2.72	0.46	0.45	168	76	4.42	5.44
N-1	>2.5	15.4	2.70	2.71	0.39	0.44	171	84	6.36	2.13
N-2	>2.5	23.1	2.72	2.71	0.27	0.39	300	89		3.97
N-3	>2.5	15.7	2.69	2.69	0.64	0.65	335	97		5.25
O-1	<2.5	5.0	2.25	2.23	7.57	8.13	308	86		
O-2	<2.5	9.0	2.37	2.33	4.65	5.07	285	101	9.56	10.61
O-3	<2.5	21.4	2.13	2.49	4.48	4.51	3,423	955	4.48	
O-4	>2.5	28.8	2.60	2.59	1.98	2.23	1,236	461	6.57	
O-5	<2.5	6.6	2.46	2.40	0.58	0.82	3,773	862	5.98	11.08
P-1	>2.5	27.5	2.62	2.62	2.28	2.23	925	366		
P-2	>2.5	13.2	2.62	2.63	2.63	2.16	1,003	422	1.24	3.11
P-3	>2.5	8.8	2.61	2.64	2.01	1.59	1,307	237	17.65	14.21
P-4	>2.5	10.0	2.59	2.60	1.94	1.91	1,510	193	10.59	17.43
P-5	>2.5	11.9	2.51	2.53	2.28	2.04	1,345	1,301	19.43	
P-6	<2.5	10.2	2.47	2.50	5.04	4.19	3,613	952	5.48	6.88
Q-1	>2.5	27.0	2.71	2.65	0.43	1.28	223	196	14.75	
Q-2	>2.5	18.7	2.65	2.66	1.09	0.87	490	36	2.68	14.57
R-1	>2.5	14.2	2.62	2.63	0.50	1.06	613	201		4.23
R-2	>2.5	6.9	2.64	2.62	0.64	0.64	494	252		0.50
R-3	>2.5	9.8	2.69	2.66	1.36	1.59	1,230	635	1.00	0.62
S-1	>2.5	57.0	2.70	2.70	0.27	1.37	168	36		
S-2	>2.5	29.5	2.70	2.70	0.67	0.76	303	169		
T-1	>2.5	41.8	2.58	2.60	3.10	2.60	1,095	498	64.61	
T-2	>2.5	33.1	2.60	2.59	1.83	1.86	1,063	486	12.00	

the regime plot, in which fractions with low specific gravities and high absorptions passed in slow cooling but appear in the "bad" area of the chart, both of these fractions, 0-1 and 0-2, contain very large pores. These pores probably prevented high hydraulic pressures during freezing and reduced expected dilations of the specimens. Further refinements of this regime plot are anticipated as increased data become available.

Prediction of Total Sample Behavior

The sample from Source P, of which 6 fractions were tested, was used in an experiment to determine if the frost susceptibility of a complete sample could be predicted from the slow-cooling results of its fractions. Three specimens, each 6 in. in diameter by 12 in. long, using the gravel as processed at the source were cast. Curing, conditioning, storage, and slow-cooling tests (6 cycles) were performed on these cylinders in exactly the same manner as the test fractions.

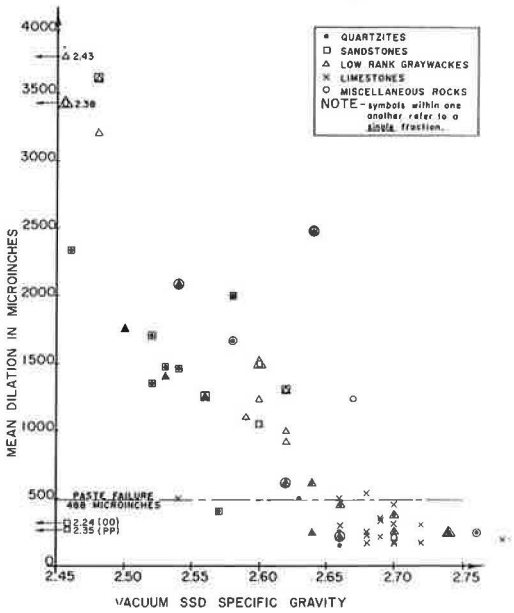

Figure 10. Comparison of average dilation and lithology of test fractions to specific gravity.

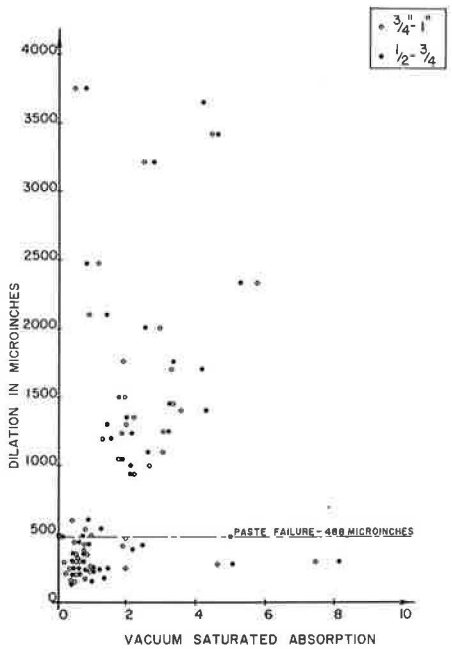

Figure 11. Comparison of slow-cooling dilation to vacuum-saturated absorption.

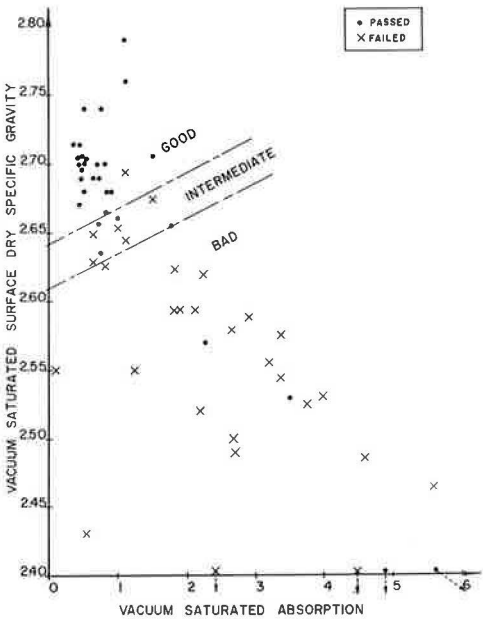

Figure 12. Frost resistance by vacuum-saturated absorption and bulk vacuum-saturated surface-dry specific gravity.

Table 4 gives an analysis of the fractions, with corrections for sample size and the 32.6 percent of the fractions that were not tested. This analysis gives the anticipated dilation per inch of specimen length. The 2 values were 83 μin./in. for the actual test on the total sample aggregate and 121.4 μin./in. predicted from the test fractions. Although the predicted value is somewhat higher than that of the actual test on the total sample, it must be remembered that only 67 percent of the sample was used in the prediction. From this difference it can be seen that the untested portion of the gravel would very likely have exhibited a considerably lower dilation than the other fractions (it is assumed to be the same in these calculations). The untested portion consisted largely of more resistant sandstones, confirming this indication of lower dilation.

TABLE 4

COMPARISON OF DILATIONS OF FRACTIONS WITH TOTAL DILATIONS

Fraction	Mean Sixth Cycle Dilation (μin.)	Decimal Portion of Total Gravel	Product (μin.)
UU	433.3	0.226	97.9
VV	426.7	0.109	46.5
YY	566.7	0.074	41.9
ZZ	733.3	0.083	60.9
AAA	506.7	0.098	49.6
BBB	2,310.0	0.084	194.0
Total		0.674	409.9

Note: Predicted sixth cycle dilation corrected for amount of sample not tested: 490.9/0.674 = 728.4 μin.; 728.4 μin./6 in. (length of fraction cylinders) = 121.4 μin./in. predicted sixth cycle dilation. Mean actual total sample dilation: 996.6 μin.; 996.6 μin./12 in. (length of total gravel cylinders) = 83.0 μin./in.

This method of prediction should be tested further, and all or nearly all the fractionated materials should be used as a basis for the predicted dilation.

Failure Criterion

Larson et al. (2) developed the following mathematical model to determine the critical dilation:

$$D_c = (L/E)\ (1 - 2\mu)\ f_t$$

where

E = modulus of elasticity,
f_t = tensile strength of the paste, and
μ = Poisson's ratio.

Six mortar specimens were made by using the same cement, water, and fine aggregate ratios as a composite of the 60 test fractions and received identical curing and conditioning. The mean values were substituted for the elastic constants, and the critical dilation was found to be 488 μin. This is interpreted as the dilation at which the elastic limit of the paste phase is reached and represents the point of incipient failure. This figure agrees well with the value of 421 μin. determined empirically by Larson et al. (2) by analysis of many dilation versus freeze-thaw cycle plots.

DISCUSSION AND CONCLUSIONS

General Observations

Aggregate fractions from 12 of the 20 aggregate sources tested are considered deleterious in that their freeze-thaw characteristics are such that paste failure occurs in 12 cycles or less. Nine of the failing sources are glacial gravels or river gravels suspected to be of glacial origin. This observation is not unexpected because gravels of glacial origin vary more widely in lithology, increasing the chance of the presence of frost deleterious materials. Generally the service record of these glacial gravels has been less satisfactory than that of quarried stones in Pennsylvania. Unfortunately, in the northern part of the state, where the glacial gravels are found, there is little ledge rock suitable for concrete aggregate.

Rapid Control Test Procedures

Based on the results of this investigation, the use of the sodium sulfate soundness test is not recommended. As shown in Figure 9, sodium sulfate soundness does not indicate frost susceptibility of coarse aggregates in concrete.

The use of the regime plot (Fig. 12) shows great promise. This method can be used as a preliminary acceptance test, and aggregates that are on the borderline or in the intermediate area can be tested by the slow-cooling method.

Lithology and Frost Resistance

Although lithologies were somewhat mixed in many of the test fractions, enough data were obtained to list basic lithologies in their order of increasing soundness as follows:

1. Chert;
2. Fine-grained, low-rank graywacke;
3. Fine-grained quartzite;
4. Argillite, siltstone, and medium- and coarse-grained, low-rank graywacke;
5. Sandstone and limestone; and
6. Medium- and coarse-grained quartzite.

Because graywackes and sandstones differ greatly in frost resistance and most engineers tend to consider graywackes as sandstones, and because fine-grained and medium- and coarse-grained quartzites also differ greatly in frost resistance, analysis by a trained petrographer is even more important than was previously thought.

With the exception of grain size, rock characteristics such as weathering and toughness, originally thought to be at least as important as rock type, were surprisingly uninfluential on frost resistance. Larson et al. (7) further discuss the relationship of rock lithologies to frost sensitivities as studied during this project.

ACKNOWLEDGMENT

This research was carried out under the auspices of the Pennsylvania Department of Transportation and the U.S. Bureau of Public Roads, Federal Highway Administration, Department of Transportation. The opinions expressed, however, are solely those of the authors and may not necessarily be shared by the Department of Transportation or the Bureau of Public Roads.

REFERENCES

1. Larson, T. D., Boettcher, A., Cady, P. D., Franzen, M., and Reed, J. R. Identification of Concrete Aggregates Exhibiting Frost Susceptibility. NCHRP Rept. 15, 1965.
2. Larson, T. D., and Cady, P. D. Identification of Frost-Susceptible Particles in Concrete Aggregates. NCHRP Rept. 66, 1969.
3. Powers, T. C. Basic Considerations Pertaining to Freezing and Thawing Tests. Proc. ASTM, Vol. 55, 1955, pp. 1132-1155.
4. Tremper, B., and Spellman, D. L. Tests for Freeze-Thaw Durability of Concrete Aggregates. HRB Bull. 305, 1961, pp. 28-50.
5. Wills, M. H., Lepper, H. A., Jr., Gaynor, R. D., and Walker, S. Volume Change as a Measure of Freezing-and-Thawing Resistance of Concrete Made With Different Aggregates. Proc. ASTM, Vol. 63, 1963, pp. 949-965.
6. Mather, K., and Mather, B. Method of Petrographic Examination of Aggregates for Concrete. Proc. ASTM, Vol. 50, 1950, pp. 1288-1313.
7. Larson, T. D., Cady, P. D., Harman, J. W., Browne, F. P., Stewart, N. B., and Bakr, T. A. Methods for Aggregate Evaluation, Durability Studies of Structural and Paving Concretes. Dept. of Civil Eng., Pennsylvania State Univ., 1969.
8. Verbeck, G., and Landgren, R. Influence of Physical Characteristics of Aggregates of Frost Resistance of Concrete. Proc. ASTM, Vol. 60, 1960, pp. 1063-1079.

Chlorides and Bridge Deck Deterioration

DONALD L. SPELLMAN and RICHARD F. STRATFULL,
Materials and Research Department, California Division of Highways

As a result of a recent bridge deck study and other related work, a mathematical expression was derived that describes the distribution of chloride in concrete as related to depth below the surface in bridge deck concrete. The validity of the expression is supported by a similar distribution of salt found in piles submerged in bay water. Data are given showing that the distribution of chloride in concrete is highly variable, and attention must be given to the number of samples when determining the average chloride content. Steel was removed from 1 bridge deck, and corrosion loss was measured. Although not structurally significant, the corrosion that had occurred was more than necessary to cause extensive cracking of the concrete. It was concluded that deck deterioration due to corrosion of the steel could be effectively prevented in new structures by the use of a noncorrosive de-icing agent, or the use of an effective sealing membrane to prevent salt intrusion. A membrane placed on a high chloride-contaminated deck is likely to accelerate corrosion. Half-cell potential measurements were made on sections of 2 bridge decks. They show that corrosion activity of the steel can be nondestructively detected by electrical measurements.

•IN COOPERATION with the U. S. Bureau of Public Roads, the California Division of Highways has been continuing its studies of the causes of corrosion of steel embedded in concrete (1, 2, 3, 4, 5, 6). This report is a phase of the current study to determine the level of chlorides in concrete that can cause corrosion of reinforcing steel.

As a result of an inspection made during 1960, it was considered that the most significant trouble observed at that time was that bridge substructures in contact with environments containing high chloride had corrosion of the reinforcing (4). A study of bridge decks made in cooperation with the Bureau of Public Roads and the Portland Cement Association during the spring of 1962 revealed that only 1 out of a group of 21 California bridge decks selected for study was reported to have corrosion of the embedded steel (7).

Because of the lack of a history of significant number of bridge deck deterioration problems prior to about 1962, it has been assumed that a major contributor to the recently observed deck deterioration has been the accelerated statewide use of de-icing salts that started about 1960. This observation is supported by the fact that in 1955 the Division of Highways was just experimenting with salt and, by 1960, 3,000 tons of salt were used in the sanding and snow-removal operation. By 1968, the use of de-icing salts had become so widespread that the estimated average tonnage being applied to California highways was about 10,000 tons per year.

During the summer of 1969, 3 construction contracts were advertised for the repair and resurfacing of 31 bridge decks. The contract bid price for the 31 bridges was about $777,000, or about $25,000 per bridge deck, or an average cost of $2.58/sq ft for the entire 300,673 sq ft of bridge decks. However, this price does not include the cost of concrete removal. It should be noted that most of these bridges are less than 10 years

Paper sponsored by Committee on Effect of Ice Control and presented at the 49th Annual Meeting.

old, and this further amplifies the role of de-icing salts as a primary cause of deterioration. Because corrosion of the deck steel has been relatively recently observed, it was decided to determine if de-icing salts are in fact penetrating the concrete and, if so, to determine the distribution and quantity of salts that are present. It is also interesting to note that 4 of the 21 bridges (7) referred to previously as having no significant signs of corrosion are included in the recent repair contracts. Repair measures were apparently not required or considered necessary at the time of that study in 1962. This illustrates that the rate of deterioration can be rapid.

GENERAL CONSTRUCTION OF CALIFORNIA BRIDGE DECKS

In general, the thickness of concrete covering over the top mat of reinforcing has been specified to be a minimum of 1½ in. in freeze-thaw areas. However, depending on the economics of bridge design and the geographic location of the bridge, the specified cover over the reinforcing has ranged from 1 to 2 in. in thickness.

Starting in about 1960, the concrete cover over bridge deck steel has been specified as 2 in. in freeze-thaw areas, and 1½ in. minimum in other areas.

As an indication of the good construction practice in California, for the 21 bridges that were investigated in the cooperative study (7), the average specified minimum cover was 1.28 in. and the actual measured minimum cover was 1.25 in. for 19 comparative measurements.

Normally, the bridge decks have been constructed of concrete having 6 sacks (94 lb each) of cement per cu yd, and a water-cement ratio of about 5 to 6 gal per sack of cement. The range of the reported water-cement ratio was 4.6 to 6.2 gal per sack of cement (7).

Beginning in about 1960, some concrete bridge decks in freeze-thaw areas had a specified minimum cement factor of 7 sacks/cu yd.

AVERAGE DISTRIBUTION OF CHLORIDES IN CONCRETE

During the spring of 1969, 16 bridge decks were sampled by obtaining 4-in. diameter cores. The number of cores obtained from each deck varied from 6 to 22. The purpose of this range in number of cores was to determine the salt content and the minimum number of cores that were necessary for some specified degree of confidence in the test results.

Because the roadway as well as bridge decks are salted in the mountainous areas of California, an exact determination cannot be made of the precise amount of salt that comes in contact with the decks. However, bridges 1 through 9 and 12 through 14 (Table 1) are on roadway sections of about 30 miles in length that receive an average of 50 tons of salt per year. These structures received an estimated 0.2 lb of salt per

TABLE 1

DISTRIBUTION OF CHLORIDES IN CALIFORNIA BRIDGE DECKS

Bridge	No. of Cores	n	Calculated Chloride Content (lb/cu yd) at Depth Below Surface											
			1 in.		2 in.		3 in.		4 in.		5 in.		6 in.	
			Mean	Standard Deviation	Mean	Standard Deviation	Mean	Standard Deviation	Mean	Standard Deviation	Mean	Standard Deviation	Mean	Standard Deviation
1-273	6	28	4.58	1.89	2.15	1.05	0.91	0.48	0.48	0.18	0.44	0.09		
2-266	6	29	3.85	1.92	2.31	1.67	0.85	0.65	0.49	0.25	0.45	0.03		
3-6119	6	25	4.42	1.54	2.72	2.31	0.85	0.40	0.40	0.13	0.40	0.00		
4-6117	6	24	7.47	1.80	2.65	0.76	1.12	0.34	0.63	0.24	0.40	0.00		
5-695	20	86	4.53	1.56	2.08	1.45	0.75	0.85	0.26	0.16	0.26	0.06	0.20	0.00
6-202	19	107	7.84	1.94	0.85	0.31	0.25	0.06	0.23	0.06	0.23	0.09	0.28	0.11
7-289	6	31	5.25	2.93	3.61	2.60	1.21	0.75	0.55	0.18	0.46	0.03	0.64	0.00
8-265	6	29	4.15	1.61	1.45	0.47	0.64	0.25	0.43	0.04	0.45	0.02		
9-6116	22	104	5.73	1.82	2.47	1.02	0.86	0.38	0.33	0.31	0.36	0.32	0.18	0.02
10-2515	7	31	1.79	1.30	1.87	1.88	1.06	0.93	0.86	0.58	0.81	0.41		
11-513	11	46	8.32	2.60	3.47	2.68	1.82	1.92	0.63	0.42	0.42	0.02	0.50	0.03
12-6112	6	30	5.81	1.39	2.44	0.35	0.74	0.21	0.41	0.02	0.42	0.02	0.44	0.00
13-244	21	94	3.58	0.96	1.50	0.80	0.43	0.24	0.32	0.06	0.41	0.05		
14-278	6	26	5.63	1.61	2.68	0.90	0.87	0.22	0.53	0.09	0.46	0.03		
15	19	81	12.5	3.76	4.77	2.72	1.07	1.23	0.464	0.248	0.394	0.139		
16	20	84	10.4	4.25	4.58	2.27	1.68	1.45	0.821	0.807	0.504	0.619		

year per sq ft of area. Bridges 15 and 16 are in salt areas in which the roadway and bridge decks receive an average of 1,000 tons of salt per year. Based on the square footage of application, it is estimated that bridges 15 and 16 have about 1 lb of salt applied per sq ft of deck surface per year.

The average chloride content for each of the 16 bridges that were sampled is given in Table 1. The chloride values shown are for the lower face of each 1-in. thick disk.

For all 16 structures, the average chloride content in the concrete where the upper mat of steel is located was found to be about 2.6 lb of chloride per cu yd of concrete. The approximate average chloride content of the concrete in the deteriorated San Mateo-Hayward Bridge averaged about 1.9 lb of chloride per cu yd of concrete (1). Therefore, it is apparent that corrosion of steel in bridge decks, girders, and piles can occur at what can be considered as relatively low levels of chloride content.

CALCULATED DISTRIBUTION OF CHLORIDES IN CONCRETE

In an effort to determine if there is a mathematical distribution of the chlorides in the concrete, the data for each bridge were plotted and a regression line was calculated by the method of least squares (8). The basic equation for the correlation was

$$\log_{10}C = (\log_{10}M)(S) + \log_{10}b \qquad (1)$$

where

C = chloride content (lb/cu yd) of a 1-in. thick disk;
M = slope of the regression line;
S = maximum depth (in.) below surface for a 1-in. thick disk; and
b = intercept of regression line on Y-axis.

When this equation is reduced to eliminate the logarithms, the equation takes the following form:

$$C = b(M)^S \qquad (2)$$

The results of the regression analysis for all 16 bridges are given in Table 2. Because the chloride content of the concrete is calculated in terms of the logarithm to the base 10, it will be observed that the standard error of the estimate (8) as given in Table 2 is an antilogarithm.

TABLE 2

CALCULATED DISTRIBUTION OF CHLORIDES IN BRIDGE DECKS

Bridge	Year Built	Length (ft)	Width (ft)	Equation Regression Analysis[a]	Standard Error of Estimate is Log_{10} of:	n	Coefficient of Correlation	Bridge Type
1-273	1960	159	84	$C = 8.55(0.471)^S$	1.63	24	0.874	Conc. grdr., cont.
2-266	1960	172	84	$C = 6.54(0.501)^S$	1.93	24	0.776	Conc. grdr., cont.
3-6119	1960	125	84	$C = 10.0(0.438)^S$	1.65	22	0.878	Conc. grdr., cont.
4-6117	1960	125	84	$C = 15.2(0.432)^S$	1.35	22	0.956	Conc. grdr., cont.
5-695	1960	136	84	$C = 11.2(0.370)^S$	1.99	78	0.851	Conc. grdr., cont.
6-202	1917	579	28	$C = 14.2(0.309)^S$	1.88	86	0.903	R.C. arch
7-289	1960	45	80	$C = 10.5(0.471)^S$	1.87	24	0.813	Conc. grdr., cont.
8-265	1960	134	84	$C = 7.07(0.472)^S$	1.43	24	0.927	Conc. grdr., cont.
9-6116	1960	250	84	$C = 16.2(0.358)^S$	1.66	83	0.913	Conc. grdr., box.
10-2515	1936	120	24	$C = 1.81(0.796)^S$	2.07	25	0.348	Conc. girder
11-513	1963	352	32	$C = 17.4(0.407)^S$	2.14	39	0.800	Conc. grdr., box
12-6112	1962	99	84	$C = 13.7(0.404)^S$	1.28	24	0.975	Conc. grdr., cont.
13-244	1959	126	28	$C = 6.95(0.433)^S$	1.64	84	0.887	Conc. grdr., cont.
14-278	1960	147	84	$C = 12.0(0.443)^S$	1.34	24	0.956	Conc. grdr., cont.
15	1959	92	39	$C = 36.7(0.306)^S$	1.99	74	0.888	Conc. grdr., cont.
16	1960	—	48	$C = 17.7(0.456)^S$	2.20	75	0.747	Conc. grdr., cont.

[a] C = chlorides, lb/cu yd; S = depth below concrete surface, in.

At the time of the calculations, only the data for bridges 1 through 14 were available; therefore, these data were combined to determine the overall average for the relationship between chloride content and depth. For the 14 bridges, the following correlation was derived by the method of least squares:

$$C = 9.60(0.441)^S \quad (3)$$

where

C = chloride content (lb/cu yd) of a 1-in. thick disk; and
S = maximum depth (in.) below surface for 1-in. thick disk, with a depth limit of 4 in.

For the n of 56 values, the coefficient of correlation was 0.917, and the standard error of the estimate was the $\log_{10}$ of 1.50.

The calculated regression line and the average chloride content are shown in Figure 1. The calculated line (Fig. 1) is parallel to but consistently less than the line that shows the average. This is because there is a normal distribution of chloride in the concrete at any particular depth. As a result, the average is the arithmetic mean. However, in the regression analysis of chloride versus depth, the mathematical relationship for the chloride content is a logarithmic function. Therefore, the mean chloride content that is calculated by Eq. 3 for each depth is not a simple arithmetic mean but, in effect, a geometric mean. The geometric mean should result in a value that is less than the simple arithmetic mean.

The simple arithmetic mean of the chloride content at each depth was calculated and the regression analysis resulted in the following equation:

$$C = 10.85(0.440)^S \quad (4)$$

For the n of 56 values, the coefficient of correlation was 0.918, and the standard error of the estimate is the $\log_{10}$ of 1.49.

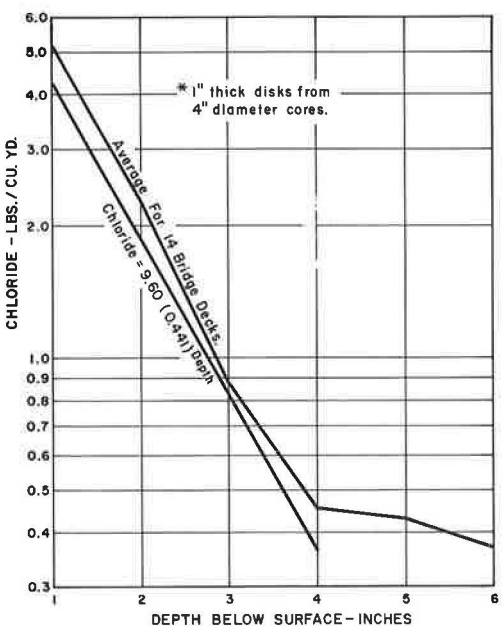

Figure 1. Average distribution of chloride in bridge decks.

Figure 1 also shows that the average chloride content of the concrete at the 5- and 6-in. depths does not follow the same slope of the line as shown for chloride values for depths of 4 in. or less. This trend in the data was typical, and none of the chloride values that were found for the concrete core disks that were obtained from 5 or 6 in. in depth was included in the regression analysis. The reason for the apparent disparity of chloride distribution at the 5- and 6-in. depth was not investigated.

In order to determine whether Eq. 1 is a basic representation of the distribution of chlorides in concrete with depth, new cores were cut from 6 continuously submerged piles that were removed in 1968 from the abandoned 40-year-old San Mateo-Hayward Bridge (1, 2, 3, 4, 5, 6). Corrosion of the reinforcing was observed in all of those sections of the piles that were exposed to San Francisco Bay water. There was no observed evidence (cracking, rust stains, or spalls) of corrosion in those sections of the piles that were continuously surrounded by the bay mud. Tables 3 and 4 give the results of this investigation.

TABLE 3

CHLORIDE IN SUBMERGED PILES EXPOSED TO BAY WATER

Average Depth Below Portland Cement Concrete Surface (in.)	Chloride Content (lb/cu yd) of 1-in. Thick Disk												
	Core 1-3	Core 1-4	Core 2-1	Core 2-2	Core 3-5	Core 3-6	Core 4-3	Core 4-4	Core 4-5	Core 5-3	Core 5-4	Core 6-3	Core 6-4
1	24.00	26.00	30.00	28.00	22.00	22.00	26.00	20.00	22.00	38.00	20.00	22.00	18.00
2	17.60	22.00	18.00	16.00	18.00	18.00	16.00	14.00	18.00	22.00	19.20	15.20	18.00
3	14.00	15.20	12.00	12.00	12.00	12.00	13.20	12.00	—	12.00	14.40	12.00	13.20
4	9.60	12.00	12.00	7.20	10.00	9.60	9.60	10.00	—	7.20	12.00	10.00	8.80
5	7.20	7.60	6.40	5.20	—	6.40	5.60	8.00	—	5.20	8.40	5.60	8.00
6	7.20	5.60	3.60	2.00	3.60	3.00	3.60	3.80	—	2.40	4.00	3.20	5.60
7	3.60	2.80	2.00	0.80	1.40	1.80	—	2.40	—	—	1.80	1.28	4.00
8	3.20	1.60	1.40	—	—	1.00	—	—	—	—	1.20	—	3.80
9	3.00	—	—	—	—	—	—	—	—	—	—	—	—

TABLE 4

CHLORIDE IN SUBMERGED PILES EXPOSED TO BAY MUD

Average Depth Below Portland Cement Concrete Surface (in.)	Chloride Content (lb/cu yd) of 1-in. Thick Disk													
	Core 1-1	Core 1-2	Core 2-3	Core 2-4	Core 3-1	Core 3-2	Core 3-3	Core 3-4	Core 4-1	Core 4-2	Core 5-1	Core 5-2	Core 6-1	Core 6-2
1	2.00	2.60	1.40	1.20	1.60	1.12	1.28	1.08	15.20	8.00	1.20	1.20	6.00	3.40
2	1.12	1.40	0.72	0.52	0.80	0.60	0.88	0.80	12.00	7.20	0.72	0.60	3.40	1.80
3	1.00	0.88	0.40	0.48	0.48	0.52	0.56	0.48	8.00	4.40	0.72	0.36	1.80	1.00
4	0.64	0.68	0.40	0.28	0.36	0.36	—	0.32	6.00	3.40	0.48	0.32	1.20	0.72
5	0.48	0.44	0.20	0.20	0.32	0.28	—	0.28	4.00	2.00	0.20	0.24	0.80	0.52
6	0.36	0.44	0.20	0.12	0.20	—	—	0.28	3.00	1.40	0.16	0.20	0.48	0.32
7	0.24	0.48	0.16	0.12	0.24	—	—	0.36	—	1.00	0.16	0.16	0.32	0.28
8	0.20	0.48	—	0.16	0.32	—	—	0.28	—	0.80	0.56	0.24	0.20	0.28
9	—	—	—	0.16	—	—	—	0.40	—	—	—	0.16	0.28	—

The 16-in. square piles were cored up to depths of 9 in., or slightly more than one-half of the pile thickness. The data were plotted and analyzed by the method of least squares, and the basic form of the equation was again found to be semilogarithmic or the same as Eq. 1.

For the sections of piling that have been continuously submerged for about 40 years, the derived relationship between the chloride content and depth was

$$C = 40.6(0.682)^S \quad (4)$$

where

C = chloride content (lb/cu yd) of a 1-in. thick disk; and
S = maximum depth (in.) below surface for a 1-in. thick disk.

For the n of 91 observations, the correlation coefficient was 0.932, and the standard error of the estimate was the $\log_{10}$ of 1.43.

For those sections of the piling that have been continuously submerged and in contact with bay mud for about 40 years, the derived relationship was

$$C = 2.35(0.747)^S \quad (5)$$

For the n of 105 observations, the correlation coefficient was 0.641, and the standard error of the estimate was the $\log_{10}$ of 2.32. The derived relationships of chloride versus depth as well as the plot of the simple average of the actual chloride content versus depth are shown in Figure 2.

CORROSION LOSS OF STEEL

A total of 47 linear feet of corroded deck reinforcing steel from bridge 15 (Table 1) was removed, and corrosion loss was measured. The method used was to measure

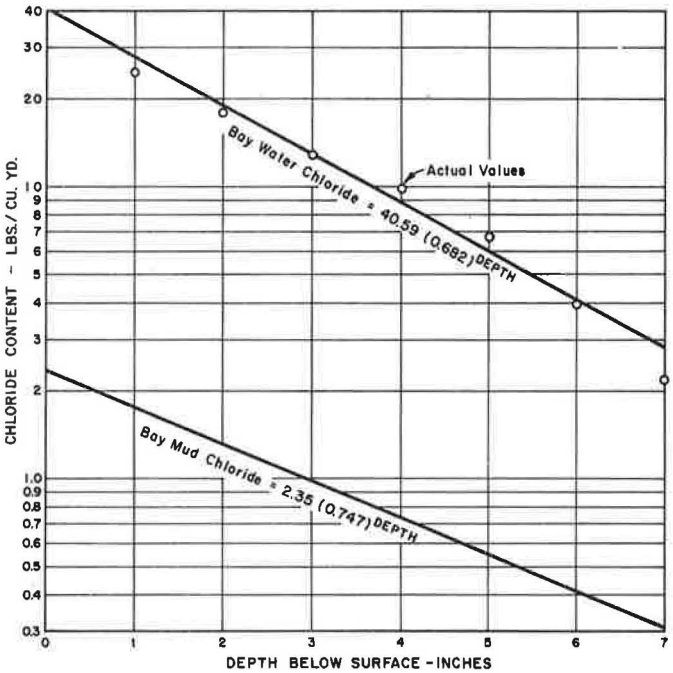

Figure 2. Chloride in concrete piling.

che maximum metal loss by means of a micrometer within each linear foot of the lightly sandblasted steel; results are shown in Figure 3 as a distribution curve.

The distribution of metal loss shown in Figure 3 has a log-normal distribution. By graphic analysis, Figure 3 shows that the mean of the maximum metal loss for each linear foot of the No. 4 reinforcing steel was 0.029 in. or 29 mils. For this particular bridge, it was apparent that 29 mils of maximum metal loss within each linear foot of steel would not significantly affect the overall strength of the structure.

Although 29 mils of maximum metal loss due to corrosion does not appear significant, it was found that in about 16 percent of the laboratory specimens a maximum metal loss of less than 1 mil was sufficient to crack a $\frac{7}{8}$-in. thickness of concrete cover (9).

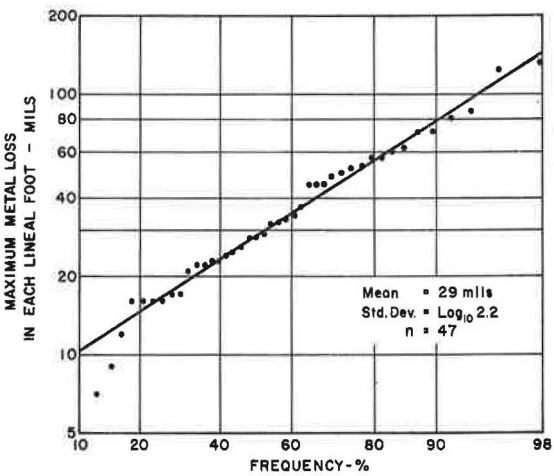

Figure 3. Corrosion of reinforcing in bridge 15.

DETERIORATION OF CONCRETE

Eleven of the 16 bridges (Table 1) are currently under contract for repair and application of a membrane; three have been repaired under a previous contract, and two are considered for complete deck restoration in the near future.

Depending on whether there has been chain traffic, the concrete deterioration has been evidenced by surface scaling as a result of tire chain abra-

sion and freeze-thaw damage, while the primary contributing factor in the bridge deck deterioration repairs is the spalling or lifting of the surface concrete. Where spalls have been removed, various degrees of corrosion of the steel have been observed.

However, the area of reinforcing steel corrosion has not necessarily been related to the total area of concrete spalling. This is not considered unusual as concrete spalls have been previously observed in the bottom of beams that extended for the entire beam width at the plane of the reinforcing, and not all of the steel was corroded (1).

SAMPLING

The data given in Table 1 were further mathematically reduced, resulting in an observation that, on the average, there is a relatively constant coefficient of variation (10) of the chloride content at any bridge or for any depth. The mean coefficient of variation for the chloride data given in Tables 1 and 4 is approximately 30 percent. With a coefficient of variation of about 30 percent, the precision in determining the chloride content in concrete will be highly contingent on the number of samples. For example, according to the recommended practice for choice of sample size (ASTM Designation E 122-58), about 35 samples would be necessary in order not to exceed a sampling error of 10 percent more than 1 in 20 times.

Because of the importance of the chloride content of concrete and the apparent 30 percent coefficient of variation that is found in the distribution of chlorides in concrete, sample size versus sample error, based on the ASTM recommended practice for sample size (10), was plotted and is shown in Figure 4. The relationship was calculated on the basis that sample error would exceed the calculated tolerable sampling error once in 20 times. These relationships should provide guidance for any future sampling program.

ELECTRICAL POTENTIALS

Previous studies have shown that electrical potential measurements could be made on the surface of the concrete, and the locations of reinforcing corrosion could be electrically detected (1, 2). The electrical potential measurements are made by the first electrical connection to the reinforcing and the second electrical connection to a saturated copper-copper sulfate half-cell. The half-cell is placed on the surface of the concrete, and the measurements are made by using a high input impedance electronic voltmeter.

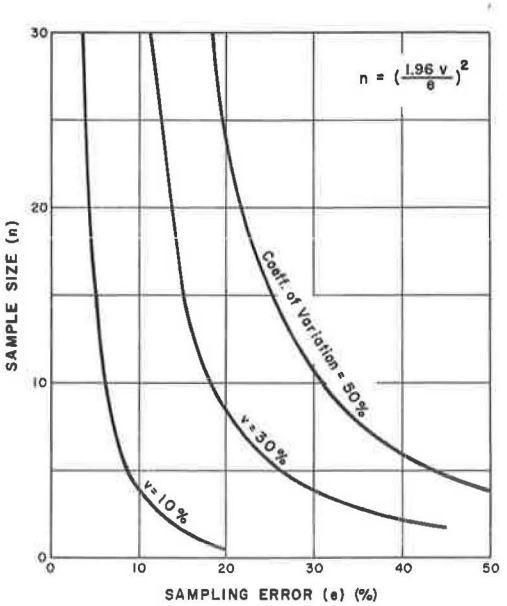

Figure 4. Sample size versus sample error.

In this study, the electrical potential, or half-cell potential of the steel, was measured over a 2-ft grid in the longitudinal and the transverse direction on sections of 2 bridge decks. Then contours were drawn through the points of equal potential.

The results of the potential survey for 1 bridge deck are shown in Figure 5. The equipotential contours only show values of -0.10 and -0.15 volt negative to the copper-copper sulfate half-cell. For this particular section of this bridge deck, there is no evidence of deterioration as determined by visual observation and by the "sounding" of the deck by means of dragging a chain over its surface to "hear" hollow areas. However, there is a relatively minor amount of deterioration visible in other locations on this bridge deck.

In previous laboratory and field studies (1, 9), it was observed that the steel was passive or noncorroding in uncracked concrete when the half-cell potential was less

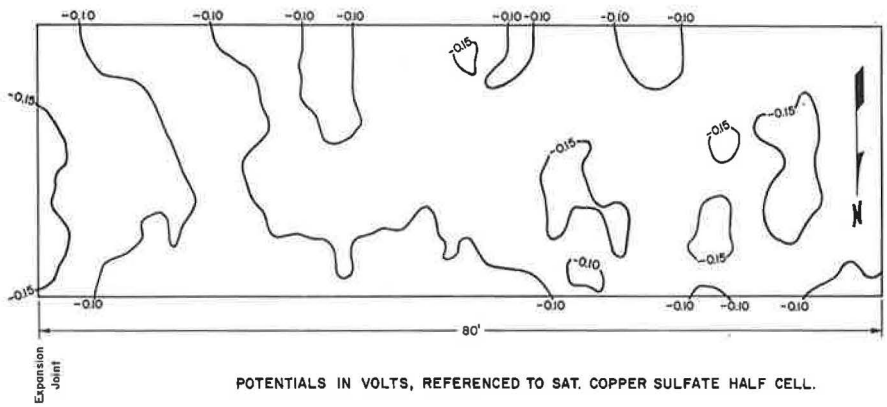

Figure 5. Equipotential contours of bridge deck 1723R.

than about 0.25 volt negative to the copper sulfate half-cell. In cracked concrete, actively corroding steel has a half-cell potential that has ranged from about -0.25 to about -0.50 volt to the copper sulfate half-cell (9).

The section of bridge deck shown in Figure 6 is in a bridge of the same age and design as 1723R, and is on parallel alignment. The only difference is that the deck of bridge 1723R currently has extensive deterioration.

The potential measurements of the bridge deck steel shown in Figure 6 were made at the same time that the repairs were being made. Except for one area, the concrete was removed from the steel at the cross-hatched locations at the time the measurements were being made. Because the salt-contaminated concrete was not completely removed from the periphery of the steel, the still partially embedded steel exhibited active potentials. It is surmised that the measured potential of the partially exposed steel is less than that which would be observed prior to concrete removal. For example, near the central area (Fig. 6), a potential contour of -0.40 volt is shown in a location of repair. The maximum recorded half-cell potential at this location was -0.43

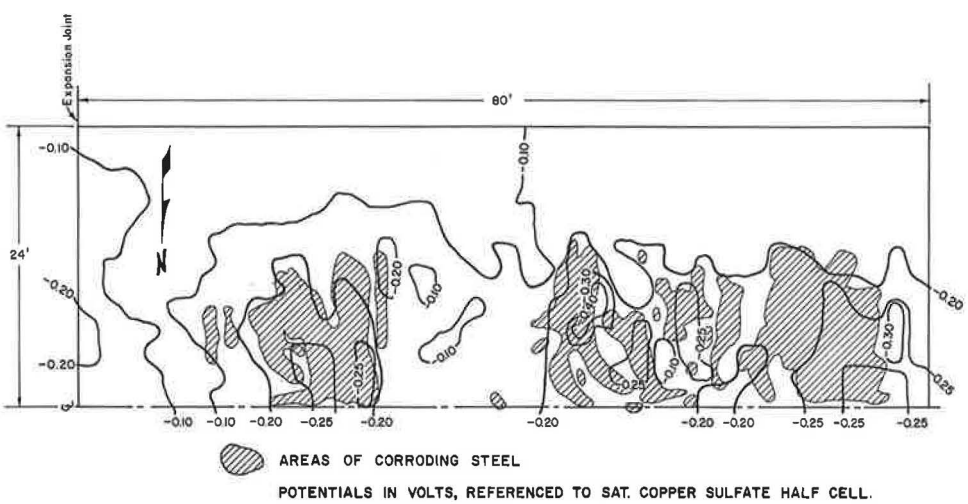

Figure 6. Equipotential contours of bridge deck 1723L.

volt. At this location the measurements of the half-cell potential of the steel were made prior to the removal of the concrete.

Figure 6 shows that there is relatively good agreement between the location of repair and the enclosed area that is delineated by the potential contour of about -0.20 volt. Also, where potential contours are less than -0.20 volt, there is a significant lack of repairs. In effect, it appears that the electrical potential contours not only establish the fact that electrochemical corrosion of the steel exists (1) but also may have significance for estimating the amount of as well as the locations for repair.

Because of the electrochemical phenomenon of the corrosion of the steel in concrete, it may be feasible to use the half-cell potential measurements of the steel not only to evaluate the corrosion activity of the steel but also to evaluate the effectiveness of repair methods for arresting the corrosion of the steel.

DISCUSSION OF FINDINGS

Although the study only encompassed a few California bridge decks, other states have made reports of their investigations on bridge deck problems (11, 12, 13).

As indicated by this study, chlorides penetrate concrete in a manner that can be mathematically described. Therefore, it is apparent that concrete cracking of bridge decks is not a prerequisite for the penetration of chloride to the surface of the steel. That corrosion of reinforcing can occur independently of cracking was established by the field investigation of the San Mateo-Hayward Bridge and laboratory studies (5, 9, 14). However, there is no question that chloride can penetrate more rapidly to the surface of steel that has a cracked concrete or poor quality concrete covering, but the lack of cracks per se in a bridge deck will not prevent the penetration of the chloride salt. Also, the presence of chloride and corrosion of the steel will be a cause of concrete cracking and spalling (1, 9).

In a previous laboratory study (9), reinforcing with $\frac{7}{8}$ in. of excellent quality concrete cover (8 sacks/cu yd, 2 in. of slump, moist-cured, and air-entrained) was found to corrode in less than 1 year when partially immersed in a salt solution. Therefore, it is apparent that a "normal" or average concrete mix per se could not be expected to prevent the penetration of salts with the resulting corrosion of the steel. However, there is no question that high concrete quality standards and practices should be strictly adhered to not only because of the corrosion factor but also because of other structural and durability factors such as shrinkage, freeze-thaw, and abrasion. In addition, with concrete of high shrinkage, the problems associated with the use of a membrane would be vastly increased because it would be necessary for the membrane to elongate and "roof over" concrete cracks.

As indicated by this study, additional cover should provide proportionate increase in the forestalling of corrosion. However, with the direct application of chloride de-icing salts to a bridge deck, significantly increasing the amount of cover over the steel may not completely prevent early deterioration because of the presence of some degree of deck cracking. For example, in California it has been reported that practically all 21 of the investigated bridge decks had some form of cracking (15). In Illinois, Minnesota, New Jersey, Ohio, and Texas, it was reported that about two-thirds of the spans and about four-fifths of the investigated bridges had some type of cracking (15).

Studies in 1962 (3) and 1966 (16) indicated that a primary cause of bridge deck cracking could be the result of drying shrinkage and of concrete age. Although these observations may be correct, it is also probable that these factors, which have caused concrete cracking, have normally been present to some overall degree throughout the history of reinforced concrete bridge deck construction.

Further evidence of the destructive role of de-icing salts was the apparent lack of significant bridge deck deterioration that was observed during the statewide survey of California bridges in 1960 (4). Also, no significant evidence of bridge deck deterioration had been reported during the yearly inspection of all bridges by engineers of the Bridge Department of the California Division of Highways prior to about 1960. Therefore, this study indicates that the primary cause of widespread accelerated bridge deck deterioration in California is the relatively recent and increased use of chloride de-icing salts.

Because of the mathematical similarity in the distribution of salt with depth in concrete decks and piling, it is important that the primary mechanism for salt penetration be thoroughly investigated.

It is speculated that chloride is distributed in bridge decks as a result of a primary mechanism of absorption by capillary action, and loss of water by evaporation to the atmosphere. If such a mechanism applies to bridge piles, then an effective method for reducing the rate of chloride penetration would be to physically restrict the loss of water vapor to the atmosphere by use of a membrane. Coating of the entire pile above and below the water line would be even more effective.

For bridge decks, it is obvious that either a protective membrane or sealant will be required to prevent the penetration of salt into the concrete, or noncorrosive de-icing chemicals should be used to prevent deterioration due to corrosion of the embedded steel.

Of course, if noncorrosive chemicals were used on bridge decks, they would also have to be used for some length on adjacent pavement because of the "tracking" of the corrosive salts by vehicles. California pavements are nonreinforced so that salt damage to pavements would be limited to scaling or other attack of non-air-entrained portions. All concrete in freeze-thaw areas is normally specified to be air-entrained.

SUMMARY AND CONCLUSIONS

Sampling and Chloride Distribution

Sixteen bridge decks with various degrees of deterioration that have been subjected to de-icing salts were cored and analyzed for chloride content. It was found that there was a basic mathematical relationship that would describe the distribution of chlorides with depth. In effect, the log of the chloride content is inversely related to the depth below the surface.

A basic mathematical expression was derived for the chloride analysis of the concrete obtained from piles that were continuously submerged in bay water. The mathematical expression for the distribution of chlorides in concrete was found to be the same for bridge decks or piling and indicated that, for each additional inch of depth, the chloride content would be reduced by approximately one-half. Therefore, the mechanism for the absorption of salt may be similar, and cracks in a concrete deck may only perform the role as a local accelerator to the incidence of corrosion.

The distribution of chloride in the concrete was found to be highly variable. On the average, the coefficient of variation of the chloride content was approximately 30 percent. Therefore, based on a coefficient of variation of 30 percent, it would be advisable to obtain not less than 6 samples in order to estimate the average chloride content. Even with 6 samples, there is a probability that 1 out of 20 average values would have a sampling error of greater than about 24 percent.

Membranes and Corrosion

Previous experience (1) has shown that application of a membrane over chloride-contaminated concrete bridge decks can result in acceleration of the corrosion. Because of the similarity between the evidence of corrosion, the distribution and the concentration of chloride in piles and in decks, and the detection of similar electrical potential activity of deck steel, the application of a membrane to a deck could also result in acceleration of the corrosion.

Metal Loss

The reinforcing steel from 1 distressed bridge deck was removed, and it was found that the mean of the maximum corrosion loss within each foot of steel was 29 mils. Although not structurally significant, this amount of corrosion loss is more than enough to cause concrete cracking and spalling. Laboratory testing showed that less than 1 mil of corrosion loss was sufficient to crack a $\frac{7}{8}$-in. thick concrete cover.

Corrosion Prevention

Based on the mechanism of corrosion and design limitations, deterioration of a nominally chloride-free (less than 0.6 lb/cu yd) concrete deck due to corrosion can be prevented by using a noncorrosive de-icing chemical, or a membrane barrier on the concrete surface. Other alternatives, such as artificial heat rather than salt to melt ice, may also prevent corrosion. Of course, this method would have to be used where there was no salting of the adjacent pavement because this could be "tracked" on the deck by traffic.

Half-Cell Potential

The half-cell potential of the reinforcing steel in sections of 2 bridge decks was measured, and it is shown that deterioration is associated with corrosion of the steel as indicated by the electrical measurements. The measurements can be used to locate actively corroding reinforcing steel in bridge decks, and should show promise in evaluating repair techniques that are considered to be arresting the corrosion of the steel.

ACKNOWLEDGMENT

This project was performed in cooperation with the U. S. Department of Transportation, Federal Highway Administration, Bureau of Public Roads. The opinions, findings, and conclusions expressed in this report are those of the authors and not necessarily those of the Bureau of Public Roads.

REFERENCES

1. Gewertz, M. W., Tremper, B., Beaton, J. L., and Stratfull, R. F. Causes and Repair of Deterioration to a California Bridge Due to Corrosion of Reinforcing Steel in a Marine Environment. HRB Bull. 182, 1958, pp. 1-41.
2. Stratfull, R. F. The Corrosion of Steel in a Reinforced Concrete Bridge. Corrosion, Vol. 13, No. 3, June 1957.
3. Stratfull, R. F. Progress Report on Inhibiting the Corrosion of Steel in a Reinforced Concrete Bridge. Corrosion, Vol. 15, No. 6, June 1959.
4. Beaton, J. L., and Stratfull, R. F. Environmental Influence on Corrosion of Reinforcing Steel in Concrete Bridge Substructures. Highway Research Record 14, 1963, pp. 60-78.
5. Stratfull, R. F. Effect on Reinforced Concrete in Sodium Chloride and Sodium Sulfate Environments. Materials Protection, Vol. 3, No. 12, Dec. 1964, p. 75.
6. Beaton, J. L., Spellman, D. L., and Stratfull, R. F. Corrosion of Steel in Continuously Submerged Reinforced Concrete Piling. Highway Research Record 204, 1967, pp. 11-21.
7. Durability of Concrete Bridge Decks, A Cooperative Study. California Division of Highways, U. S. Department of Transportation, and Portland Cement Association, Rept. 3, 1967.
8. Brownlee, K. A. Industrial Experimentation. Chemical Publishing Co., Brooklyn, 1949.
9. Spellman, D. L., and Stratfull, R. F. Laboratory Corrosion Test of Steel in Concrete. Materials and Research Dept., California Division of Highways, Research Rept. M&R 635116-3, Sept. 1968.
10. Manual on Quality Control of Materials. ASTM, Spec. Tech. Publication 15-C, Jan. 1951.
11. A Study of Deterioration in Concrete Bridge Decks. Div. of Materials and Research, Missouri State Highway Commission, Jefferson City, Progress Rept. on Investigation 59-2A, Oct. 1965.
12. Bukovatz, J. E. Bridge Deck Deterioration Study, Part 7, Weathering Test of Reinforced Concrete Slab With Various Depths of Steel. Planning and Research Dept., State Highway Commission of Kansas, Topeka, 1968.
13. Hughes, R. D., and Scott, J. W. Concrete Bridge Decks, Deterioration and Repair. Div. of Research, Kentucky Department of Highways, Frankfort, June 1969.

14. Ost, B., and Monfore, G. E. Penetration of Chloride Into Concrete. Jour. of PCA Research and Dev. Laboratories, Vol. 8, No. 1, Jan. 1966, pp. 46-52.
15. Durability of Concrete Bridge Decks, A Cooperative Study. Portland Cement Assn., Rept. 5, 1969.
16. Stewart, C. F., and Neal, B. F. Factors Affecting the Durability of Concrete Bridge Decks. Highway Research Record 226, 1968, pp. 50-68.

Durability of Concrete Bridge Decks—A Review of Cooperative Studies

CLIFFORD L. FREYERMUTH, PAUL KLIEGER, DAVID C. STARK, and HARRY N. WENKE, Research and Development Division, Portland Cement Association

The paper summarizes the results of concrete bridge deck durability studies made by the Portland Cement Association in cooperation with the U. S. Bureau of Public Roads and 10 state highway departments. Condition surveys were made of over 1,000 randomly selected decks in California, Illinois, Michigan, Minnesota, New Jersey, Ohio, Texas, and Virginia to assess the extent of deterioration. Detailed field and laboratory investigations were made on 68 decks in Kansas, Michigan, California, and Missouri to determine the causes of deterioration. Attention is given to scaling, cracking, and spalling. Scaling is not a particularly serious problem and has been kept under control—although not eliminated—with use of air-entrained concrete. The observed scaling is usually associated with deficiencies in the entrained air void systems and with inadequate deck drainage. Many forms of cracking are of secondary importance because they do not lead to more serious forms of deck distress. Longitudinal cracking is sometimes found on the thicker slab-type bridges and apparently results from subsidence of high slump concrete around the reinforcing bars. Transverse cracking is the form most often encountered. Shrinkage and thermal volume changes in the concrete apparently are the primary factors producing these cracks. Surface spalling, a major problem in some states, is the result of internal expansive forces in the concrete generated by the corrosion of top reinforcing bars. Cracks over bars, shallow concrete cover over bars, and permeable concrete allow the de-icing chemical solutions to reach the bars and cause the corrosion. Recommendations for improved durability involve the use of higher quality concretes, improved construction practices, and attention to design details that have an influence on durability. Attention is also invited to 2-course bonded construction (such as is used for industrial floor construction) as an alternative to single course bridge deck construction.

•THIS PAPER is based on studies of concrete bridge deck durability begun in 1961 by the Portland Cement Association in cooperation with the U. S. Bureau of Public Roads and 10 state highway departments. The scope of the study program was described in an earlier paper (1). The initial objectives were to (a) assess the extent of bridge deck durability problems in various parts of the country, (b) determine the causes of the deterioration, (c) develop recommendations for obtaining improved durability of new bridge deck construction, and (d) develop methods for retarding any deterioration on existing bridges. It is believed that considerable progress has been made toward achievement of the first 3 objectives. However, the study has not developed sufficient data in regard to the fourth objective.

The source data for the studies were obtained from in-service bridge decks by means of 2 types of field investigations. Detailed investigations were made of a limited number

Paper sponsored by Committee on Effect of Ice Control and presented at the 49th Annual Meeting.

of decks in 4 states for the purpose of determining causes of deterioration. The second type of field inspection was made on a statistically representative sampling of bridge decks in 8 states, including 2 states in which detailed investigations were made. The purpose of this portion of the study was to estimate the extent of deterioration, but other related information was also gathered. In both types of studies, the bridges were selected from those built on the federal-aid highway system from 1940 to 1962.

For purposes of the study, the types of deterioration were defined as scaling, cracking, and spalling. Figure 1 shows some typical forms of deterioration. Scaling was described as light, medium, heavy, or severe scaling according to the depth of concrete that was affected. Six classifications of cracking were defined primarily on the basis of directional trend: transverse, longitudinal, diagonal, pattern or map, D, and random. Surface spalls were defined originally as small and large, but there is no real distinction between the two other than size. Joint spalls and popouts were also included in the studies, but there were usually minor problems, and they will not be discussed in the present paper.

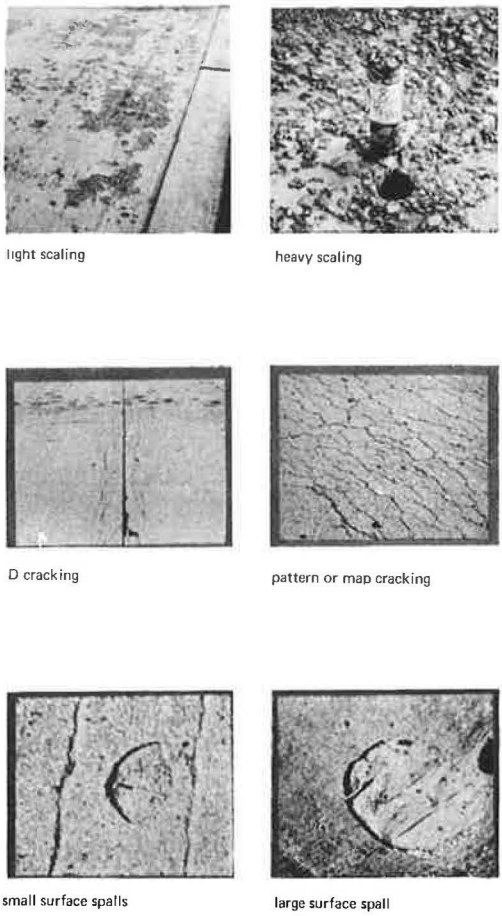

Figure 1. Examples of deterioration.

EXTENT AND SEVERITY OF BRIDGE DECK PROBLEMS

The random surveys were made to obtain quantitative information about the kinds of durability problems that occur on concrete bridge decks, and about the extent and the severity of the distress. The data also permitted some evaluation of the influence that factors such as deck age, bridge type, and use of air-entrained concrete have on the occurrence of the various types of defects.

Survey Method

The states included in the random surveys are given in Table 1 along with the number of bridges and spans studied in each state. In order to obtain a high level of uniformity of reporting, a special seminar was held for the participants in the survey. Data for

TABLE 1

RANDOM SURVEY STATES

State	Bridges	Spans	State	Bridges	Spans
Michigan	140	432	Illinois	158	516
Minnesota	110	353	Virginia	140	452
Ohio	146	442	Texas	132	803
New Jersey	123	321	Total	1,097	3,955
California	148	636			

each bridge were recorded on standard data sheets. Scaling was recorded as an estimated percentage of the affected span's deck area for the average severity condition ranging from light scale to severe scale. Occurrences of any of the 6 classifications of cracking were reported as being light, medium, or heavy. The numbers of large and small surface spalls were recorded for each span. Information was also gathered concerning the occurrence of joint spalls, popouts, and rusting of reinforcement.

The survey information on the data sheets was transferred to standard punched cards for processing by machine compilers. These compilations provided the source data that are presented and analyzed in an earlier report (6). In the comments that follow, only the major findings from this portion of the study are summarized.

Scaling

Scaling was found in all 8 states, but the incidence varied considerably from state to state. Virginia and Texas had the highest percentages of scaling, approximately 40 percent of the spans. In Illinois, Michigan, New Jersey, and Ohio from 20 percent to 30 percent of the spans had scaling. Decks in Minnesota had relatively little scaling; approximately 13 percent showed scaling. The insignificant amount of scaling in California occurred in an area where exposure is severe and where de-icing chemicals are used.

Although these percentages appear high, the scaling encountered in the 8 states was not too severe. Light scale, the least severe condition, accounted for 90 percent of the scaled spans. Furthermore, the scaling that occurred on about half of the scaled spans affected less than 8 percent of the deck area. Older decks usually had a higher incidence of scaling than newer decks. There was no marked trend toward greater incidence of scaling on the decks that carried the larger volumes of traffic.

The random survey data clearly illustrate the improved scale resistance of air-entrained over non-air-entrained concrete. Figure 2 shows that, compared with the air-entrained decks, the non-air-entrained decks had a higher incidence of scaling more extensive scaling on an area-affected basis, and more of the severe forms of scaling by a ratio of about $2\frac{1}{2}$ to 1. Furthermore, the most extensive scaling was found in the 2 states that either did not use air-entrained concrete or began to use it at a relatively late date.

Cracking

Some form of cracking occurred on about two-thirds of the spans; the remainder may be regarded as having no readily visible cracking. Of the 6 classifications of cracking mentioned previously, D-cracking was virtually nonexistent; longitudinal cracking, diagonal cracking, and pattern or map cracking were not encountered with great frequency.

Transverse cracking was the form most frequently observed in each of the 8 states. About one-half of the spans had transverse cracking, with the large majority of these being described as having light transverse cracking. The incidence of transverse cracks appeared to increase with increasing age of deck and also with increasing span length. The superstructure type appeared to exercise some control over the occurrence of these cracks. Incidence of transverse cracks was greater on continuous spans than on simple spans, and was somewhat greater on structural steel spans than on reinforced concrete spans. Prestressed concrete spans and reinforced concrete simple spans generally had the lowest incidences of transverse cracking.

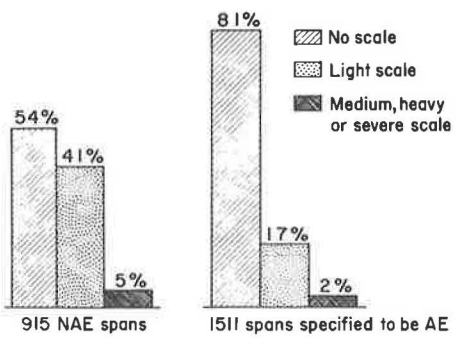

Figure 2. Influence of air entrainment on occurrence of scaling.

Surface Spalling

A significant amount of spalling was found in 4 of the 8 states. In Illinois about 25 per

of the spans showed surface spalling. In Ohio, Michigan, and Texas approximately 10 percent of the spans showed spalling. A negligible amount was observed in California, Minnesota, New Jersey, and Virginia.

Spalled bridges on the average contained about 10 surface spalls, while spalled spans on the average contained about 5 spalls. Older decks generally had a higher incidence of spalls than newer decks. Decks carrying higher volumes of traffic and those on a higher class of highway had a slightly higher incidence of surface spalls than less traveled decks on lower class highways. Span length, span continuity, bridge material, and superstructure type appeared to have little influence on the incidence of surface spalling. The indications are that decks in urban areas had a higher incidence than decks in rural areas.

Without doubt, surface spalling is the most serious and troublesome form of bridge deck defect. The deck is weakened locally, reinforcement is usually exposed, and riding qualities are impaired. Repair work is difficult and expensive, and there is no assurance that a repaired deck may not spall again.

Decks that scaled did not necessarily spall. The state that had the highest incidence of surface spalling had one of the lower incidences of scaling, and the states that had the highest incidences of scaling had little surface spalling.

Factors that contribute to surface spalling and the means for preventing this form of deck distress will be described later. At this point it might be noted that no one factor amenable to study by the procedures of this random survey could be singled out as a principal contributor to the surface spalling problem.

THE CAUSES OF BRIDGE DECK DISTRESS

Detailed investigations were made in Kansas, Michigan, California, and Missouri for the purpose of determining causes of deterioration. Decks were chosen that would illustrate a variety of types and degrees of deterioration, bridge age, location, and superstructure type. The selected decks were not necessarily typical of conditions in e state.

Investigation Procedure

The field inspections were made by a team representing the state highway department, the U. S. Bureau of Public Roads, and the Portland Cement Association. Table 2 gives the number of cores taken from the decks. Measurements were made of concrete cover over reinforcing steel. The cores were examined by various techniques in the laboratory. Air void characteristics were measured by the linear transverse method (PCA cores) and by the high-pressure method (BPR cores). Concrete quality was studied microscopically and was checked by pulse velocity measurements. The petrographers gave special attention to cracks in the cores to ascertain time of formation and possible causes. Concentration of chlorides as a function of depth was determined. Plans, specifications, and construction records were studied for possible correlation with the deterioration observed in the field.

The data and findings of the detailed investigations were presented in earlier reports (2, 3, 4, 5).

TABLE 2

DETAILED INVESTIGATION STATES

State	Bridges	Cores		
		PCA	BPR	Total
Kansas	18	128	122	250
Michigan	13	42	21	63
California	20	170	54	224
Missouri	17	143	44	187
Total	68	483	241	724

Scaling

Scaling to varying degrees of severity was observed on both non-air-entrained and air-entrained decks. When cores from these decks were studied in the laboratory, the scaling was almost invariably associated with either a total lack of entrained air, or with deficiencies in the air void systems of the intentionally air-entrained concretes.

Linear traverse measurements of cores from non-air-entrained decks

TABLE 3

COMPARISON OF AIR VOID PARAMETERS OF AIR-ENTRAINED CONCRETES HAVING UNIFORM AND NONUNIFORM AIR VOID DISTRIBUTIONS

State	Air Void Distribution	Percent Air	Voids per Linear In.	Specific Surface ($in.^2/in.^3$)	Void Spacing Factor (in.)[a]
Michigan	Uniform	2.2-8.0	4.1-18.0	485-1,145	0.004-0.010
	Nonuniform	3.5-5.2	7.0-9.2	645-870	0.006
California	Uniform	2.2-8.6	4.1-22.8	690-1,180	0.003-0.009
	Nonuniform	1.8-6.8	3.3-15.7	735-1,450	0.004-0.010
Missouri	Uniform	2.7-6.6	4.6-15.8	475-1,100	0.004-0.009
	Nonuniform	2.9-10.1	5.0-18.6	490-1,150	0.003-0.010

[a]Based on assumed paste content of 25 percent.

resulted in calculated void spacing factors, $\bar{L}$, greater than 0.019 in., i.e., well in excess of the 0.008 to 0.010 in. limit that is generally considered necessary to protect cement paste during freezing in the presence of de-icer solutions. However, there were large areas of many non-air-entrained decks that had been subjected to de-icing chemicals and that had not scaled. It is believed that effective drainage of these areas eliminated one of the conditions that is necessary before scaling can occur. This point will be mentioned again later.

Deficiencies in the air void systems of intentionally air-entrained concretes were manifested in 3 ways: (a) differences in air content from one portion of a deck to another, (b) a lack of air in thin irregular zones at the wearing surface of the concrete, and (c) nonuniform distribution of air voids throughout the depth of the concrete.

Large differences of air contents measured in cores from a single deck are indicative of batch-to-batch variations. However, this condition was detected on only a few of the bridges; there was generally good control of air contents in most of the decks in each state.

Nearly all of the observed scaling or incipient scaling in air-entrained concretes was attributed to nonuniform air void distribution, particularly when this occurred in thin irregular zones at the wearing surface. In cores displaying this condition, the horizontal microcracks, which are indicative of incipient scale, would typically be found in the air-deficient zones. Detection of this condition could be made only by microscopic examination. Furthermore, the results of linear traverse measurements (ASTM C 457) of the full length vertical sections of the whole cores failed to disclose the the existence of these zones. Similar air void parameters were measured by this averaging technique for cores having both uniform and nonuniform air void distribution (Table 3).

Several cores in the investigation contained uniform air void distribution and satisfactory void spacing factors, but displayed light surface scaling. It is likely that the aforementioned air-deficient zones were once present at the wearing surfaces of these concretes, but they have since scaled to the level where an adequate protective air void system was encountered.

The observed nonuniformities in air contents and air void distribution appear to be the result of a number of factors. Batch-to-batch variations in air content may result from inadequate control of concrete batching and mixing operations. Thin, irregular zones deficient in air may result from improper placing and finishing procedures.

It was reasoned that cores from scaled areas might contain, on the average, an amount of chlorides different from that contained by companion cores from non-scaled areas. Quantitative analyses were made to learn if this was the case; however, the results indicated no substantial or significant differences for cores in the 2 groups.

In addition to these concrete properties, deck drainage has an important influence on the occurrence of scaling. Scaling was confined to the gutter areas of 32 of the 38 scaled decks (both air-entrained and non-air-entrained) and extended beyond the gutters on 4 other decks. The more extensive scaling in the gutter areas is undoubtedly brought about by the tendency for water and de-icer solution to pond in these areas.

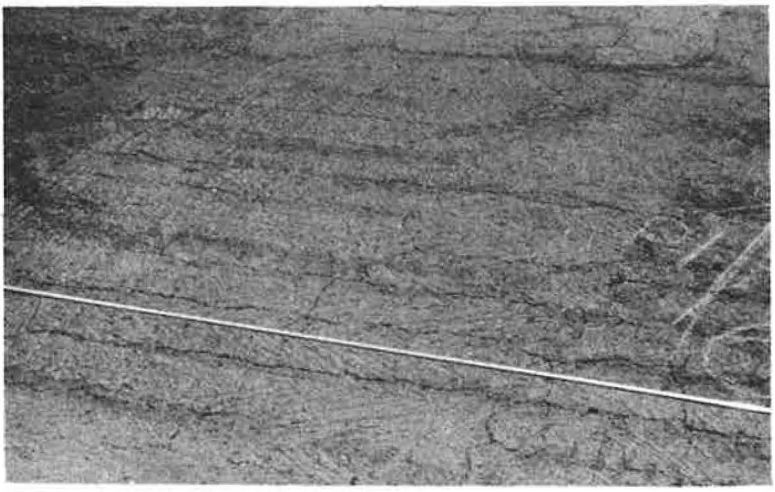

Figure 3. Heavy longitudinal cracking.

Cracking

Figure 3 shows heavy longitudinal cracking on a solid slab bridge. The cracks are relatively wide, are readily visible, and occur over each line of top longitudinal reinforcement. The cracks are not in the direction that would be expected of cracks due to dead loads or live loads, and their width and location indicate that these are not structural cracks. An apparent factor in the cracking found on the thicker concrete slab bridges is restraint to subsidence of the concrete (settlement during bleeding) imposed by the fixed reinforcement, or by void tubes in hollow slab bridges. Resistance to subsidence tends to result in cracking over and parallel to the top reinforcement, horizontal cracking at the sides of the bar, and a void beneath the bar—a situation that is aggravated as concrete slump increases.

Transverse cracking was the predominant form of cracking encountered in decks supported by longitudinal steel or concrete girders. The cracks usually developed in patterns characteristic of the superstructure type. Decks on steel girders tended to have rather uniformly spaced transverse cracking over the entire length of the deck. Decks supported by concrete girders, on the other hand, tended to have closely spaced tight transverse cracking in the negative moment areas over the supports and relatively little transverse cracking in the positive moment areas of the span. The significant longitudinal dead-load stresses that are developed in the decks of the concrete bridges apparently influence the transverse crack pattern, as compared to the uniformly spaced transverse crack pattern on the steel bridges that have only small dead-load stresses in the deck.

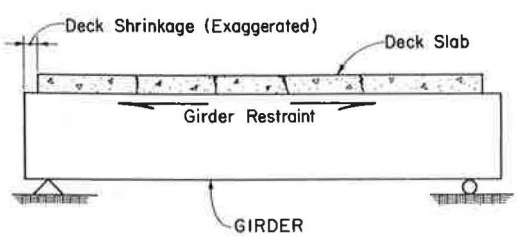

Figure 4. Girder restraint to longitudinal volume change.

The detailed investigations indicate that shrinkage and thermal volume changes of the concrete are particularly significant factors in the formation of transverse cracks. Figure 4 shows one aspect of the volume change effect in which the longitudinal steel girders restrain the shrinkage of the deck slab. The effect is less in decks supported by concrete girders because the difference in shrinkage between slab and girder is less. Restraint to overall shrinkage is also provided by the reinforcement in the deck slab.

Another aspect of shrinkage is the stresses induced by the differential drying rate through the thickness of the slab, as shown in Figure 5 for a slab drying from 2 faces. These stresses are in addition to the stresses induced by the overall shortening of the deck shown in Figure 4.

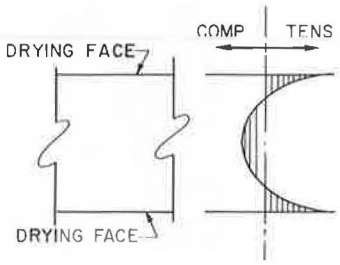

Figure 5. Distribution of shrinkage stresses through thickness of slab.

The pattern of transverse cracks shown in Figure 6 occurred on a deck with "trussed" or bent bars as part of the transverse reinforcement. The cracks developed only where the bent bars were near the top of the slab. It is believed that the reinforcement causes this type of cracking partially by the restraint to subsidence effect mentioned previously and, also, because the bar subsequently restrains the shrinkage of the top surface of the slab. The great majority of transverse cracks on decks supported by longitudinal girders were observed to occur directly over top reinforcing bars. In addition to providing restraint to shrinkage, these cracks are believed to form over bars because the bars act as stress risers in the concrete section under tension.

Spalling

Transverse and longitudinal cracks over reinforcement are of concern primarily because they may be contributing factors in the development of surface spalls. Figure 7 shows a core taken from a deck with an incipient surface spall. The black spot near the top of the core is a section of the reinforcing bar. The photo shows the typical crack over the reinforcing bar and, also, the cracks radiating from the bar that form the spall surface. Figure 8 shows a closer view of the bar, and the cracking may be seen to be associated with the cap of corrosion products on the top of the bar. This phenomenon—in which the corrosion products simply break away or push off the concrete over the top of the bar—was observed on nearly every reinforcing bar in cores taken through surface spalls.

Surface spalls were found frequently over bars with inadequate cover. In the Missouri detailed investigation (5), 13 cores were taken through reinforcement from sound areas of bridge decks. The average cover on the bars in these cores was $1\frac{3}{4}$ in. In

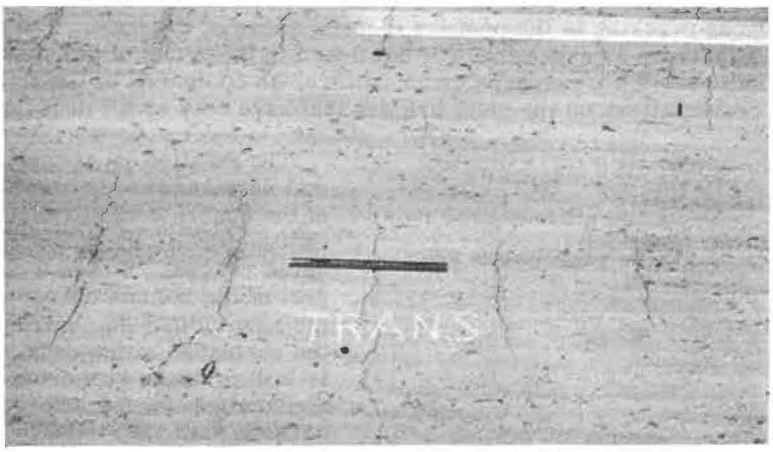

Figure 6. Transverse cracks over trussed reinforcing bars.

Figure 7. Core through incipient surface spall.

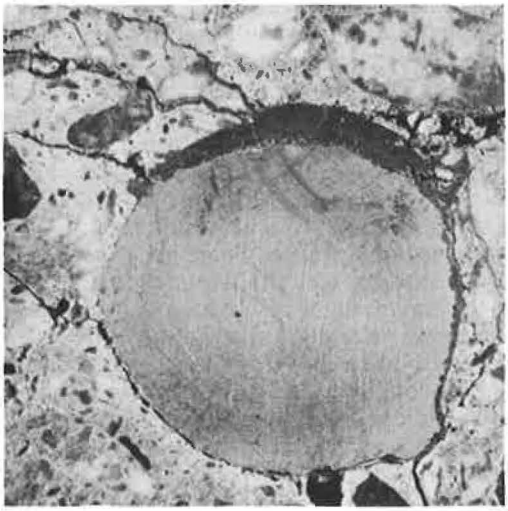

Figure 8. Corroded reinforcing bar (detailed view of core shown in Figure 7).

12 cores taken through spalled areas, the average cover was $1\frac{1}{4}$ in. However, there was not a consistent or direct relationship between depth of cover and the occurrence of surface spalls in the cores studied.

More than a thousand quantitative chemical analyses for chloride content as a function of depth were made on ground-up samples of the mortar in the cores. These analyses showed progressively higher chloride contents in (a) cores from sound decks, (b) sound cores from spalled decks, and (c) spalled cores from spalled decks (Fig. 9). This may reflect a higher permeability of spalled decks, or that more chlorides have been placed on the spalled decks. In either case, the higher chloride content at the level of the reinforcement has been shown to be related to the problem of corrosion and spalling.

It was mentioned previously that the random survey results indicated an apparent lack of influence on the part of factors such as superstructure type (steel versus concrete members), span length, or superstructure continuity (simple spans versus continuous spans) with the occurrence of surface spalling. All of these factors significantly influence the vibration characteristics of bridge superstructures. Although little data are available on the subject, it is reasoned by many that superstructure vibrations are a basic factor in bridge deck deterioration—primarily in transverse cracking and surface spalling.

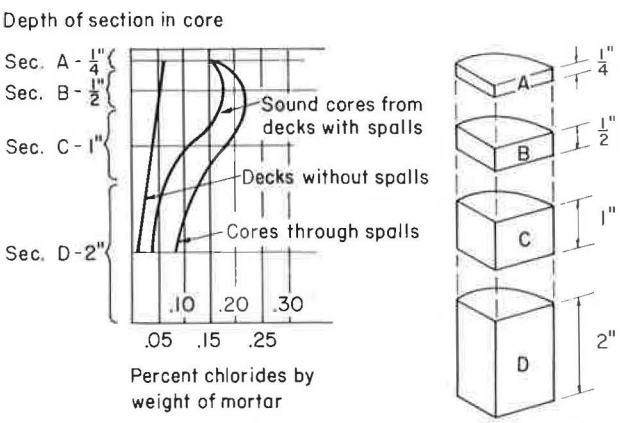

Figure 9. Average chloride distribution as a function of depth of concrete.

In order to develop some data, the theoretical natural frequencies of vibration were calculated for 46 of the superstructures from the 4 detailed investigations, and the results were compared to the conditions

of the decks. The following types of superstructures were included: composite and noncomposite simple span steel bridges, simple span concrete bridges, noncomposite continuous span steel bridges, and continuous span concrete bridges. Calculations were made by considering both composite and noncomposite action for the steel spans, and gross section and transformed cracked section for the concrete spans. The calculations revealed no relationship between high or low frequency of vibration, or high or low dynamic impact values, and the condition of the bridge decks. It is emphasized, however, that this finding is only relevant to the levels of "flexibility" represented by the bridge designs studied, which reflect design practices used between 1940 and 1960. Many of these designs are very conservative compared to present practices.

To summarize, the basic cause of surface spalling is considered to be the corrosion of the top layer of reinforcement as a result of the use of de-icing chemicals. Cracks located over and parallel to the reinforcement, shallow cover, permeable concrete, and pressures developed by the freezing of water or de-icer solution in this weakened region contribute to the formation of spalls. Although the direct blows of vehicle tires undoubtedly contribute to the breaking up of the weakened concrete, the vibration characteristics of the bridges studied do not appear to be a primary factor in surface spalling.

SUGGESTIONS FOR IMPROVED DURABILITY

The massive use of de-icing chemicals on bridge decks, which has developed largely during the past 10 to 15 years, represents a significant increase in the severity of exposure conditions for reinforced concrete bridge decks. In order to provide durable decks in this type of environment, more attention must be given to design, construction, and quality of concrete for bridge decks.

Design recommendations for slab-on-beam bridges are shown in Figure 10. A minimum concrete cover of 2 in. is recommended over the top slab reinforcement. The 2-in. cover must be of dense, impermeable, low water-cement ratio concrete in order to provide an effective barrier against penetration of chlorides and corrosion of steel. The primary transverse top bars have been placed below the longitudinal "shrinkage and temperature" bars. This is a related measure for controlling the widths of shrinkage cracks that form over and parallel to the primary reinforcement.

Another design feature that has not received adequate attention in relation to bridge deck durability is drainage of the deck. The number, location, size, and details of the deck drains should be sufficient to drain the deck even in the event that some minor imperfection should develop during deck construction.

Consideration should also be given to the use of the 2-course bonded construction technique for initial construction of concrete bridge decks. The details of this type of

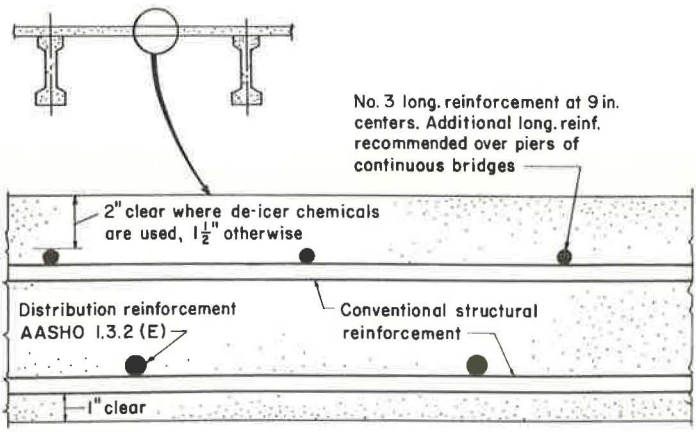

Figure 10. Design recommendations for slab-on-beam bridges.

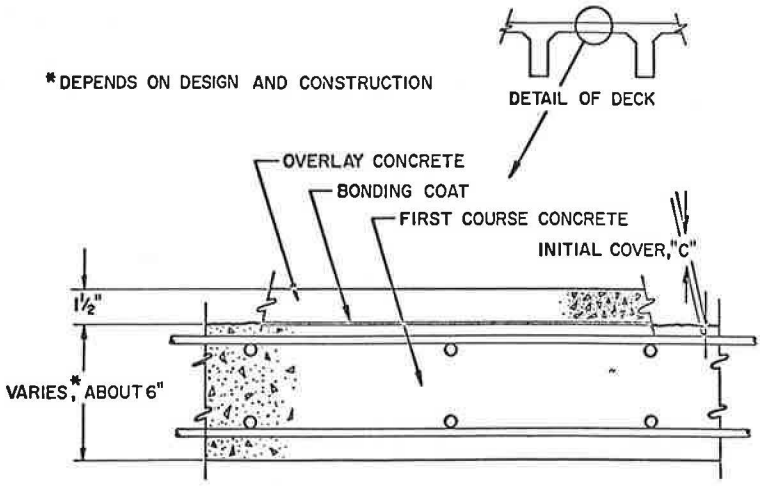

Figure 11. Two-course bonded construction.

construction (which is widely used for industrial floors) are shown in Figure 11. The surface course would be of very high-quality, low-slump, air-entrained concrete bonded to the first course with a portland cement, or an epoxy, bonding coat. The use of high-quality aggregates might be justified for the surface course, and precautions would be taken to obtain low shrinkage characteristics for the surface course. The technique tends to minimize the effect of restraint to subsidence by the reinforcement, and ensures that a specified amount of cover is obtained over the top reinforcement with placement of the overlay.

In regard to concrete quality, it is recommended that concrete used for bridge decks should conform to the specifications given in Table 4. The 4,500 and 4,000 psi compressive strengths are recommended on the basis of durability considerations, regardless of the values assumed for the purpose of structural design of the deck slab.

It is apparent from these cooperative studies, and from bridge deck studies made by many others, that inadequate construction practice has played a major role in the development of many present durability problems. Examples of shallow cover, ponding of water in gutters, high water-cement ratio pastes at the wearing surface, excessive

TABLE 4

SUGGESTIONS FOR QUALITY OF BRIDGE DECK CONCRETE

Maximum Size of Concrete Aggregate (in.)	Maximum Water-Cement (gal/bag)	Minimum Cement Content (bag/cu yd)	Air Content (±1 percent)	Slump (±½ in.)	Minimum 28-Day Compressive Strength[a] (psi)
Freeze-Thaw Areas					
½	5	7.6	8	2½	4,500
¾	5	7.0	7	2½	4,500
1	5	6.6	6	2½	4,500
1½	5	6.2	5.5	2½	4,500
Areas of No Freeze-Thaw					
½	5.5	7.0	5.5	2½	4,000
¾	5.5	6.4	5	2½	4,000
1	5.5	6.0	4.5	2½	4,000
1½	5.5	5.6	4	2½	4,000

[a]Not more than 20 percent of the strength tests should have values less than those indicated here.

variations in air content, improper finishing, inadequate curing, and other durability-reducing practices have all been observed, and are described in the volume of literature on this subject. Although the problems are generally recognized, much remains to be done to provide the adequate inspection and to obtain the improved practices that are required.

ACKNOWLEDGMENT

The views expressed in the paper are those of the authors and do not necessarily reflect the views of the U. S. Bureau of Public Roads or of the cooperating state highway departments.

REFERENCES

1. Klieger, P., and Fountain, R. S. A Cooperative Bridge Deck Study. HRB Bull. 323, 1962, pp. 23-25.
2. Durability of Concrete Bridge Decks, A Cooperative Study: Kansas Detailed Investigation. Portland Cement Assn., Rept. 1, 1965.
3. Durability of Concrete Bridge Decks, A Cooperative Study: Michigan Detailed Investigation. Portland Cement Assn., Rept. 2, 1965.
4. Durability of Concrete Bridge Decks, A Cooperative Study: California Detailed Investigation. Portland Cement Assn., Rept. 3, 1967.
5. Durability of Concrete Bridge Decks, A Cooperative Study: Missouri Detailed Investigation. Portland Cement Assn., Rept. 4, 1967.
6. Durability of Concrete Bridge Decks, A Cooperative Study: Random Surveys. Portland Cement Assn., Rept. 5, 1969.
7. Durability of Concrete Bridge Decks, A Cooperative Study. Portland Cement Assn., Final Report, in press.

Laboratory and Field Tests on Concrete Sealing Compounds

J. RYELL and B. CHOJNACKI, Department of Highways, Ontario

This report describes field and laboratory tests to determine the effects of concrete curing compounds, concrete surface-sealing compounds, and products described as combined curing and sealing compounds on the resistance of air-entrained and non-air-entrained concrete to freezing and thawing in the presence of de-icing salts. Emphasis is placed on the performance of a boiled linseed oil-kerosene mixture as a surface sealer. The report concludes that the performance of sealing compounds applied to hardened concrete is not impressive and recommends that the present general practice of applying 2 coats of linseed oil-kerosene solution to exposed new concrete bridge decks and pavements in Ontario be discontinued. The most important single factor in the attainment of durable concrete is that the concrete be properly air-entrained. In this respect a vigorous policy of ensuring that concrete is air-entrained should be pursued by personnel engaged in concrete quality control in highway work.

•THE ADOPTION OF AIR-ENTRAINMENT by the Department of Highways, Ontario, in the early 1950's reduced, but did not eliminate, the incidence of surface scaling on exposed concrete. This initial lack of success with air-entrainment can be attributed to a poor specification (3 to 5 percent air) and insufficient control to ensure that the placed concrete was air-entrained. Protective coatings were then used as a means of preventing or arresting the deterioration of concrete. It seemed logical that if concrete could be kept dry, and water and de-icing salts could be prevented from entering the concrete, it would remain durable.

A silicone treatment for asphalt-covered concrete bridge decks was initiated in 1956, but abandoned in 1961 when it was apparent that silicone did not prevent scaling. A 2-coat boiled linseed oil-kerosene mixture was tried on concrete pavement in 1959 and later used for all concrete that might be exposed to de-icing salts. The laboratory and field tests that led to these decisions have been reported previously by Smith (1) and Hussell (2). The air content specified for structural concrete (¾ in. coarse aggregate) was increased to 5 to 7 percent in 1957.

In spite of these measures, some exposed concrete continued to scale. For example, a long section of concrete pavement in Ottawa has a very objectionable degree of surface deterioration after 9 years. This concrete received an initial 2-coat application of boiled linseed oil and kerosene.

In 1962 the department's inspectors were instructed to determine the air content of each truckload of concrete to be placed in exposed locations and to reject all concrete containing an insufficient volume of air. These measures, and those previously mentioned, have almost eliminated scaled concrete on present-day department work. As an example no significant scaling has occurred on the approximately 2 million sq yd of concrete pavement and exposed bridge decks constructed on the Toronto bypass of Highway 401 between 1964 and 1969. The field tests described in this report were initiated in 1960 when the values of silicones and linseed oil solutions were being investigated, and at a time when epoxy resin coatings were widely recommended for the

Paper sponsored by Committee on Curing of Concrete and presented at the 49th Annual Meeting.

protection of concrete. The gradual change from wet burlap curing to curing with a resin-type white-pigmented compound that took place from 1965 onward raised doubts as to whether the linseed oil compound could penetrate into the concrete and effectively seal the surface. Surface brushing prior to application of the linseed oil removed little of the curing compound film. During this period various chlorinated rubber compounds were marketed in Ontario with claims that their application as a curing compound provided protection against the penetration of moisture into the matured concrete.

The laboratory tests described in this report were initiated in 1965 to evaluate the effect of a linseed oil treatment on concrete cured with a resin-type curing compound. In addition 4 chlorinated rubber compounds were tested to evaluate their efficiency as sealing compounds when applied to plastic or hardened concrete.

MATERIALS TESTED

The materials tested can be divided into 3 groups depending on their functions, and each group into types depending on the material composition. The group and types of the materials were as follows:

1. Concrete curing compounds. Material C-1, used only in the laboratory tests, was a white-pigmented hydrocarbon resin-based compound with a mineral spirits-type solvent. It was applied to the finished concrete surfaces by spraying immediately after the water sheen had disappeared. The rate of application was 200 sq ft/gal.
2. Concrete curing and sealing compounds. Three white-pigmented chlorinated rubber-based materials, CS-1, CS-2, and CS-3, and 1 clear chlorinated rubber-based material, CS-4, were included in the laboratory tests only. Compound CS-1 was a chlorinated rubber-epoxy mixture. Each material was applied to the finished concrete surface by spraying immediately after the water sheen had disappeared. The rate of application was 200 sq ft/gal.
3. Concrete surface-sealing compounds. The boiled linseed oil, S-1, was diluted with kerosene in proportions 1:1 by volume. In the laboratory tests the material was sprayed onto the surface of the concrete at an application rate of 375 sq ft/gal for each coat. All specimens received 2 coats. In the field tests the material was brushed onto the concrete at an application rate of 200 sq ft/gal for the first coat and 260 sq ft/gal for the second coat. Field sections were treated with 1 or 2 coats.

The linseed oil emulsions, used only in the laboratory tests, were mixed with water in proportions 1:1, S-1-1, or 2:1, S-1-2, by volume. Each material was applied in 2 coats by spraying at a rate of 375 sq ft/gal for each coat.

The chlorinated rubber compounds, S-2 clear and S-3 containing a fugitive dye, were used only in the laboratory tests. The materials were applied by spray to the concrete surface at the rate of 200 sq ft/gal. Compound S-3 was a chlorinated rubber-epoxy mixture.

The 2 white-pigmented products, CS-1 and CS-3 referred to earlier, were also tested in the laboratory as surface-sealing compounds. The application rate was 200 sq ft/gal.

The epoxy resin compound S-4 was used only in the field tests. Two coats were brushed onto the concrete at the following application rates for each coat:

Compound	Sq Ft/Gal
S-4-0 (no solvent)	104
S-4-1 (epoxy to solvent 2:1 by volume)	192
S-4-2 (epoxy to solvent 1:1 by volume)	292

The solvent-soluble silicone, S-5, and the water-soluble silicone, S-6, were used only in the field tests. The materials were applied by brush at a rate of 167 sq ft/gal for each coat. Panels were treated with either 1 or 2 coats. The solvent-soluble silicone contained 5 percent solids and the water-soluble silicone 3 percent.

LABORATORY TESTS

The materials tested in the laboratory were evaluated by using 2 types of scaling specimens, air-entrained and non-air-entrained concrete, and a number of curing procedures (S-1 only). Tables 1, 2, 3, and 4 give the curing procedures, the surface treatments, and the scale ratings of the test slabs.

Concrete Mixes

Both the air-entrained and non-air-entrained concrete mixes were proportioned to have a cement content of 525 ± 10 lb/cu yd of concrete and a slump of 3 ± ¼ in. The air-entrained concrete had an air content of 6 ± ½ percent. Concrete materials were a type 1 cement, a ¾-in. crushed dolomitic limestone coarse aggregate, a natural fine aggregate, and a vinsol resin air-entraining agent. The concrete was mixed in a 3½-cu ft rotating drum mixer.

Fabrication of Specimen Slabs

Two types of scaling slabs were fabricated. Type A specimens were cast in a mold with a granular base to simulate pavement concrete; type B specimens were cast on a nonabsorptive base to simulate bridge deck concrete. Eight type B slabs were made from mixes LO-20 and LO-21. Four type A and 4 type B (series LO) or 2 type A and 2 type B (series 100 and 200) were made from other concrete batches. Slabs were 9 by 12 by 4 in. (depth) and cast in epoxy-coated plywood molds.

TABLE 1

SCALING TEST RESULTS OF CURING COMPOUNDS

lab Type and Number	Type of Curing	Sealing Compound	Day Scale Test Started	Type of Slab Casting	Scale Rating[a] by Number of Freeze-Thaw Cycles								
					10	20	30	40	50	75	100	125	150
AEC[b]													
LO-11-1	C-1[c], LA28	None	28th	A[d]	0.75	1.25	2.25	3.25	3.25	5.00	—	—	—
				B[e]	1.00	1.50	2.25	3.75	3.75	5.00	—	—	—
LO-11-2	C-1, LA28	S-1[f]	28th	A	0	0	0	0.50	0.50	1.25	3.25	3.50	4.00
				B	0	0	0	0.75	0.75	1.25	2.75	3.25	4.25
LO-16-1	C-1, LA28	None	28th	A	0	0	0	0	1.00	1.75	2.50	2.75	3.50
				B	0	0	0.25	0.50	0.75	1.25	1.50	1.50	1.75
LO-16-2[g]	C-1, LA28	S-1[f]	28th	A	0	0	0	0	0.50	1.50	1.75	2.75	3.25
				B	0	0	0.25	0.25	0.25	0.50	0.75	0.75	1.25
LO-18-1	C-1, LA28	None	28th	A	0	0	0	0	0.25	0.25	0.25	0.50	0.50
				B	0	0	0	0	0	0.75	1.50	1.75	2.50
LO-18-2	C-1, LA28	S-1[f]	28th	A	0	0	0	0.25	0.50	1.00	1.00	1.00	1.50
				B	0	0	0	0	0	0.50	0.75	0.75	0.75
LO-20-1	C-1, LA28	None	28th	A	—	—	—	—	—	—	—	—	—
				B	1.00	2.00	2.50	3.00	3.25	4.00	4.00	4.50	4.50
LO-20-2	C-1, LA14	None	14th	A	—	—	—	—	—	—	—	—	—
				B[h]	1.50	2.00	3.50	3.75	4.00	4.00	4.50	4.50	4.50
LO-20-3	MR3[i]+LA25[j]	S-1[f]	28th	A	—	—	—	—	—	—	—	—	—
				B	0	0	0	0	0	1.00	3.50	5.00	—
LO-20-4	MR14+LA14	S-1[f]	28th	A	—	—	—	—	—	—	—	—	—
				B	0	0	0	0	0	0.75	1.75	2.75	4.75
NAEC[k]													
LO-21-1	C-1, LA28	None	28th	A	—	—	—	—	—	—	—	—	—
				B	1.50	3.50	5.00	—	—	—	—	—	—
LO-21-2	C-1, LA14	None	14th	A	—	—	—	—	—	—	—	—	—
				B	5.00	—	—	—	—	—	—	—	—
LO-21-3	MR3+LA25	S-1[f]	28th	A	—	—	—	—	—	—	—	—	—
				B[l]	0	0	0	0	0	1.00	5.00	—	—
LO-21-4	MR14+LA14	S-1[f]	28th	A	—	—	—	—	—	—	—	—	—
				B	0	0	0.50	2.00	2.00	5.00	—	—	—

[a]The scale ratings shown represent either the average of 2 slabs or, when 1 slab reached a rating of 5.0, the rating of the remaining slab.
[b]Air-entrained concrete.
[c]White-pigmented resin-type curing compound.
[d]Slabs cast on sand bases.
[e]Slabs cast in watertight molds.
[f]Linseed oil-kerosene mixture.
[g]Surface wire-brushed before application of linseed oil-kerosene mixture.
[h]One slab reached 5.0 at 135 cycles.
[i]Curing in moist room at 73 F and approximately 100 percent relative humidity for 3 days.
[j]Air dry-curing at 73 F for 25 days.
[k]Non-air-entrained concrete.
[l]One slab reached 5.0 at 70 cycles.

TABLE 2

SCALING TEST RESULTS OF CURING AND SURFACE SEALING COMPOUNDS

Slab Type and Number	Type of Curing	Sealing Compound	Day Scale Test Started	Type of Slab Casting	Scale Rating[a] by Number of Freeze-Thaw Cycles								
					10	20	30	40	50	75	100	125	150
AEC[b]													
100	CS-4 LA28	CS-4[c]	28th	A[d]	0	0.50	0.50	0.50	0.50	0.75	1.00	1.00	1.25
				B[e]	0	0.50	0.50	0.50	0.50	0.75	1.00	1.00	1.00
101	CS-1 LA28	CS-1[f]	28th	A	0	0	2.00	2.50	3.00	3.25	3.25	4.25	4.25
				B[g]	0.25	0.25	4.25	4.25	4.50	4.50	4.50	4.50	5.00
102	CS-2 LA28	CS-2[h]	28th	A	0	0	1.25	2.25	2.75	2.75	3.00	3.50	4.00
				B[g]	0	0	1.75	3.25	3.25	3.00	3.00	3.50	4.00
103	CS-3 LA28	CS-3[h]	28th	A	0	0	0.50	1.00	2.50	2.75	3.00	3.00	3.25
				B	0	0	0.75	0.75	2.50	3.00	3.00	3.75	4.25
199	MR14[i]+LA14[j]	None	28th	A	0	0.50	0.50	0.50	0.50	0.50	0.50	0.50	0.50
				B	0.50	0.75	0.75	0.75	0.75	0.75	0.75	0.75	0.75
NAEC[k]													
100N	CS-4 LA28	CS-4	28th	A	0	0.50	0.50	0.50	0.50	0.50	2.50	3.75	5.00
				B	0.25	3.25	5.00	—	—	—	—	—	—
101N	CS-1 LA28	CS-1	28th	A	0.50	0.50	5.00	A + B reached 5 at 25 cycles					
				B	0	0	5.00						
102N	CS-2 LA28	CS-2	28th	A	0	2.25	2.75	3.75	5.00	—	—	—	—
				B	0	4.50	5.00	—	—	—	—	—	—
103N	CS-3 LA28	CS-3	28th	A	0	0.50	2.00	2.50	3.50	4.50	5.00	—	—
				B	0	0	1.00	1.50	3.00	3.50	3.75	4.50	4.50
199N	MR14+LA14	None	28th	A	0.50	0.75	1.50	2.00	4.50	4.50	5.00	—	—
				B[l]	0.50	3.00	4.00	4.00	5.00	—	—	—	—

Note: On slabs treated with a curing and surface-sealing compound, the product was sprayed onto the surface of the plastic concrete immediately after cessation of bleeding.

[a]The scale ratings shown represent either the average of 2 slabs or, when 1 slab reached a rating of 5.0, the rating of the remaining slab.
[b]Air-entrained concrete.
[c]Clear chlorinated rubber product.
[d]Slabs cast on sand bases.
[e]Slabs cast in watertight molds.
[f]White-pigmented epoxy chlorinated rubber product.
[g]One slab reached 5.0 at 55 cycles.
[h]White-pigmented epoxy chlorinated rubber product.
[i]Curing in moist room at 73 F and approximately 100 percent relative humidity for 14 days.
[j]Air dry-curing at 73 F for 14 days.
[k]Non-air-entrained concrete.
[l]One slab reached 5.0 at 35 cycles.

TABLE 3

SCALING TEST RESULTS OF SURFACE SEALING COMPOUNDS—BOILED LINSEED OIL

Slab Type and Number	Type of Curing	Sealing Compound	Day Scale Test Started	Type of Slab Casting	Scale Rating by Number of Freeze-Thaw Cycles								
					10	20	30	40	50	75	100	125	150
AEC[a]													
LO-1-1	MR3+LA25	None	28th	A[b]	1.25	1.25	1.75	1.75	1.75	1.75	2.25	2.25	2.50
				B[c]	0.50	0.50	1.50	1.50	1.50	1.50	1.75	1.75	2.00
LO-1-2	MR3+LA25	S-1[d]	28th	A	0	0	0	0.50	1.00	1.75	2.50	2.50	3.00
				B	0	0	0.50	0.50	1.75	3.00	3.00	3.25	3.25
LO-2-1	PF3[e]+LA2	None	5th	A	1.00	1.00	1.25	1.50	1.75	1.75	1.75	2.00	2.00
				B	0.50	0.75	1.50	1.75	2.00	2.00	2.00	2.00	2.00
LO-2-2	PF3+LA2	S-1[f]	5th	A	0	0	0	0.25	0.50	1.00	3.00	4.00	4.00
				B	0	0	0.50	1.00	1.00	1.25	4.00	4.50	4.50
LO-3-1	PF7+LA2	None	9th	A	0.50	0.50	0.50	0.50	0.50	0.50	0.50	0.50	1.00
				B	0.75	1.00	1.25	1.75	2.25	2.25	2.50	2.75	2.75
LO-3-2	PF7+LA2	S-1[g]	9th	A	0	0	0	0	0	0.25	0.75	1.50	1.75
				B	0	0.25	0.25	0.50	1.00	1.50	2.50	3.50	3.50
LO-4-1	MR14+LA14	None	28th	A	0.25	0.75	0.75	0.75	0.75	0.75	0.75	1.00	1.00
				B	0.25	0.75	0.75	0.75	0.75	1.00	1.00	1.00	1.00
LO-4-2	MR14+LA14	S-1[h]	28th	A	0	0	0	0	0	0	0.50	0.50	0.50
				B	0	0	0	0	0	0	0	0.25	0.50
LO-5-1	MR14+LA14	S-1[i]	28th	A	0	0	0	0	0	0	0.50	1.00	1.00
				B	0	0	0	0	0	0	0.25	0.50	0.75
LO-5-2	MR14+LA14	S-1[j]	28th	A	0	0	0	0	0	0.75	1.75	1.75	2.00
				B	0	0	0	0	0	1.25	2.50	2.50	2.50
LO-13	MR3[k]+LA25[l]	S-1[d]	28th	A	0	0	0.25	0.25	1.25	2.25	3.00	3.25	3.25
				B	0	0	0.50	0.50	0.75	1.25	2.00	3.50	3.75
LO-14	MR3+LA25	S-1-1[d]	28th	A	0	0	0.50	0.75	2.00	2.50	2.50	2.50	2.50
				B	0	0	0.25	0.75	1.25	1.75	2.00	2.00	2.00
LO-15	MR3+LA25	S-1-2[d]	28th	A	0	0	0.50	0.50	0.50	2.75	2.75	2.75	2.75
				B	0	0	0.50	0.50	1.25	2.25	2.50	2.75	2.75

[a]Air-entrained concrete.
[b]Slabs cast on sand bases.
[c]Slabs cast in watertight molds.
[d]Applied on 21st and 22nd day after slab fabrication.
[e]Curing with a polyethylene film at 73 F for 3 days.
[f]Applied on 3rd and 4th day after slab fabrication.
[g]Applied on 7th and 8th day after slab fabrication.
[h]Applied 3 and 27 hr after removal from moist room.
[i]Applied on 15th and 16th day after slab fabrication.
[j]Applied on 16th and 17th day after slab fabrication.
[k]Curing in moist room at 73 F and approximately 100 percent relative humidity for 3 days.
[l]Air dry-curing at 73 F for 25 days.

TABLE 4

SCALING TEST RESULTS OF SURFACE SEALING COMPOUNDS—OTHER THAN BOILED LINSEED OIL

Slab Type and Number	Type of Curing	Sealing Compound	Day Scale Test Started	Type of Slab Casting	Scale Rating[a] by Number of Freeze-Thaw Cycles								
					10	20	30	40	50	75	100	125	150
AEC[b]													
200	MR14[c]+LA14[d]	S-2[e]	28th	A[f]	0	0	0.25	0.50	0.50	0.50	0.50	0.75	1.25
				B[g]	0	0	0.75	1.00	1.00	1.25	1.50	1.50	2.00
201	MR14+LA14	CS-1[h]	28th	A	0	0	0	0	0	0.50	0.50	0.50	1.50
				B	0	0	0	0	0	0.50	0.50	0.50	1.25
203	MR14+LA14	CS-3[i]	28th	A	0	0	0	0.50	0.50	0.50	0.50	0.50	0.75
				B	0	0	0	0	0	0.50	0.50	0.50	1.25
204	MR14+LA14	S-3[j]	28th	A	0.25	0.25	0.25	0.25	0.25	0.25	0.25	0.25	0.25
				B	0.50	0.50	0.50	0.50	1.00	1.00	1.00	1.25	1.75
299	MR14+LA14	None	28th	A	0.75	0.75	0.75	0.75	0.75	0.75	1.00	1.00	1.75
				B	1.00	1.00	1.00	1.00	1.00	1.00	1.00	1.25	1.50
NAEC[k]													
200N	MR14+LA14	S-2	28th	A[l]	0.50	1.25	2.75	4.00	4.00	5.00	—	—	—
				B	0	0.75	3.00	4.75	5.00	—	—	—	—
201N	MR14+LA14	CS-1	28th	A	0	5.00	—	—	—	—	—	—	—
				B[m]	0	4.25	4.50	5.00	—	—	—	—	—
203N	MR14+LA14	CS-3	28th	A	0	1.75	1.75	5.00	—	—	—	—	—
				B	0	1.50	3.75	5.00	—	—	—	—	—
204N	MR14+LA14	S-3	28th	A	0.75	3.00	3.50	5.00	—	—	—	—	—
				B	3.50	5.00	—	—	—	—	—	—	—
299N	MR14+LA14	None	28th	A	2.50	5.00	—	—	—	—	—	—	—
				B	2.75	5.00	—	—	—	—	—	—	—

Note: On slabs treated with a surface-sealing compound, the product was sprayed onto the surface of the hardened concrete 1 day after removal of the slabs from the moist room.

[a]The scale ratings shown represent either the average of 2 slabs or, when a slab reached a rating of 5.0, the rating of the remaining slab.
[b]Air-entrained concrete.
[c]Curing in moist room at 73 F and approximately 100 percent relative humidity for 14 days.
[d]Air dry-curing at 73 F for 14 days.
[e]Clear chlorinated rubber product.
[f]Slabs cast on sand bases.
[g]Slabs cast in watertight molds.
[h]White-pigmented epoxy chlorinated rubber product.
[i]White-pigmented chlorinated rubber product.
[j]Epoxy chlorinated rubber product with red fugitive dye.
[k]Non-air-entrained concrete.
[l]One slab reached 5.0 at 40 cycles.
[m]One slab reached 5.0 at 20 cycles.

Each specimen was cast by filling the mold with concrete and compacting with 75 strokes of a $\frac{5}{8}$-in. standard tamping rod. Excess concrete was removed and the surface leveled with 2 passes of a 1-in. wide screed using a sawing motion. Immediately after the water sheen disappeared, the surface was burlap dragged (1 pass). The type of curing is given in Tables 1, 2, 3, and 4.

Application of the Compounds

If a curing or a curing and sealing compound, was to be applied, a groove was made around the edges of the slab, and it was sealed with a wax immediately following the burlap dragging. The curing and the curing and sealing compounds were applied soon after the burlap dragging operation. The times the sealing compounds were applied are given in Tables 1, 2, 3, and 4.

Demolding of the Specimens

Each slab was demolded the day before the scaling test was started and a 1 by 1 in. epoxy mortar dike was cast around the edges to retain the sodium chloride solution. After the dike was made, the slab was left at normal laboratory air conditions for approximately 24 hours.

Scaling Test

The day after the dike was cast the surface of the slabs was flooded with a 3 percent sodium chloride solution to a depth of $\frac{1}{2}$ in. and freeze-thaw cycling was started. The freeze-thaw cycle was obtained by placing the slabs in a walk-in cold room at -10 F overnight and thawing them the next day at normal laboratory air temperature. After each 5 cycles, the slabs were washed and the solution was replaced.

The progress of scaling was observed after each 5 freeze-thaw cycles by visually comparing the scaling of the test slabs with the scaling of standard slabs. The standard slabs had scale ratings of 0 to 5 as follows:

Condition	Rating
No scale	0
Scattered spots of light scale without exposure of the coarse aggregate	1
Light scale over most of the surface with several spots slightly exposing coarse aggregate	2
Scattered spots of moderately deep scale with exposure of the coarse aggregate	3
Moderately deep scale over the entire surface	4
Deep scale over the entire surface	5

The test was discontinued after 150 freeze-thaw cycles or when the slab reached a scale rating of 5 whichever occurred first. After exposure to 150 freeze-thaw cycles, slabs LO-1 to LO-5, untreated or treated with linseed oil, were drained of salt solution and stored dry at normal laboratory air conditions for 15 days. During this period, one of the type A and one of the type B of the untreated and of the linseed oil-treated slabs were treated with 2 coats of linseed oil (seventh and eighth day). Seven days after the new treatment, all the slabs were exposed to further scaling tests for a total of 300 cycles.

LABORATORY TEST RESULTS AND DISCUSSION

The test results are given in Tables 1 through 4 and are shown in Figures 1, 2, and 3, separately for each group of materials. Each figure in the tables represents an average scale rating of 2 slabs. Slabs with the same general identification, e.g., LO-11-1 and LO-11-2, were made from the same batch of concrete.

Type of Specimen

The difference in scaling between the type A and type B slabs was analyzed at 50 and at 150 cycles. In both cases the A slabs cast on the sand bases generally scaled slightly less than the B slabs cast in watertight bases. This is in agreement with the test results obtained by Timms (3).

Curing Compounds

This series of tests was designed to measure the effect of a linseed oil treatment on air-entrained specimens cured with a white-pigmented curing compound. Additional

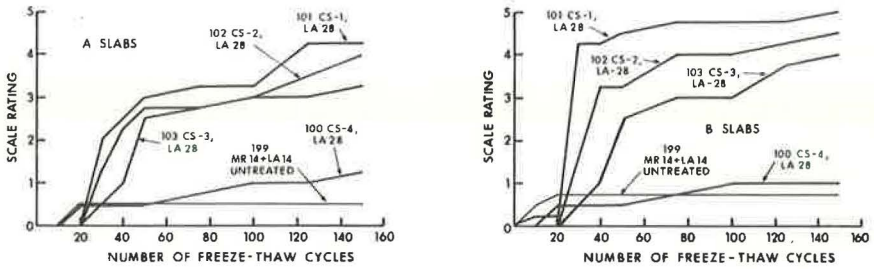

Figure 1. Effect of curing and surface-sealing compounds on the scaling resistance of air-entrained concrete.

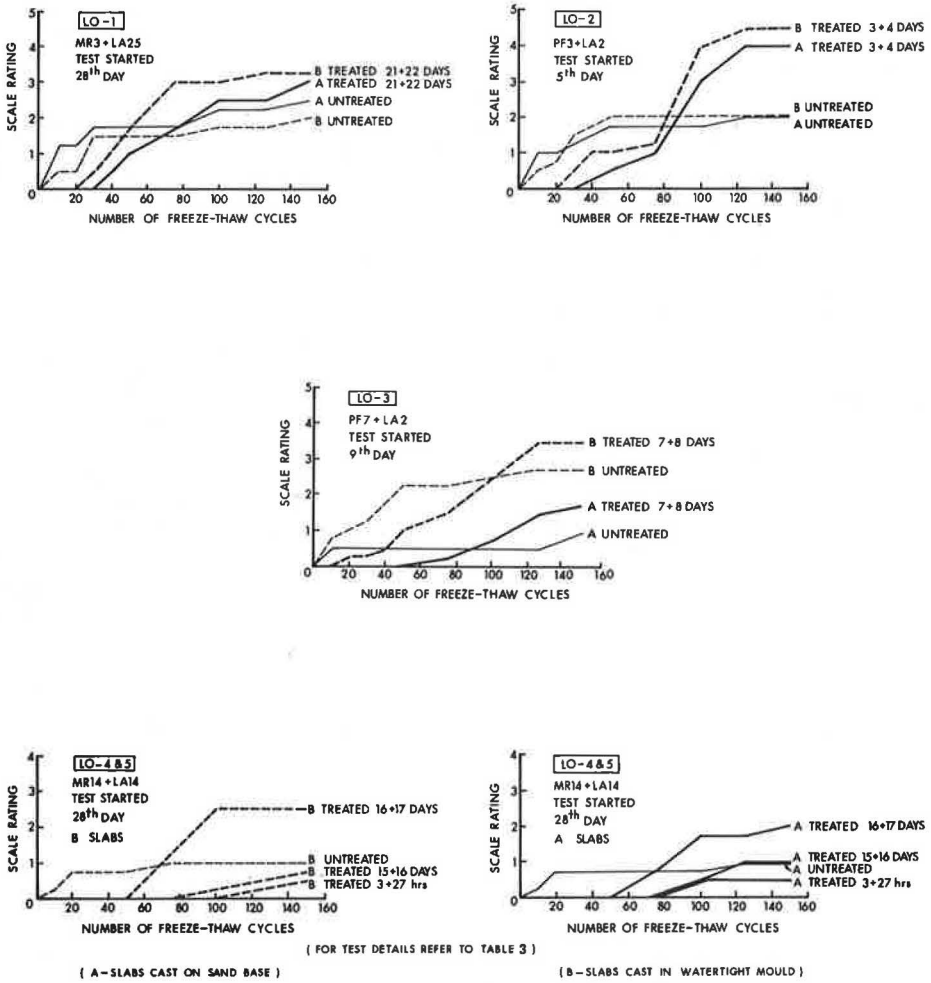

Figure 2. Effect of surface-sealing compounds (boiled linseed oil) on the scaling resistance of air-entrained concrete.

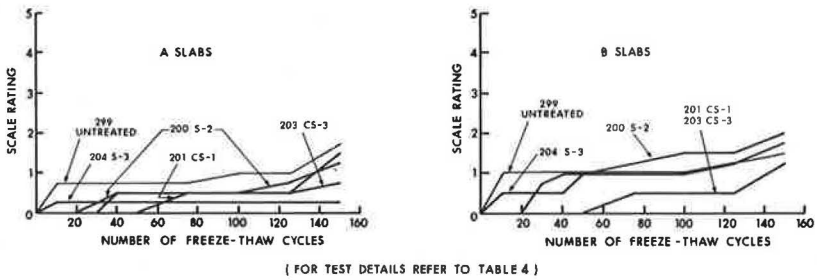

Figure 3. Effect of surface-sealing compounds (other than boiled linseed oil) on the scaling resistance of air-entrained concrete.

tests were carried out to compare the durability of untreated specimens cured with a curing compound with the durability of moist-cured, linseed-oil treated slabs on both air-entrained and non-air-entrained concrete.

In general on air-entrained concrete, it was observed that the curing compound film had peeled from the surface of the specimens after exposure to 10 to 40 freeze-thaw cycles. Slabs treated with the boiled linseed oil-kerosene mixture retained the film for a somewhat greater number of freeze-thaw cycles than the untreated slabs. The boiled linseed oil-kerosene mixture retarded the progress of scaling; at 50 cycles the treated concrete had a lower scale rating than the untreated concrete. This reduction in scaling was due to a higher resistance of the curing membrane to peeling rather than to the penetration of the concrete by the boiled linseed oil-kerosene mixture. During application of the boiled linseed oil-kerosene mixture, it was observed that the film of the curing compound softened somewhat and hardened again after evaporation of the solvent. It is thought that this change in character of the protective film is responsible for the improved resistance to salt scaling. Visual observations of cut sections of slabs, treated with linseed oil, indicated that the solution did not penetrate through the film of the curing compound into the concrete.

Moderate wire-brushing of the membrane-cured surface prior to application of the linseed oil in specimens LO-16-2 did not remove the membrane from the low spots, and it is unlikely that much penetration of linseed oil into the concrete was achieved. A comparison of the 4 sets of the LO-20 slabs shows that linseed oil-treated, moist-cured specimens had a much better scale resistance after 50 cycles than the membrane-cured concrete. The durability of these sets of specimens after 150 cycles, however, was very similar.

Non-air-entrained specimens (LO-21) also show that the untreated membrane-cured concrete has a much lower durability at 50 cycles than the boiled linseed oil-kerosene treated, moist-cured concrete. However, once scaling commenced on the treated specimens, the concrete surfaces deteriorated at a high rate.

Curing and Surface-Sealing Compounds

Each of the 3 white-pigmented curing and sealing compounds, CS-1, CS-2, and CS-3, started to peel from the slabs after exposure to approximately 5 cycles (Table 2 and Fig. 1). In most cases, the membrane completely peeled from the slabs at approximately 25 cycles. Figure 1 shows that at 50 as well as at 150 cycles all the air-entrained concrete slabs (101, 102, and 103) cured with the white-pigmented materials (CS-1, CS-2, and CS-3) had a much higher scale rating than the moist-cured concrete (199) and the concrete (100) cured with a clear curing and sealing compound (CS-4).

The non-air-entrained concrete slabs (100N) of type A cured with the clear curing and sealing compound (CS-4) had a considerably lower initial scaling than the slabs cured moist or with the white-pigmented compounds. The slabs cured with the white-pigmented compounds and the moist-cured slabs (101N, 102N, 103N, and 199N) had little scaling up to 20 cycles; after 20 cycles the scaling progressed at a high rate. Type B slabs scaled rapidly after approximately 10 cycles.

The curing and sealing compound film protects the concrete against scaling as long as it remains in an unbroken state on the surface of the concrete. Because the compound is applied when the concrete is saturated surface dry, it does not penetrate the concrete. It forms a film on the surface of the concrete, and once this film is broken and peels the protection is lost. The variation in the scaling of the slabs is at least partially due to the variation in the number of cycles at which the film peels off.

Surface-Sealing Compounds

The boiled linseed oil-kerosene treatment of the concrete surfaces had a retarding effect on the progress of scaling up to approximately 75 cycles (Table 3 and Fig. 2). After this number of freeze-thaw cycles, the untreated specimens with some exceptions (LO-4-2 and LO-5-1) scaled less than the treated specimens regardless of the type of slabs or the method of curing.

Slabs LO-4-2, which received a 14-day moist-curing and a linseed oil treatment 3 and 27 hr after removal from the moist room, exhibited a very high durability and had little scaling at 150 freeze-thaw cycles. This suggests that the moisture content of the concrete at the time the linseed oil is applied has an important effect on the scale resistance of the concrete and that a long period of drying out of the concrete prior to the application of the sealer may not be beneficial to concrete durability. Snyder's work leads to a similar conclusion (4).

The untreated control slabs, regardless of curing condition or age at commencement of test, had relatively good resistance to scaling; specimens cured in the moist room or under polyethylene film for 7 days or longer had a higher durability than slabs with a short curing period (3 days). A similar order of performance can be observed for the linseed oil-treated slabs. On non-air-entrained concrete using 2 curing procedures, the linseed oil treatment postponed concrete scaling for 20 or 50 cycles, but after that time the slabs scaled very rapidly.

The 2 linseed oil emulsions evaluated in a brief test program had an effect on the scale resistance of air-entrained concrete generally similar to that of the linseed oil-kerosene mixture (LO-13 to LO-15).

Slabs in the series LO-1 to LO-5 with an initial linseed oil treatment generally benefited from retreatment at 150 freeze-thaw cycles, whereas slabs without an initial treatment showed apparently no benefit from being treated at 150 cycles. However, the maximum increase in the scale rating of the originally treated slabs, between 150 and 300 cycles, was 2.5 in contrast to the maximum increase in the scale rating of the originally untreated slabs of only 0.5.

Figure 3 shows that the effect of chlorinated rubber surface sealers on the resistance of air-entrained concrete to scaling was negligible. Both the untreated and treated slabs had good durability, and little difference in scaling at 150 cycles is evident. Some products delayed the start of scaling for up to 50 cycles.

The chlorinated rubber products had little effect on the resistance to scaling of the non-air-entrained concrete. Both treated and untreated slabs scaled rapidly. It is interesting to compare the effect of the 3 chlorinated rubber products when tested as curing and sealing compounds and tested as sealing compounds only (Figs. 1 and 3). The 2 white-pigmented products (CS-1 and CS-3) performed much better when applied to the hardened concrete as a sealing compound. The clear product (CS-4 and S-2) had a similar effect on the scaling resistance of the concrete for the 2 applications. In the case of the white-pigmented products, it is thought that the penetration of the chlorinated rubber into the surface of the hardened concrete resulted in a more durable protective membrane.

FIELD TESTS

The field tests were carried out on a 2,200-ft length of curb and gutter section of the Queen Elizabeth Way near Bronte, Ontario. The curb and gutter form part of the boulevard on the 6-lane section of the controlled-access highway. Part of the test area is located on the structure crossing Bronte Creek, and the remainder is on the east approach to the bridge. The northwest and southeast curb and gutter on the structure and the northwest curb and gutter on the approach form the test area. This section of the Queen Elizabeth Way has an annual average daily traffic (AADT) volume of 38,900 vehicles and receives many salt applications each winter to maintain a bare pavement.

The test section consists of 102 panels of bridge curb and gutter and 100 panels of pavement curb and gutter. Sealing compounds were applied to 157 panels, and 45 panels formed the untreated control sections. Products S-1, S-4, S-5, and S-6 were applied to the pavement section; and products S-1, S-5, and S-6 were applied to the bridge section (Table 5). Panels for each product and control panels were laid out consecutively along the test section.

After each winter the test area was inspected and each panel rated by using the same system as used in the laboratory tests. Photographs of the standard slabs were used in the field inspection; in rating the panels no reference was made to previous

TABLE 5

SEALING COMPOUNDS USED IN FIELD TESTS

Sealing Compound	Product Description	Number of Coats	Number of Test Panels in Location Indicated		
			Pavement C and G	Bridge C and G	Total
S-1	Boiled linseed oil-kerosene mixture	1 or	6	20	26
		2	13	6	19
S-4-0	Epoxy resin, no solvent	2	4	—	4
S-4-1	Epoxy resin, 33 percent solvent	2	7	—	7
S-4-2	Epoxy resin, 50 percent solvent	2	8	—	25
S-5	5 percent solvent-soluble silicone	1 or	—	20	20
		2	19	6	25
S-6	3 percent water-soluble silicone	1 or	—	18	18
		2	20	6	26
Control untreated panels			18	26	44

Note: The 4 sealing compounds were applied, in addition, to a short section of non-air-entrained pavement curb and gutter, 1 panel for each sealer.

observations. The average scale ratings of the treated and untreated panels are given in Table 6 and shown in Figure 4.

Construction Details

The concrete sections were cast between September 17 and November 3, 1960, as part of a normal department construction contract. Concrete was supplied from a ready-mixed plant (10 miles from the job site) to the following specification: cement content, 525 lb/cu yd; maximum slump, 2½ in.; air content, 6 ± 1 percent; and lignin water reducing admixture ¼ lb/87½ lb of cement. The admixture and air-entraining agents were intentionally omitted from one load of concrete to produce a 60-ft section of non-air-entrained concrete on the pavement section of the test area. The concrete was cured with 2 layers of burlap that was kept wet for a period of 4 days after placement of the concrete.

Application of Sealing Compounds

The sealing compounds were applied to the concrete on October 29, November 14, and November 16, 1960. The average air temperature during the period of application on these 3 days was 60, 55, and 55 F respectively.

The concrete in the bridge curb and gutter section was 31 or 32 days old, and the concrete in the pavement curb and gutter section was 11 to 46 days old at the time of application of the sealing compounds. The concrete surface was clean and dry. With the exception of the linseed oil-kerosene solution (S-1), the materials dried rapidly and the second coat, where specified, was applied the same day. Table 5 gives the number of panels and the number of coatings for each of the sealing compounds.

TABLE 6

SUMMARY OF SCALE RATINGS IN FIELD TESTS

Location[a]	Sealing Compound	Product Description	No. of Coats	No. of Panels	Average Scale Rating		
					2 Years	5 Years	7 Years
P and B[b]	None		None	44	1.0	1.1	1.5
P and B	S-1	Linseed oil-kerosene mixture	1 and 2	45	0.7	1.6	2.4
P and B	S-6	3 percent water-soluble silicone	1 and 2	44	0.7	0.9	1.4
P and B	S-5	5 percent solvent-soluble silicone	1 and 2	45	0.8	1.1	1.7
P	S-4	Epoxy resin	2	19	0.8	0.7	1.0
All Panels				197	0.8	1.1	1.7

Note: Non-air-entrained concrete section not included.

[a]P and B = pavement and bridge; P = pavement only. [b]Untreated control sections.

Tests on Concrete Cores

In 1965, eleven 6-in. diameter cores were drilled from the test section. The surface of each core was ground and polished, and the parameters of the air void system were determined by using linear traverse and modified point count techniques (ASTM C 457). With the exception of the purposely non-air-entrained concrete, and 1 core taken from the pavement curb and gutter, the concrete in the test section appeared to contain an adequate system of air voids for high freeze-thaw durability.

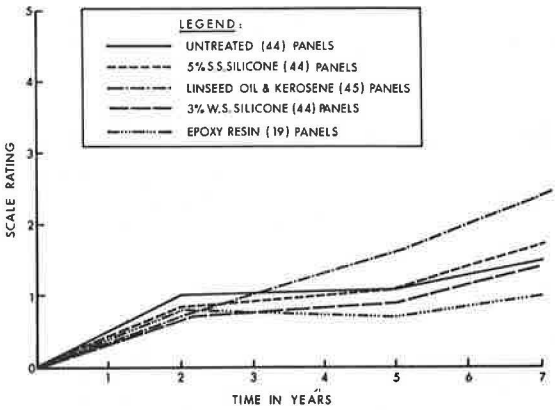

Figure 4. Field test performance of treated and untreated air-entrained sections (average ratings plotted).

FIELD TEST RESULTS AND DISCUSSION

The average scale rating of the 197 panels (purposely non-air-entrained concrete not included) was as follows: after 2 years, 0.8; after 5 years, 1.1; and after 7 years, 1.7. Thus, in general, the concrete in the test sections had excellent durability. The average type of deterioration, i.e., a light scaling over part or all of the test panels, is in fact loss of a thin skin of surface laitance that must be accepted as normal for site-cast concrete subject to freeze-thaw conditions with de-icing salts on the surface.

The absence of large differences between the durability of the various test sections precludes any dramatic evidence of good or bad performance of the sealing materials. The untreated control panels generally performed well, pointing again to the very adequate performance of quality entrained concrete.

Some trends in performance of the 4 surface sealers are evident and these are discussed.

Effect of Location

It is known that concrete in a bridge deck slab has a more severe exposure condition than concrete in a pavement because the deck slab can freeze from both sides. During precipitation at low temperatures ice may form on a bridge deck earlier than it forms on the adjacent pavement.

The most severe concrete deterioration to the curb and gutter occurred at the west end of the bridge where in a length of 300 ft, 16 of 24 panels were rated 3 or higher after 7 years. Tests on a core taken from a panel with a rating of 4.5 indicate that the concrete below the scaled surface was adequately air-entrained. The relatively poor performance of this section of concrete is attributed to loss of air in the near-surface portion of the concrete curb and gutter. Variations in concrete finishing techniques such as overworking of a nonplastic surface with water sprinkled onto the concrete might account for such loss of air.

The average ratings of the untreated panels, the panels treated with the linseed oil-kerosene mixture, and the panels treated with the 2 silicones, indicate no significant difference in the performance of concrete curb and gutter on the bridge and adjacent to the pavement.

Effect of Linseed Oil-Kerosene (S-1)

When compared with the untreated control concrete, the concrete treated with linseed oil generally had marginally increased durability up to 2 years and significantly decreased durability at 7 years. The reduced durability of the linseed oil-treated concrete after 7 years will not in all probability affect the service life of the concrete; but, as the data show, an initial 2-coat application of the material is not efficient as a

permanent surface sealer. The data indicate little difference in the performance of concrete on the bridge or on the pavement sections, or of concrete treated with 1 coat or 2 coats of linseed oil-kerosene mixture.

Effect of 5 Percent Solvent-Soluble Silicone (S-5)

The silicone sealer had no significant effect on the durability of the concretes and, in general, silicone-treated concrete performed in a similar way to the untreated control concrete. Two coats of silicone did not produce a more durable concrete than 1 coat.

Effect of 3 Percent Water-Soluble Silicone (S-6)

Regardless of location or number of coats of silicone applied, there appeared to be no significant difference between the durability of silicone-treated concrete and the durability of the untreated control concrete.

Effect of Epoxy Resin (S-4)

The thin film of epoxy resin that remained on the surface of the concrete after application quickly deteriorated, and after 7 years of exposure there is little evidence of the epoxy film.

The epoxy resin coating appeared to have a slight beneficial effect on the durability of the concrete, and the average 7-year scale rating of 1 is the lowest scale rating of any of the test sections. The scale rating of the epoxy-treated concrete decreased slightly between 2 and 5 years (Table 6). This is indicative of the limitations of a visual scale rating system and not a reflection of actual performance of the concrete.

After 7 years of exposure, concrete treated with undiluted epoxy (4 panels only) exhibited almost no surface scaling, and more than half of all the epoxy-treated panels had a rating of less than 1. It should be noted that there are no epoxy-treated panels on the bridge curb and gutter section.

Non-Air-Entrained Concrete

After 7 years of exposure the 5 panels of non-air-entrained concrete on the pavement section of the curb and gutter exhibit significant deterioration. None of the 4 sealers applied to this concrete (S-1, S-4, S-5, and S-6) had a beneficial effect on durability. The degree of surface scaling on this concrete, although not yet a reason for replacing the curb and gutter section, would be highly objectionable on an exposed bridge deck or concrete pavement.

CONCLUSIONS

The field and laboratory tests warrant the following conclusions:

Untreated Concrete

1. Untreated moist-cured, air-entrained concrete generally has excellent durability.
2. Untreated non-air-entrained concrete has poor durability.

Curing Compounds

3. Air-entrained concrete cured with a resin-type white-pigmented curing compound has a lower durability than moist-cured concrete.
4. The application of a linseed oil-kerosene mixture to concrete cured with the resin-type curing compound will postpone the start of surface scaling.

Curing and Surface-Sealing Compounds

5. There is considerable variation in the performance of the combined curing and sealing compounds. Air-entrained concrete treated with the clear chlorinated rubber

product has excellent durability; concrete treated with the white-pigmented chlorinated rubber products has a significantly lower durability than untreated moist-cured concrete.

Surface Sealing Compounds

6. An initial application of a linseed oil-kerosene treatment to moist-cured air-entrained concrete will reduce the surface scaling during the early life of the concrete but results in a small increase in scaling at later ages.
7. Retreatment of scaled concrete with a linseed oil-kerosene mixture has a beneficial effect on concrete durability.
8. There is no significant difference between the performance of an emulsion-type linseed oil and that of a boiled linseed oil-kerosene mixture.
9. The 2 silicone sealers, evaluated only in the field tests, have no significant effect on concrete durability.
10. The epoxy resin sealer, evaluated only in the field tests, has a beneficial effect on concrete durability when applied undiluted in 2 coats.
11. Chlorinated rubber sealing compounds applied to moist-cured air-entrained concrete delayed the start of scaling and in most cases resulted in some improvement in durability throughout the test.
12. In most cases the sealing compounds tested delayed the start of scaling on non-air-entrained concrete. The initial application of a sealing compound on non-air-entrained concrete did not, in any test, result in permanently durable concrete.

EFFECTS OF TRAFFIC WEAR AND CONCRETE SURFACE TEXTURE

Two factors not present in either the laboratory or the field tests must be taken into account when the test data are considered so that a fair assessment can be made on the value of the sealing compounds when applied to concrete pavements and bridge decks. These factors are the effect of traffic wear on the life of the sealing compound and the effect of the standard Ontario wire-broom surface texture on the uniformity of penetration of sealing compounds.

Traffic Wear

The wear from normal rubber-tired traffic rapidly removes the film of white-pigmented resin curing compound from the surface of the hardened concrete, and it must be assumed that chlorinated rubber compounds will perform no better. Thus any compound applied initially as a curing compound to the plastic concrete and having no penetration into the concrete cannot be considered as acting as an efficient sealing material once traffic uses the pavement. This factor would also negate the improvement that a linseed oil treatment produced on membrane-cured concrete in the laboratory tests because traffic would quickly remove this "resealed" membrane.

The relatively new problem of wear due to studded tires (5) must also be considered because not only will a surface membrane be very rapidly destroyed but the depth of wear in the wheel tracks during 1 winter will equal or exceed the penetration depth of a linseed oil solution, which according to Stewart and Shaffer (6) is absorbed to less than 0.01 in.

Concrete Surface Texture

The wire-broom texturing operation currently used on concrete pavement and exposed bridge deck construction in Ontario produces closely spaced grooves $\frac{1}{8}$ to $\frac{3}{16}$ in. in depth. A low viscosity sealing compound such as linseed oil applied to such a surface cannot produce uniform penetration of the concrete. Most of the solution will rapidly drain into the grooves resulting in greater penetration there but with less sealer and thus less penetration on the ridges of the pavement.

REAPPLICATION OF SEALING COMPOUNDS

There is evidence from this and other studies that frequent reapplication of sealing compounds may be more effective than only an initial application. Although some testing in this project was concerned with reapplication, it has not been generally considered in the study because of the unacceptable procedure of closing busy urban streets and highways for the time necessary to clean the pavement, apply the sealing compounds, and allow the pavement surface to dry.

RECOMMENDATIONS

Based on this study, the following recommendations are made regarding the control of air-entrainment, the curing of concrete, and the use of concrete sealing compounds on pavement and bridge deck construction in Ontario.

1. The most important single factor in the attainment of durable concrete is that the concrete be properly air-entrained. In this respect a vigorous policy of ensuring that concrete is properly air-entrained should be pursued by personnel engaged in quality control work.
2. The use of white-pigmented curing compounds as an alternative to wet burlap curing should be continued. Although the laboratory tests indicate that membrane-cured concrete is less durable than moist-cured concrete field experience shows that its scale resistance is adequate.
3. The department's present practice of applying 2 coats of linseed oil-kerosene mixture to exposed new construction, i.e., bridge decks and pavements, should be discontinued.
4. The ineffective chlorinated rubber-based curing and sealing products should not be used.
5. Where concrete develops surface scaling during service, it should be treated annually with a low-cost sealing material such as linseed oil. Where the distressed concrete is not a traveled pavement surface, for example the top of a bridge pier, 2-coat treatment of epoxy resin is preferable.

REFERENCES

1. Smith, P. Observations on Protective Surface Coatings for Exposed or Asphalt-Surfaced Concrete. HRB Bull. 323, 1962, pp. 72-94.
2. Hussell, D. J. T. Freeze-Thaw and Scaling Tests on Silicone-Treated Concrete. Highway Research Record 18, 1963, pp. 13-32.
3. Timms, A. G. Factors Affecting Resistance of Portland Cement Concrete to Scaling Action of Thawing Agents. Public Roads, Vol. 28, No. 7, April 1955.
4. Snyder, M. J. Protective Coatings to Prevent Deterioration of Concrete by Deicing Chemicals. NCHRP Report 16, 1965.
5. Schonfeld, R., and Smith, P. Pavement Wear Due to Studded Tires and the Economic Consequences in Ontario. Research Branch, Department of Highways, Ontario, Rept. RR152, 1969.
6. Stewart, P. D., and Shaffer, R. K. Investigation of Concrete Protective Sealants and Curing Compounds. Highway Research Record 268, 1969, pp. 1-16.

Discussion

C. E. MORRIS, National Flaxseed Processors Association—The authors state that the reduction in scaling of test slabs treated with boiled linseed oil-kerosene mixture was due to the higher resistance of the treated curing membrane to peeling. There appear to be no data substantiating this conclusion.

It is also stated that visual observations of cut sections of slabs of concrete treated with linseed oil indicate that the solution did not penetrate through the film of the c' \g

compound into the concrete. It is agreed that penetration of concrete by linseed oil solutions is difficult to detect by ordinary visual observations. Gast, Kubie, and Cowan reported at the 1970 meeting of the HRB Committee on Curing of Concrete that a technique has been developed for measuring precisely the penetration of linseed oil into concrete. They show that penetrations of 1 to 3 mm are accomplished into blocks cured either with polyethylene sheeting or with resin-based or wax-based liquid membrane-forming commercial curing compounds when the oil is applied as a 50/50 mixture by volume of boiled linseed oil and mineral spirits.

Mineral spirits is a much preferred solvent to kerosene because its properties are defined by ASTM, AASHO, and U. S. Government specifications. Kerosene, on the other hand, is less precisely defined and may also contain greasy residues. Hence, it is probable that much better penetrations will be achieved without a tendency to form a varnish-like coating if proper application rates and procedures are observed.

The formation of a varnish-like coating on the surface may well be the cause of nonpenetration. This varnish layer tends to peel off the surface as it weathers, taking with it a thin layer of mortar sufficient to affect the scale rating. Moreover, the scaled areas are then exposed to subsequent attacks by de-icing salts.

The authors agree that reapplication would be effective in preventing the onset of scaling but state that the "unacceptable" procedure of closing busy streets and highways makes the procedure unfeasible. It should be pointed out that experience has shown that regular applications are highly beneficial when performed on a regular schedule. The recommended procedure is the application of 1 single coat 1 year (50-100 freeze-thaw cycles) after the initial application of a 50/50 mixture of boiled linseed oil and mineral spirits at the rate of 225 sq ft/gal. Subsequent coats should be applied at 2- to 3-year intervals depending on the severity of conditions. By proper scheduling during the warm season of the year, it is possible to apply the coating to 1 lane at a time, and the lane need be closed for not more than 4 hours during the period of relatively light traffic. In most cases drying will occur well within this time and, in the cases where it does not, the judicious application of silica sand will obviate any skidding or safety hazard.

A point should also be made of the rate of application reported. The quantities used are about double those presently recommended. These heavy applications may well be the cause of the varnishing and nonpenetration reported in this study.

J. RYELL and B. CHOJNACKI, Closure—The first point made by Mr. Morris concerns the effect of a linseed oil treatment on concrete cured with a membrane compound. In the report we have stated that the linseed oil softened the hardened membrane film somewhat, and it is suggested that this change in the character of the membrane was responsible for the improved resistance to scaling. In any case the membrane treated with linseed oil resisted the process of disintegration or "peeling," as we have called it, better than the untreated membrane-cured concrete. This longer life of the treated membrane is not specifically shown in the tables; its effect is evident from the performance of the salt scaling slabs.

Mr. Morris refers to a committee report of Gast, Kubie, and Cowan that indicates penetration of linseed oil through a film of membrane-curing compound. Subsequent discussion among the authors and another investigator appears to confirm this. We look forward to publication of the work by Gast, Kubie, and Cowan; it should add much to our knowledge of the effect of membranes on the durability of concrete.

It is suggested by Mr. Morris that mineral spirits are a much preferred solvent to kerosene because apparently kerosene may contain greasy residue that produces a varnish-like coating to the concrete. The problems of greasy residues or varnish-like coatings have not occurred in Ontario, and we doubt very much that substitution of mineral spirits for kerosene in our tests would have increased the penetration of linseed oil, or affected the durability of the concrete in any significant way.

The statement in the report covering the "unacceptable" procedure of closing busy streets and highways for the reapplication of linseed oil is certainly a debatable one. In any case, each highway authority will decide for itself just what is unacceptable. The authors doubt that much will be accomplished in closing a highway for 4 hours. Under most conditions the total operation—arranging traffic control, applying the sealing compound, drying out, and removing signs and barricades—for a sufficient length of highway to make the application an economical one will occupy a full working day. The authors do not agree that application of silica sand to a linseed oil treatment that has not dried will obviate skidding. For modern high-speed traffic, it almost certainly will not.

In the last paragraph of the discussion, Mr. Morris refers to "varnishing and nonpenetration reported in this study." We wish to point out that no such phenomena were reported. We agree that the application rate of linseed oil in the field trials was much heavier than is now commonly recommended. In 1960 there was less information on the optimum application rate of linseed oil, and the material was brushed onto the concrete in an amount consistent with what it would take. The application rate did not appear overgenerous. In any case it is difficult to imagine how a heavy application could be less effective than a lighter one.

We would like to thank Mr. Morris for his pertinent and interesting discussion.

Effectiveness of Corrosion Inhibitors and Their Influence on the Physical Properties of Portland Cement Mortars

R. J. CRAIG and L. E. WOOD, School of Civil Engineering, Purdue University

This paper presents the results of laboratory studies using some of the various chemical corrosive admixtures in order to determine their action on physical properties of cement mortar mixes. The compression and splitting tensile strength tests as well as the workability of these mixes were used to determine the influence of the chemical additives on the cement mortar mixes. The ability of these chemical admixtures to prevent corrosion in reinforced concrete was investigated by 2 methods: anodic polarization and visual tests. In these tests, small reinforcing bars were embedded in cement mortar and examined at a later date. Calcium chloride was added in varying amounts along with rust inhibitors to observe their effect on the physical and corrosive protection properties.

•THE PROBLEM OF CORROSION in reinforced concrete has been given considerable attention in the past few years. There have been cases of corrosion that have led to expensive maintenance and repair. The California Division of Highways has had specific problems with bridges near a marine environment. The San Mateo-Hayward Bridge is a good example of corrosion of reinforcing steel in a marine environment. The stirrups in some places have completely disintegrated. There is spalling of the concrete because of the action of corrosion. Where there are cracks in the concrete, rust stains appear on the concrete surface. There have been similar deteriorations in structures located in Florida (1), Texas, Malaya, and South Africa (9).

The presence of calcium chloride has also caused severe corrosion in reinforced concrete, especially under steam-cured conditions. The use of chloride salts as deicers in the northern states has caused deterioration in bridge decks. The salts have penetrated the protective coatings of some bridges and caused corrosion of the reinforcing steel.

The review of literature (3, 15 through 34), which was limited to the addition of inhibitors to portland cement as protective measures, yielded a list of chemicals that in previous studies gave indication of being effective in reducing corrosion attack. The recommended compound groups were chromates, phosphates, hypophosphites, alkalies, and fluorides. The chemicals used in past studies that showed good results in resisting corrosion in reinforced concrete were barium, strontium, lead, and potassium chromates; calcium and silicon fluorides; sodium nitrite; sodium benzoate and sodium metasilicate; ethyl aniline and calcium lignosulfonate; aluminum acetate; chrome oxide; chrome carbides; chlorate; thirourea; and calgon and mercaptobenzothiazole. The review of literature indicated a lack of knowledge concerning the effects of these chemical inhibitors on the physical properties of the mortar or concrete. From this list of chemicals, sodium nitrite, sodium benzoate, and potassium chromate were chosen for this study.

MATERIALS

The basic mortar mix used in this study consisted of 3 different components: cement, Ottawa sand, and water. The corrosion inhibiting chemicals that were added to the

Paper sponsored by Committee on Metals in Highway Structures and presented at the 49th Annual Meeting.

basic mortar mix in varying proportions were selected on the basis of past work by researchers.

Cement

A type 1 normal portland cement that came from the same clinker batch was used in this investigation. This precaution was to ensure that the cement had the same chemical composition. Thus a difference in the physical properties could not be related to a difference in the chemical composition of the cement. The chemical and physical properties of the cement used were not investigated.

Chemicals

The selection of chemicals that serve as rust inhibitors had to be carefully made. The chemical inhibitors used in this study must act as rust inhibitors in cement paste, must cover the different types of inhibitors that can be used, and must be practical and easy to use in field operations. The selection was based on work that had been performed by other investigators studying the effectiveness of chemical rust inhibitors. The chemicals selected for this investigation were as follows:

1. Sodium nitrite. This chemical is one in the nitrite salt group that acts as an anodic rust inhibitor. It has been recommended by many researchers as a very effective chemical rust inhibitor. Sodium nitrite showed passivation at low concentrations. These concentrations were approximately 1 percent by weight of cement.
2. Potassium chromate. This chemical represents the chromates, the other main type of salt, that are effective as anodic rust inhibitors. The effective concentration of this salt is approximately twice that of the sodium nitrite.
3. Sodium benzoate. This chemical, which is one in the anodic inhibitor group, required large concentrations to have a beneficial effect in passivation.
4. Calcium chloride. This salt is a very widely used accelerator that is added tc concrete. It has been found by some investigators to cause corrosion of reinforcing steel in concrete. This chemical was added in varying amounts with the rust inhibitors, and its effect on the physical properties of the paste was observed.

Aggregates

To ensure that the aggregate introduced no variation in the results, standard grade natural silica sand from Ottawa, Illinois, that met ASTM Specification C 109 was used. This sand was used in both the compressive and splitting tensile mortar specimens.

Water

The water used in the cement mortar mix was distilled water obtained from the Sanitary Engineering Laboratories. The temperature of the mixing water was kept between 68 and 72 F. The amount of water put into a mortar mix was kept constant. The chemicals were dissolved in the water before the proper amounts were measured.

OUTLINE OF INVESTIGATION

The object of this study was to determine the influence of certain chemical rust inhibitors on some physical properties of cement mortar mixes that had varying amounts of calcium chloride present. These properties were workability, compressive strength, and splitting tensile strength. Also under investigation was the effectiveness of the admixtures to serve as chemical rust inhibitors. There has been some concern recently with the corrosion of steel in reinforced concrete. Investigations have been directed toward finding different chemical admixtures that will prevent corrosion, but there has been very little effort expended on what would happen to the properties of the hardened paste when these admixtures are added.

In the field, the presence of calcium chloride at times has proved to be a cause in corrosion of reinforcing steel in concrete. Because this chemical is widely used in field practice, various percentages were used in this investigation.

To obtain a true picture of the behavior of the strength properties and workability, an experimental model was set up. The amounts and types of chemicals, materials, procedures, and apparatus were decided. The order in which the specimens were to be cast and tested was developed in a somewhat random procedure. A random mathematical table was used to decrease the day-to-day personal differences in the procedure. The specimens that were to be cast were divided into 3 series. These series, based on the amount of time for curing, were 3-day, 7-day, and 28-day tests. In each series, different combinations of chemical corrosive admixtures were prepared. These 30 different combinations were picked in a random manner from a table of random numbers. Because of the time element in preparing the specimens, this was the extent of randomization of specimens. In each of these 30 combinations, 6 specimens were made: 3 compressive strength specimens and 3 splitting tensile strength specimens. During each casting, 6 different combinations could be made.

It was desirable to evaluate workability of the various combinations because of the necessity of knowing whether the various mixtures could be placed in the field. The flow table was used for measuring the workability of the mixes. This method seemed to give a good indication of this parameter.

There has been some difference of opinion on whether chemical rust inhibitor admixtures produced a passivation of the steel. These opinions were (a) that chemical rust inhibitors would prevent corrosion, (b) that the effectiveness of the inhibitors would be lost after a few years because of leaching, and (c) that the presence of the inhibitors would have no effect. The effectiveness of the 3 chemicals for passivation of the reinforcing steel was investigated by 2 different methods: anodic polarization and visual observation of the piece of reinforcing steel in the split specimen. The ages at which these were to be tested were 4 days for the anodic polarization and 270 days for the visual observations.

APPARATUS AND PROCEDURE

Preparation of Mortar Mixtures

The cement mortar mix proportions remained constant throughout this study. The mix proportions of water, cement, and aggregate were 1:2:5.5 by weight. This gave a good workable mix for all of the chemicals used in this study. The aggregate-cement ratio was taken from ASTM Specification C 109. The amount of water was determined on a trial-and-error basis by flow table measurements prescribed by ASTM Designation C 230. The flow for a nil batch was appromixately 80 percent. The chemicals were added to the mixing water before the water was measured.

The quantities of water, cement, and aggregate were measured to the nearest gram. The chemicals added to the mix were measured to the nearest tenth of a gram. Each batch-day consisted of the making of 36 specimens. That was 6 combinations of 3 compressive and 3 tensile strength specimens. The mixing and casting room temperature was controlled at 68 to 72 F. The relative humidity fluctuated from 50 to 70 percent.

The mechanical mixer used was a Hobart model with a 250 cu in. capacity that conformed to ASTM Designation C 305-64T. The mixing procedure that was adopted for all specimens was the one prescribed in this specification.

Each mix batch contained enough for all compressive and splitting tensile specimens for that particular combination in its series. Flow table measurements were taken immediately after mixing. These measurements were a means for determining the consistency of the mixes; they were also used as a means for determining the workability of the mixes. The flow table conformed to ASTM Designation C 230-61T.

Casting and Curing of Specimens

After it was mixed, the mortar was then cast into molds. The molds used for the compressive strength specimens conformed to the standard 2-in. cube molds of ASTM Specification C 109. The splitting tensile test specimens were formed in 2-in. diameter by 4-in. high cylindrical molds. The placing and compacting were accomplished according to ASTM Specification C 109.

The specimens used in the study of the anodic polarization effectiveness were mixed in the same manner as the compression and splitting tensile specimens. The pieces of steel that were set in the mortar mix had 2 paraffin coats that were placed 2 in. apart to set up a known area of bar surface exposed to the cement mortar. After 24 hours, the specimens were stripped of the paper cup molds and divided into 3 groups. Each group consisted of 1 specimen of each combination as previously described. One group was left exposed to the air at 72 F and 50 to 70 percent relative humidity. The other 2 groups were placed in tap water. After 9 months, one group that was in the water was then subjected to a saltwater bath. The other 2 groups were tested at this time.

Compressive and Splitting Tensile Tests

The compressive and splitting tensile strength measurements were made according to ASTM Specification C 109. Careful alignments were made in placing the specimens in the correct position under the floating head of the testing machine. For the splitting tensile specimens, ¼- by 1- by 6-in. pressed masonite was used for the bearing strips.

The compressive strengths were determined by

$$\sigma_{comp} = \sum \frac{P}{A}$$

where

σ_{comp} = compressive strength, psi;
P = sum of failure loads of the specific combination; and
A = sum of the cross-sectional areas of the specimens, in^2.

The splitting tensile strengths were determined by

$$T = \sum \frac{2P}{ldn}$$

where

T = splitting tensile strength, psi;
P = sum of the failure loads of a specific combination;
l = length, in.;
d = diameter, in.; and
n = number of specimens.

Effectiveness Studies of the Admixtures in Mortar Mix

The specimens were placed in water saturated with calcium hydroxide. An external voltage was applied to the steel reinforcing bar that was in the specimen and was acting as an anode and to a platinum electrode that was acting as a cathode. The potential of the steel was measured relative to a saturated calomel electrode by means of a vacuum tube voltmeter. This apparatus was used for the specimens that were 7 days old.

The anodic effectiveness of the rust inhibitors was performed by measuring the steel potential as a function of the polarization current density per unit area of anode. Definite current values were established between the steel anode and the platinum cathode, starting with the open circuit or zero current value, and the resulting potentials of the anode relative to the calomel electrode were measured. After a potential measurement, the current was increased to the next definite value, and the potential was read again after 5 minutes. This procedure was continued for 7 to 10 five-minute intervals. This procedure is shown in Figure 1 and is the same procedure that was used in the Portland Cement Association study (15).

A visual test was performed on the remaining specimens to determine the effectiveness of the various chemical additives in retarding corrosive attack after 9 months

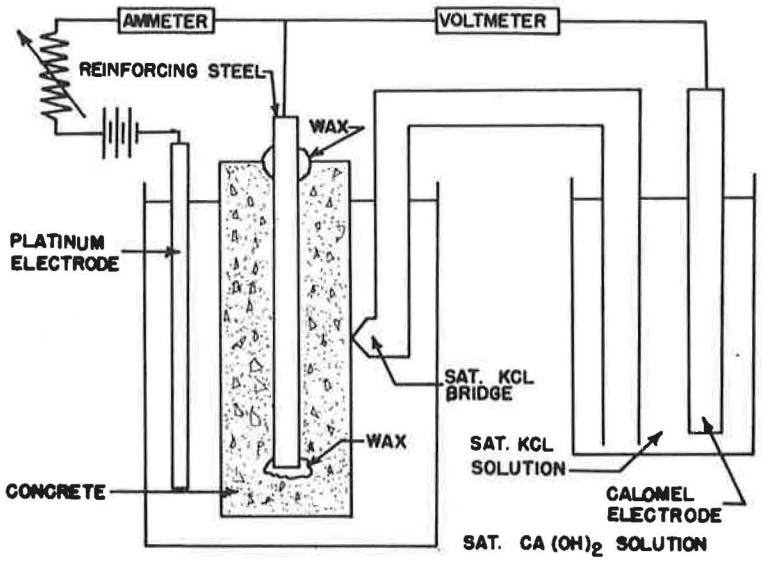

Figure 1. Circuit diagram for polarization measurements (15).

curing. The specimens containing the reinforcing steel were split longitudinally, and the effectiveness was measured by the percentage of corrosion and the severity of attack.

$$\text{Percentage of corrosion} = \frac{Ac}{A_t}$$

where

Ac = corrosive surface on the reinforcing embedded in concrete; and
A_t = total area embedded in concrete (between 2 wax spots).

The corrosion severity was rated from 1 to 5 as follows:

Condition	Rating
Very thin film	1
Thick film	2
Small pitting	3
Medium pitting	4
Severe pitting	5

DISCUSSION OF TEST RESULTS

Physical Properties Observed During Testing

The chemicals that were utilized in this study produced significant physical changes when added to the mortar mixes. The chemical admixtures when mixed with the mortar gave the surface of the specimens different colored appearances. These color changes were not uniform across the surface. The potassium chromate actually gave the mix a light green cast. Most of the other salts produced a whitish color on the surface. While the specimens were kept under controlled curing conditions, the aqueous salt solutions leached to the outer surface of the specimens and formed a thin scum around the outside.

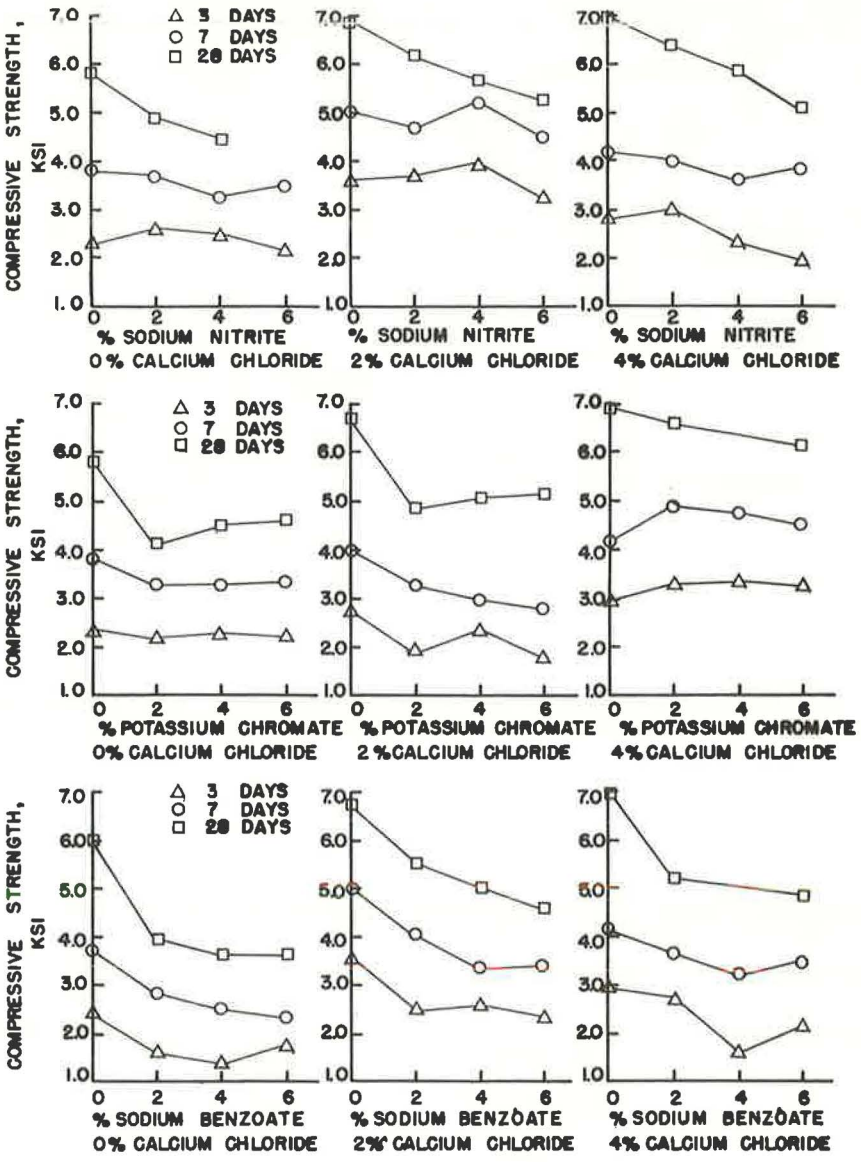

Figure 2. Influence of varying amounts of chemical corrosion inhibitors with specific amounts of calcium chloride on compressive strength of standard mortar cubes.

Compression Strength Test Results

The compressive strength results are shown in Figure 2. Because of the number of combinations and amounts of additives used in this study, compression strength test results will be discussed according to the varying amounts of calcium chloride.

For 0 percent calcium chloride, very little change in compressive strength of mortars was observed at 3 and 7 days with increasing amounts of sodium nitrite and potassium chromate. Increasing amounts of sodium benzoate showed some decrease in compressive strength at 3 and 7 days. A marked decrease in strength at 28 days for increasing amounts of chemicals was observed. The maximum decrease of 28 da

for potassium chromate, sodium nitrite, and sodium benzoate were approximately 33, 20, and 40 percent respectively.

The second set of mixes was based on 2 percent calcium chloride. The potassium chromate addition decreased the compressive strengths approximately 20 percent for all concentrations. As the amounts of sodium nitrite were increased, compressive strength for the various mixes decreased in a somewhat linear fashion to a maximum value of 25 percent for the 28-day strength. Increasing amounts of sodium benzoate decreased the compressive strength again in a linear fashion to a maximum value of 35 percent for the 28-day strength.

The third set of mixes was based on 4 percent calcium chloride. Increasing amounts of potassium chromate and sodium nitrite both gave a linear decrease in compressive strength amounting to a maximum of 20 percent and 30 percent respectively for the 28-day strengths. Increasing amounts of sodium benzoate resulted in strength decreases but did not follow a linear pattern. The maximum reduction in strength was 35 percent at 28 days.

Splitting Tensile Strength Test Results

The splitting tensile strength results, shown in Figure 3, varied with the type of rust inhibitor employed. Both sodium nitrite and sodium benzoate produced a decrease in

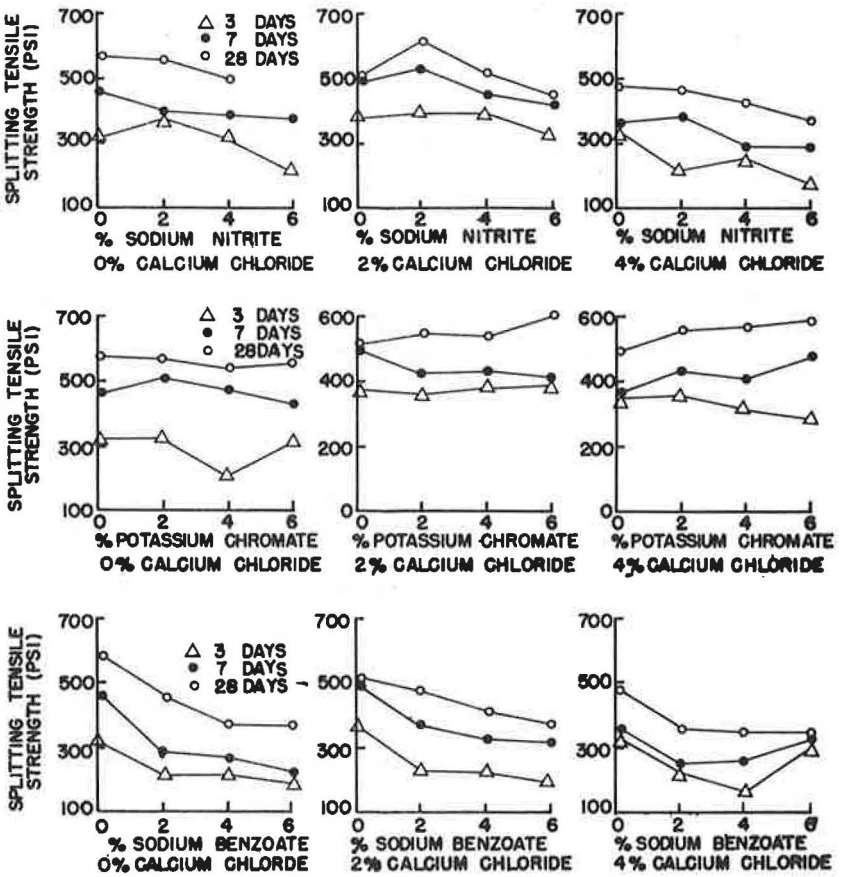

Figure 3. Influence of varying amounts of chemical corrosion inhibitors with specific amounts of calcium chloride on splitting tensile strength of mortar cylinders.

TABLE 1

VISUAL OBSERVATIONS OF REINFORCED MORTAR SPECIMENS FOR ABILITY OF MIXTURES TO PREVENT CORROSION

CaCl (percent)	Chemical		Corrosion—Percentage Exposed Surface						Rating
	Compound	Percent	0	20	40	60	80	100	
0			o -						—
2				o -					4
4					o -				24
0	$NaNO_2$	2	o -						—
0	$NaNO_2$	4	o -						—
2	$NaNO_2$	2	o -						—
2	$NaNO_2$	4	o -						—
0	$Na_3C_7H_5O_2$	4	o -						—
0	$Na_3C_7H_5O_2$	6	o -						—
2	$Na_3C_7H_5O_2$	4			o			-	52
2	$Na_3C_7H_5O_2$	6			-			o	5
0	K_2CrO_4	2	o -						—
0	K_2CrO_4	4	o -						—
2	K_2CrO_4	2			o -				5
2	K_2CrO_4	4		-	o				15

Note: o = specimens cured in air; - = specimens cured in water.

the splitting tensile strength with an increase in the amount of rust inhibitor. This held true for the 0, 2, and 4 percent calcium chloride groups. The maximum reduction was between 20 and 30 percent.

For the case of increasing amounts of potassium chromate with 0 percent calcium chloride, very little change in splitting tensile strength was observed at 3, 7, and 28 days. For increasing amounts of potassium chromate with 2 percent calcium chloride, very little change in strength was observed for 3 and 7 days. At 28 days a slight increase in splitting tensile strength was obtained. With 4 percent calcium chloride, creasing amounts of potassium chromate showed very little change in strength at 3 days, but showed an increase in strength at 7 and 28 days.

Effectiveness of Inhibitors in Reducing Corrosion

In the potential current measurements for the cement mortar mixes, passivity was indicated by a sudden sharp rise in potential at low current densities. The use of the anodic inhibitors, sodium benzoate and potassium chromate, resulted in passivity for

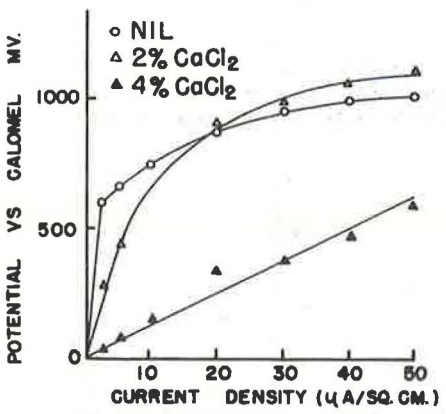

Figure 4. Effect of calcium chloride on anodic polarization of steel in reinforced concrete.

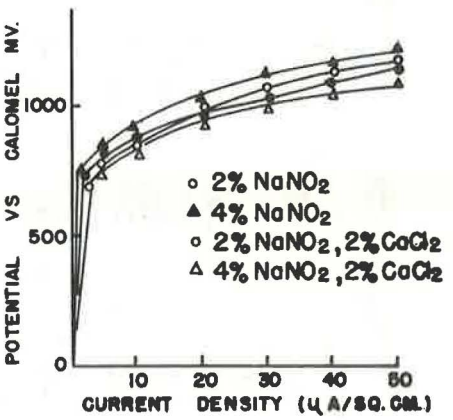

Figure 5. Effect of sodium nitrite on anodic polarization of steel in reinforced concrete.

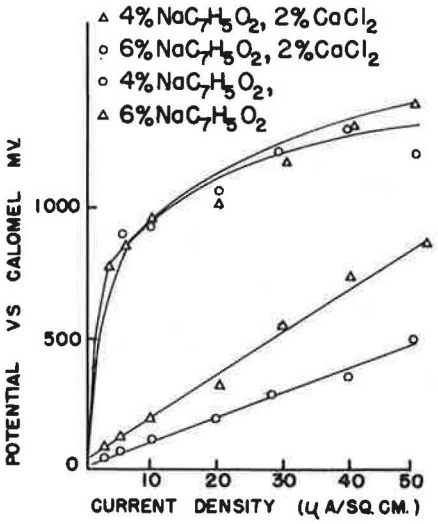

Figure 6. Effect of sodium benzoate on anodic polarization of steel in reinforced concrete.

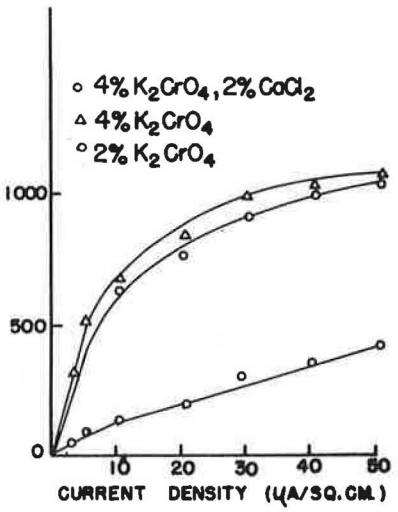

Figure 7. Effect of potassium chromate on anodic polarization of steel in reinforced concrete.

specimens with no calcium chloride in the mix. These same anodic inhibitors displayed no passivity with 2 percent calcium chloride. The sodium nitrite gave indications of being the only anodic inhibitor studied to have passivity when combined with calcium chloride in the mix. The 0 and 2 percent calcium chloride when combined with sodium nitrite gave indications of being passive (Figs. 4, 5, 6, and 7).

When split and examined visually, specimens that were exposed in air and water for 10 months gave similar results to those of the anodic polarization study. From the data given in Table 1, all specimens with 0 percent calcium chloride showed no corrosive action on the reinforcing bar. The only chemical rust inhibitor that showed passivation with calcium chloride was the sodium nitrite inhibitor. The remaining chemical rust inhibitors and calcium chloride showed 10 to 40 percent corrosion area except for the sodium benzoate, which showed 40 to 100 percent. The nil specimens as predicted showed no corrosion because of the pH of the mortar mix. As the percentage of calcium chloride increased in the specimens, the corrosive surface area increased. Similar results were observed for both the air- and water-cured specimens.

Workability of Mixes

The flow table measurements, although a measure of consistency of the mixes, will be used to present a relative picture of the effect of the various salts on the workability. These measurements seemed to give a good indication of the amount of work necessary to place the mortar in the molds (Fig. 8).

The calcium chloride mortar mixes gave a maximum flow of 93 percent at 2 percent calcium chloride and an identical flow of 74 percent at 0 and 4 percent calcium chloride.

The maximum increase in flow was 10 to 25 percent and occurred at 2 percent salt additions. Increased amounts of anodic salts decreased the flow value of the resulting mixes from these maximum values.

The combined mixes of 2 percent calcium chloride and anodic salts decreased the flow of the 2 percent calcium chloride. The flow values for the different salts remain almost constant for the different concentrations of salts except for the 2 percent sodium benzoate whose flow was approximately the same as that of the 2 percent calcium chloride.

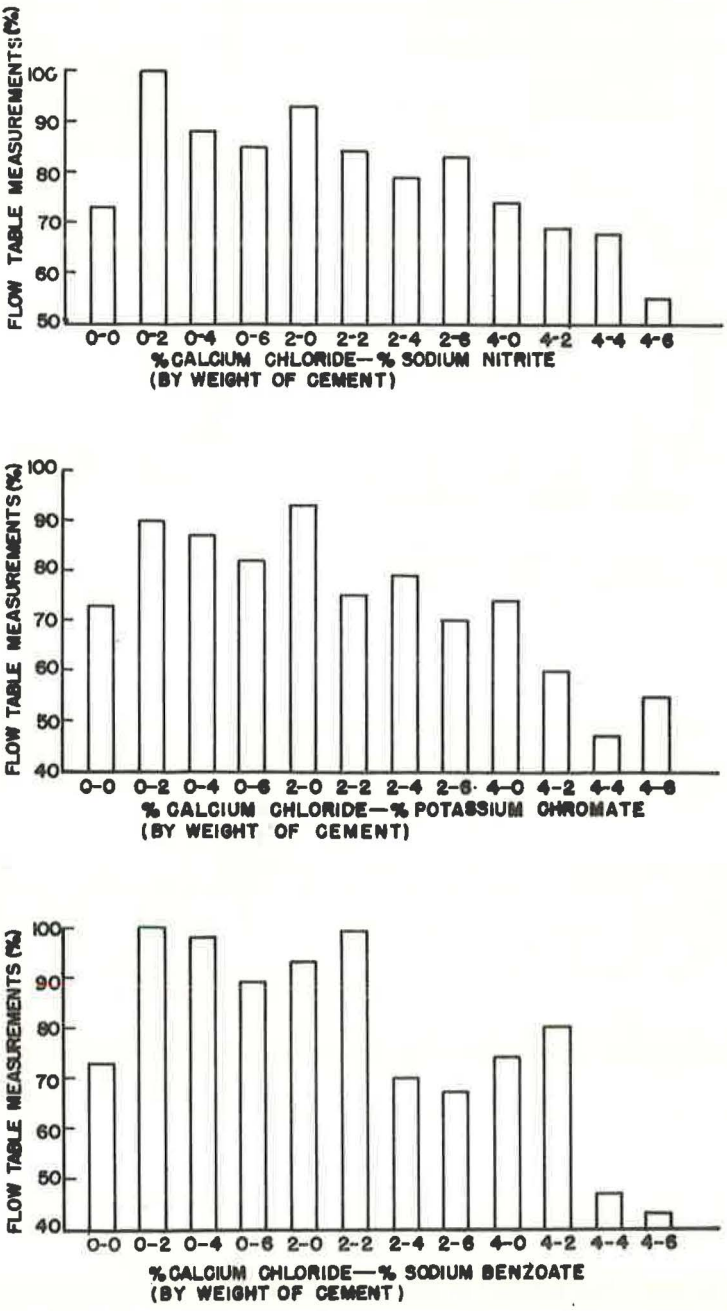

Figure 8. Influence of varying amounts of chemical corrosion inhibitors and calcium chloride on flow table measurements of mortar mix.

The 4 percent calcium chloride and anodic salt combinations behaved somewhat in the same manner as the 2 percent calcium chloride and anodic salt combinations. The flows were all decreased for the 4 percent calcium chloride sets except for the 2 percent sodium benzoate.

CONCLUSIONS

The results of this investigation showed no general trend for all chemical corrosion reducing admixtures under investigation in this study. The results of each individual admixture were presented in the foregoing sections, and only general conclusions will be drawn in this section. Based on this stipulation, the following statements concerning the effects of the various admixtures on the physical properties of portland cement mortars are presented.

1. Sodium nitrite was found to be the only effective chemical reducing admixture of the three that were under investigation.
2. The 28-day compressive strength of mortar mixes is decreased when the anodic rust inhibitors were added to the mix.
3. The presence of the chemical rust inhibitors in the cement mortar mixes increased the fluidity of these mixes. The maximum increase in fluidity occurred with the additions of 2 percent of the inhibitors.
4. The addition of calcium chloride to the cement mortar mixes with the chemical corrosion reducing admixtures decreased the gain in the fluidity obtained when the inhibitors were used by themselves.
5. Calcium chloride present in a cement mortar mix creates a corrosive environment for the reinforcing bar.
6. The mode of corrosion of the reinforcing steel rated from mild to severe pitting as opposed to the desired thin film corrosion when the various chemical admixtures were present in the cement mortar mix.

REFERENCES

1. Mozer, John D., Bianchini, A. C., and Kesler, Clyde E. Corrosion of Reinforcing Bars in Concrete. ACI Jour., Proc. Vol. 62, 1965, pp. 909-931.
2. Hausmann, D. A. Electrochemical Behavior of Steel in Concrete. ACI Jour., Proc. Vol. 61, 1964, pp. 171-187.
3. Moskvin, V. M., and Alekseev, C. N. Methods of Increasing the Resistance to Corrosion of Reinforcement in Reinforced Concrete Structural Members. Beton I Zhelezobeton, No. 1, 1957, pp. 28-29. In Russian.
4. Borgman, C. W. Basic Principles of Metallic Corrosion. In Corrosion of Metals, American Society of Metals, Cleveland, Feb. 1946, pp. 1-29.
5. Pollitt, Alan A. The Causes and Prevention of Corrosion. Ernest Benn, London, 1923, 222 pp.
6. Shalon, R. and Raphael, M. Influence of Sea Water on Corrosion of Reinforcement. ACI Jour., Proc. Vol. 55, 1959, pp. 1251-1268.
7. Ten Year Report on the Long-Time Study of Cement Performance in Concrete. ACI Jour., Proc. Vol. 49, 1953, p. 601.
8. Dean, W. E. Four Lanes Across Tampa Bay at Low Cost. Eng. News-Record, Sept. 20, 1950.
9. Halstead, W., and Woodworth, L. A. The Deterioration of Reinforced Concrete Structures Under Coastal Conditions. Trans. South Afr. Inst. Civil Eng., April 1955, pp. 1-20; also discussion, Oct. 1955, pp. 353-372.
10. Lewis, D. A., and Copenhagen, W. J. Corrosion of Reinforcing Steel in Marine Atmospheres. Corrosion, Vol. 15, No. 7, July 1959, pp. 383t-388t.
11. Monfore, G. E., and Ost, E. Penetration of Chloride Into Concrete. Jour. of PCA Research and Dev. Laboratories, Jan. 1966, pp. 46-52.
12. Griffin, D. L., and Henry, L. R. The Effect of Salt in Concrete on Compressive Strength, Water Vapor Transmission and Corrosion of Reinforcing Steel. Proc. ASTM, Vol. 63, 1963, pp. 1046-1076.
13. Cornet, I. A Short Course in Corrosion. National Assn. of Corrosion Engineers, Univ. of California, Berkeley, 1953, 119 pp.
14. Lavinovich, V. E. Reducing Corrosion in Reinforced Concrete by Addition of Salts. Tekh. Inform., Leningrad. Glavn. Stroitel, Upravlen. pri Leningrad. Gor Ispolnitel n. Komitete 3, 1957, pp. 8-11.

15. Gouda, V. K., and Monfore, G. E. Rapid Method for Studying Corrosion Inhibition of Steel in Concrete. Jour. of PCA Research and Dev. Laboratories, Sept. 1965, pp. 24-31.
16. Admixtures for Concrete. ACI Jour., Proc. Vol. 60, 1963, pp. 1481-1523.
17. Kondo, Y., Takeda, A., and Hideshima, S. Effects of Admixtures on Electrolytic Corrosion of Steel Bars on Reinforced Concrete. ACI Jour., Proc. Vol. 56, 1959, pp. 299-312.
18. Arber, M. G., and Vivian, H. E. The Action of Some Corrosion Inhibiting Admixtures in Mortar. Australian Jour. of Applied Science, No. 12, pp. 435-439.
19. Meier, F. W. Corrosion-Resistant Cements. U. S. 3, 187, 825 (cl. 106-89), April 30, 1963; Ger. Appl., June 4, 1958, 2 pp.
20. Teuber, D., and Eichenlaub, V. Acceleration of Cement Hardening With Simultaneous Corrosion Protection for Steel Reinforcement. East Ger. 35, 910 (cl. CO46), March 25, 1965; Appl., Jan. 12, 1962, 2 pp.
21. Enisherlova, S. G., and Beskov, S. D. Protection for the Corrosion of Reinforcement Steel in Dense Concrete. Uch. Zap. Mosk. Gor. Ped. Inst., No. 181, pp. 154-67.
22. Lind, S. E. G. Reinforced Concrete. Sweden 92, 537, June 8, 1938.
23. W. Werke, GmbH. Corrosion Inhibition of Steel in Concrete. Germany 1, 021,778, Dec. 27, 1957 (cl. 80b).
24. Lewis, J. I. M., Mason, C. E., and Brereton, D. Sodium Benzoate in Concrete. Civil Engineering, Vol. 51, No. 602, Aug. 1956, pp. 881-882.
25. Berthier, R. M. The Corrosion of Iron, Especially Concrete Reinforcements. Revue Materiaux de Construction et de Travaux Public, No. 511.
26. Arber, M. G., and Vivian, H. E. Inhibition of the Corrosion of Steel in Mortar. Australian Jour. of Applied Science, No. 12, 1961, pp. 339-347.
27. Seckin, W. Inhibition of Corrosion in Concrete Reinforcement. Rocla Pipes, Ltd., Australia 219,650, Jan. 20, 1959.
28. Cessna, J. C. Armature Corrosion in Siliceous Concrete. Lietuvos TSR Moks. Akad., Statybos ir Architekt. Inst., Straipsniu Rinkinys, No. 1, 1958, pp. 159-166.
29. Moskvin, V. M., and Alekseev, S. N. Protection of Reinforcements in Porous Concretes From Corrosion. Stroitel'stvo I Arkhitektura, No. 8, 1959, pp. 144-150.
30. Bregman, J. I. Corrosion Inhibitors.
31. Wood, L. E. Protecting of Reinforcing Steel. U. S. Army Engineer Division, Ohio River Corps. of Eng., Sept. 1963.
32. Gewertz, M. W., Tremper, B., Beaton, J. L., and Stratfull, R. F. Causes and Repair of Deterioration to a California Bridge Due to Corrosion of Reinforcing Steel in a Marine Environment. HRB Bull. 182, 1958, pp. 1-41.
33. Tripler, Jr., A. B., White, E. L., Haynie, F. H., and Boyd, W. K. Methods for Reducing Corrosion of Reinforcing Steel. NCHRP Rept. 23, 1966.
34. Calcium Chloride Admixture in Concrete. Structural and Railways Bureau, Portland Cement Assn.

The New Model of Hardened Portland Cement Paste

STEPHEN BRUNAUER, IVAN ODLER, and MARVIN YUDENFREUND,
Institute of Colloid and Surface Science and Department of Chemistry,
Clarkson College of Technology

Feldman and Sereda reject the Powers model of the structure of hardened portland cement paste on the ground that the BET surface area and the porosity of D-dried pastes as measured by water vapor adsorption is wrong because four-fifths of the uptake of water is interlayer water and not adsorbed water. They propose that nitrogen adsorption measures the surface approximately correctly and, on the basis of these ideas, present a new model of paste structure. The present paper shows that water vapor adsorption measures the surfaces and porosities of D-dried pastes correctly, whereas nitrogen measures only part of the surface and porosity. D-dried pastes have no interlayer water nor adsorbed water. Pore structure analysis shows that nitrogen cannot penetrate into many large pores. Completely hydrated D-dried pastes of the same cement have the same surface area when measured by water adsorption regardless of w_o/c, whereas nitrogen areas vary by a factor of almost 3. The data of Feldman and Sereda show that their quick-drying procedure is approximately equivalent to P-drying. P-dried pastes contain both interlayer water and adsorbed water. The energies of binding of these 2 types of water strongly overlap; consequently, they cannot be separated by tests of reversibility. Furthermore, because of the different drying procedure, no conclusion can be drawn from the experiments of Feldman and Sereda for D-dried pastes. The authors of the new model contend that no equilibrium is reached in the surface area measurements by water adsorption on D-dried pastes. It is shown in the present paper that equilibrium was reached in these measurements but was not reached in most of the experiments of Feldman and Sereda. Their desorption isotherms, as well as the loops, by which they attempt to test reversibility, represent nonequilibrium conditions. The main conclusion of the paper is that the authors know of no properly interpreted evidence to date that contradicts the Powers model.

•RECENTLY A NEW MODEL of the structure of hardened portland cement paste has been presented by Feldman and Sereda (1) to replace the old model, called the Powers model. Although much has been added to the original ideas of Powers by his co-workers at the Portland Cement Association, by himself, and by other researchers all over the world, the basic ideas of the model have remained unchanged. The model proposed by Powers and Brownyard (2) achieved an immediate success by correlating 2 physical properties, the surface area and the porosity of the paste, with vital engineering properties such as strength, volume changes, and permeability. The correlation was semi-empirical; further research has removed much of the empiricism and has brought about a more fundamental understanding of the structure of paste.

Paper sponsored by Committee on Basic Research Pertaining to Portland Cement and Concrete and presented at the 39th Annual Meeting.

The surface area and the porosity of the paste were measured by the BET method (3) using water vapor as the adsorbate not only by Powers but by many others, including Brunauer and his co-workers. Feldman and Sereda attempt to show that the use of water vapor for measuring the surface areas and porosities of cement pastes is wrong, and that the correct or almost correct values are obtained by nitrogen adsorption. If this statement is correct, the Powers model falls or must be greatly modified. If the statement is wrong, the model of Feldman and Sereda falls or must be greatly modified.

WATER SURFACE VERSUS NITROGEN SURFACE

The problem of water versus nitrogen surface area was settled by Brunauer, Kantro, and Weise 10 years ago in a paper on the surface energy of tobermorite gel (4). The name tobermorite gel is being replaced now by the less definite term C-S-H gel. The gel is the calcium silicate hydrate produced in the paste and "bottle" hydration of tricalcium silicate (Ca_3SiO_5 or C_3S) and β-dicalcium silicate (β-Ca_2SiO_4 or C_2S); it is also produced in the ball-mill hydration of C_2S. On the basis of Bernal's suggestion, Brunauer named these hydrates of varying composition simply tobermorites; later, on the suggestion of H. F. W. Taylor, he changed the name to tobermorite gel and abbreviated it in some of his papers to tobermorite (G). Because in the present paper numerous references will be made to the papers of Brunauer and his co-workers, the name tobermorite gel will be retained to avoid confusion.

One of the most basic facts of surface science is that atoms, ions, or molecules in the surface have higher energies than those in the body. These excess energies were first calculated by Born and Stern (5) 10 years before the first experimental determinations were made, and all of the numerous theoretical calculations and all of the numerous experimental determinations that have been made since 1919 have led to the same result. The experimental demonstration is very simple: If a substance appears in 2 different states of subdivision, the one with the higher specific surface area has the higher heat of solution.

Brunauer, Kantro, and Weise (4) made 14 different preparations of tobermorite gel by hydrating C_3S and C_2S in different ways, and plotted the heats of solution against the specific surface areas. The slope of such a plot gives the surface energy, which is usually expressed in erg/cm^2. The surface areas were measured by water vapor adsorption for samples of all 14 preparations and by nitrogen adsorption for samples of 8 preparations. The water areas ranged from 244 to 376 m^2/g. In an earlier work, one of the present authors calculated the specific surface area from crystal structure data (6). He showed that if the tobermorite gel sheets are 2 molecular layers thick, the surface area should be 377 m^2/g; if they are 3 molecular layers thick, it should be 251 m^2/g. The values experimentally obtained were closer to these limits than the experimental error. Here is then a strong indication that water adsorption measures the true surface of tobermorite gel. The external plus interlayer surface of tobermorite gel is 755 m^2/g.

The nitrogen surface areas ranged from 100 to 21 percent of the areas measured by water. Whereas the water areas correlated excellently with the heats of solution, the samples with higher surface giving higher heats of solution, there was no such correlation with the nitrogen surface areas. The authors concluded: "That nitrogen does not measure the true surface of tobermorite can be seen from the following considerations. As Figure 1 shows, the heat of solution of tobermorite in D-35 is about 8 cal/g larger than that of the tobermorite in D-28, but the surface area of the former is only about half as large, as measured by nitrogen adsorption (Table VI). This would indicate a negative surface energy, an absurdity. Several other pairs of preparations would, likewise, lead to negative surface energy values." It may be added that nitrogen adsorption for some of these pairs indicated not merely negative surface energies, an absurdity in itself, but large negative surface energies.

The explanation of the nitrogen results is simple. The heats of solution measure the excess energy residing in the entire surface, whereas nitrogen adsorption measures only a part of the surface, which leads to the absurd negative surface energies. In contrast, the water surface areas gave a positive surface energy of 386 erg/cm^2. This an interesting figure.

Earlier, Brunauer, Kantro, and Weise determined the surface energy of calcium hydroxide (7) and hydrous amorphous silica or silanol (8). The value of the former is 1,180 and of the latter, 129 erg/cm^2. The surface areas were measured by nitrogen adsorption, which is an important point to be noted.

The surface energy of a substance depends on the nature and the geometric arrangement of the surface. The calcium hydroxide consisted of almost perfect crystals; the hydrous silica was completely amorphous. Tobermorite gel is intermediate between these extremes; it is very poorly crystallized, and its X-ray diffraction pattern consists of only 3 lines. In addition, the calcium silicate hydrate is what Brunauer has called with some license a "chemical mixture" of calcium hydroxide and hydrous silica. On the basis of these 2 facts and also on theoretical grounds, one can predict that the surface energy of tobermorite gel should be roughly the geometric mean of the surface energies of calcium hydroxide and hydrous amorphous silica. The figure obtained for tobermorite gel on the basis of water surface areas was very close to that.

In later work, the same authors redetermined the surface energy of tobermorite gel (9). The original work was based on 14 preparations—7 obtained by the hydration of tricalcium silicate and 7 obtained by the hydration of dicalcium silicate. The later work was based on 70 C_2S pastes, 58 C_3S pastes, and 27 alite pastes. Not only was the sample larger, but also the theoretical evaluation was more accurate. The new value was 450 erg/cm^2; still roughly the geometric mean of the surface energies of calcium hydroxide and hydrous amorphous silica. Furthermore, the lowest surface measured for any of about 150 mature pastes was 243 m^2/g, and the highest was 387 m^2/g; values still within experimental error were those calculated by Brunauer from X-ray data for tobermorite gel sheets consisting of 3 and 2 molecular layers respectively. These data are in line with electron microscopic observations, which indicate that the thickness of the sheets is the order of a unit cell. (In the new model, the thickness of the sheets is around 15 molecular layers.) In the early stages of hydration, higher surface areas were obtained, ranging up to nearly 600 m^2/g, indicating that the gel also contained sheets of a single molecular layer.

The conclusion from all this is that nitrogen adsorption measures only a part of the surface, whereas water vapor measures the true and correct surface. A corollary of this conclusion is that at p_o, the saturation pressure of the vapor, water measures the total porosity of the paste, whereas nitrogen measures only a part of the porosity.

It may be worth mentioning that Wittman determined the surface energy of completely hydrated cement paste by a much less accurate method than that described above, and obtained a very rough value of 400 erg/cm^2 (10). The main interest in this work is that both the theoretical approach and the experimental approach were totally different from ours. If the surface of tobermorite gel were less than one-fifth as large as that measured by us, which is the contention of the new model, the surface energy would be more than 5 times as large as ours, roughly 2,300 erg/cm^2, or twice as large as that of $Ca(OH)_2$. There is no surface energy in the literature as high as this value.

This brings up the question as to whether the tobermorite gel in portland cement pastes has the same surface area as in pastes of the calcium silicates. The question was answered long ago, but the results were not published. Verbeck obtained excellent water adsorption data for numerous completely or almost completely hydrated portland cement pastes of widely differing compositions at a relative humidity of 36 percent. For many of these pastes v_m values were also available; these values represent the number of molecules necessary to cover the entire surface with a single adsorbed layer. It was found that the adsorption at 36 percent relative humidity and v_m differed by a very nearly constant factor—a result that a surface chemist would expect. By least squaring Verbeck's data and using the constant factor, Brunauer calculated the average specific surface area of the tobermorite gel produced by C_3S and C_2S in the hydration of portland cements. Not only were the results within the range of 2- and 3-layer tobermorite sheets discussed earlier, but also the calculated area produced in the hydration of C_2S was significantly lower than that produced by C_3S. This was in complete agreement with the results obtained in the hydration of C_3S and C_2S; and later Kantro, Brunauer, and Weise advanced a mechanism of the hydration process that explains the fact that tobermorite gel in C_3S pastes has a higher specific surface area than in C_2S pastes (11).

All surface areas discussed were obtained for D-dried pastes. This designation is applied to pastes equilibrated at the vapor pressure of ice at -78 C, which is 5 by 10^{-4} mm of mercury. Another type of drying, designated as P-drying, will also be discussed. This applies to pastes dried at the equilibrium vapor pressure of magnesium perchlorate dihydrate and tetrahydrate, which is 8 by 10^{-3} mm of mercury. Because the vapor pressure at P-drying is 16 times as high as that at D-drying, the drying is less complete; and it will be seen that at D-drying all adsorbed water is removed, whereas at P-drying a considerable amount of adsorbed water remains on the surface.

The question may be legitimately raised as to whether D-drying alters the surface area of the cement paste. This question is not pertinent to the present discussion, because Feldman and Sereda also performed their experiments on samples that were subjected to what they called the "equivalent" of D-drying (more about this later). Nevertheless, the question is of considerable interest.

In the first drying of a cement paste, the total porosity decreases, and the evaporable (or adsorbed) water decreases. It is possible, therefore, that the surface area also decreases; in other words, the surface areas measured by water adsorption on D-dried samples may possibly be lower than the surface areas of undried pastes. There is, however, an important indication that this is not so. Powers and his co-workers determined the surface areas of 4 undried, saturated pastes by permeability measurements, each at 4 different temperatures, and obtained remarkably close agreement with the BET areas obtained by water vapor adsorption after D-drying of the pastes. For the 4 pastes, prepared with water-cement ratios of 0.4, 0.5, 0.7, and 0.8, the permeability areas were 525, 525, 525, and 500 m^2/cm^3 respectively, and the BET areas were 528, 524, 517, and 524 m^2/cm^3 respectively. The porosities of the 4 pastes were 0.391, 0.467, 0.510, and 0.554 respectively. These results have not been published as yet.

One other important experiment will be mentioned before we pass to a different subject. Copeland determined the specific surface area of a paste by small angle X-ray scattering, and obtained almost exact agreement with the surface area of the D-dried paste (measured, of course, by water vapor adsorption).

THE PROBLEM OF INTERLAYER WATER

Feldman and Sereda contend that about four-fifths of the adsorbed water in D-dried samples is interlayer water, i.e., water between the molecular layers inside the tobermorite gel sheets. Feldman (12), aware of our results that show that D-dried samples do not soak up water even when immersed in water (6), explained this by stating that the interlayer water was already inside the gel sheets before we immersed the sample in water. However, he failed to consider the other results in the same paper. The density of the tobermorite gel showed that the spacing between the layers, the c-spacing, was 9.3 Å, which is the distance of closest approach between the calcium silicate hydrate layers. At this distance, there is no interlayer water in the sheets. Furthermore, the layers stick to each other with such force that even soaking in water does not separate the layers. Obviously, therefore, at the relative humidities of 0.07 to 0.33, used in the BET surface area determinations, water cannot enter between the layers.

The chemical formula of D-dried tobermorite gel, which has a molar CaO/SiO_2 ratio of 1.5, is $Ca_3Si_2O_7 \cdot 2H_2O$. Bernal proposed the structural formula of $Ca_2[SiO_2(OH)_2]_2[Ca(OH)_2]$, which is only partly correct (13). On the basis of our experience of about a decade and a half, a more correct representation would be $Ca_2[SiO_2(OH)_2]_2[x(CaO \cdot H_2O)]$, where x may be more or less than 1. When the CaO/SiO_2 ratio is 1.5, x is equal to 1, but it would be erroneous to write $Ca(OH)_2$ instead of $CaO \cdot H_2O$, because the water can be relatively easily removed by drying, leaving the CaO in the gel. At D-drying this water is completely removed, as indicated by the chemical formula given. We visualize this molecule of water as interlayer water, whereas the 2 other molecules of water belong to the structure of the calcium silicate hydrate, possibly as indicated by our modification of Bernal's structural formula. Phosphorous pentoxide has smaller vapor pressure than D-drying, yet prolonged exposure of D-dried samples to P_2O_5 removed only a small percentage of the water.

D-drying removes all but a small part of the interlayer water. Usually, but not always, we obtained values a small percentage in excess of 2.0 molecules; longer drying would probably have removed this. Exposure to P_2O_5 removed this excess. The amount of adsorbed water was less than 0.01 mole per mole of SiO_2 (6).

The situation is very different at P-drying. The chemical formula of P-dried tobermorite gel having a CaO/SiO_2 ratio of 1.5 is $Ca_3Si_2O_7 \cdot 2.80H_2O$, and part of the extra 0.8 mole of water is interlayer water and part of it is adsorbed water. The two were determined in the following manner. Part of a hydrated C_3S paste was D-dried, and another part was P-dried. The same was done for a C_2S paste. The adsorption on the P-dried samples in the BET region of relative humidities was smaller than the adsorption on the D-dried samples. This was attributed to the fact that the P-dried samples contained some adsorbed water on their surfaces. The amount of adsorbed water was 0.26 mole; consequently, the other 0.54 mole was between the layers. The chemical formula of P-dried tobermorite gel was, therefore, $Ca_3Si_2O_7 \cdot 2.54H_2O$. The density of the gel indicated an average c-spacing of 10.2 Å, thus, clearly showing the presence of interlayer water. Furthermore, the P-dried samples, when immersed in water, very slowly in the course of days picked up some additional interlayer water, in contrast with the D-dried samples. The uptake was so slow that it was safe to assume that in the adsorption measurements on P-dried samples, which were performed at relative humidities of 0.07 to 0.33, no water went between the layers.

The value of 10.2 Å, obtained from the density measurements of P-dried pastes for the c-spacing, is obviously an average value. There is about half a mole of interlayer water per mole of gel, but the increase of approximately 1 Å in the c-spacing is not sufficient to accommodate water molecules. The explanation is that some of the tobermorite gel sheets do not contain interlayer water, but others do, which accounts for the average value obtained.

The main conclusions of this section are that there is practically no interlayer water in D-dried tobermorite gel, but there is a considerable amount of interlayer water in P-dried gel, probably about half of the maximum amount that can go between the layers. There is another important conclusion that can be drawn from these data. Even though the tobermorite gel could accommodate more than the 0.54 mole of water per mole of gel, which is between the layers in P-dried samples, 0.26 mole of water did not go between the layers but was attached to the surface. This illustrates the fact, long before known to us, that the combined water and the adsorbed water each have a spectrum of binding energies, and that the 2 spectra strongly overlap. The average binding energy of the interlayer water is greater than the average binding energy of the adsorbed water, but the most firmly bound part of the adsorbed water has a higher energy of binding than the most weakly bound part of the combined water. Thus, a separation of adsorbed and combined water on the basis of reversibility, as claimed in the new model, is impossible because the reversibility at a given humidity depends overwhelmingly on the binding energies.

These data, though conclusive by themselves, are not the only ones that show that there is very little or no interlayer water in D-dried cement pastes. One other set of experiments will now be cited (14), which by itself is as conclusive as the data given earlier. Table 1 gives data for pastes prepared from the same portland cement; w_o/c

TABLE 1

BET SURFACES, TOTAL POROSITIES, AND HYDRAULIC RADII OF PORTLAND CEMENT PASTES

w_o/c (1)	S_{H_2O} (m^2/g) (2)	S_{N_2} (m^2/g) (3)	$S_{H_2O} - S_{N_2}$ (m^2/g) (4)	V_{H_2O} (ml/g) (5)	V_{N_2} (ml/g) (6)	$V_{H_2O} - V_{N_2}$ (ml/g) (7)	r_{H_2O} (Å) (8)	r_{N_2} (Å) (9)	r in (Å) (10)
0.35	208.0	56.7	151.3	0.1264	0.0748	0.0516	6.1	13.2	3.4
0.40	202.6	79.4	123.2	0.1776	0.1059	0.0717	8.8	13.3	5.8
0.50	194.6	97.3	97.3	0.2615	0.1792	0.0823	13.4	18.4	8.5
0.57	193.8	132.2	61.6	0.3110	0.2493	0.0617	16.0	18.9	10.0
0.70	199.6	139.5	60.1	0.4008	0.2758	0.1250	20.1	19.8	20.8

is given in column 1. The pastes with $w_o/c = 0.35$, 0.40, and 0.50 were hydrated for 12 years, the 2 others for 2½ years. Columns 2 and 3 give the BET surface areas measured by water vapor and nitrogen adsorption, respectively, and column 4 gives the difference, i.e., the surface inaccessible to nitrogen. Columns 5 and 6 give the total porosities, measured by the adsorption of water vapor and nitrogen, respectively, and column 7 gives the difference, i.e., the pore space inaccessible to nitrogen.

The volume divided by the surface is called hydraulic radius. It is a measure of the average width of the pore system. If a pore is visualized as a cylinder, the hydraulic radius is one-half of the radius of the cylinder; and if a pore is assumed to be bounded by 2 parallel plates, the hydraulic radius is one-half of the distance between the plates. Columns 8, 9, and 10 give the hydraulic radii of the pore system accessible to water, that accessible to nitrogen, and that inaccessible to nitrogen respectively.

From the point of view of our discussion, column 10 has great significance. The hydraulic radius for the paste made with $w_o/c = 0.70$ shows that nitrogen cannot penetrate into very large pores. The smallest hydraulic radius, that obtained for the paste with $w_o/c = 0.35$, is 3.4 Å for the pores inaccessible to nitrogen. This is equivalent to a distance of 6.8 Å between 2 parallel plates (or 2 layers); thus, even this value is much too large to be attributed to water occupying interlayer spaces.

The reason for the inability of nitrogen to penetrate into large pores is given in the paper (14). The pores have very narrow necks; they are what the surface chemists call "ink-bottle" pores. The difference between the penetrating abilities of nitrogen and water depends not only on the difference between the sizes of the molecules but also on 2 additional factors. The first is that a water molecule has a strong dipole, which is strongly attracted to the ionic surfaces of the compounds in hydrated cement, whereas the attraction for the nonpolar nitrogen is very much smaller. The second factor is concerned with rates. The constrictions in the necks of the pores present an energy barrier to the diffusion of the molecules into the pores. This is called activated diffusion. The barrier may be larger for nitrogen than for water because of the differer between the sizes of the molecules, but let us assume that the energy of activation is the same for both. Then, because of the temperature difference (298 versus 77 K), water should pass over the energy barrier 50 times as rapidly as nitrogen. Even for water, it takes 2 to 3 weeks to equilibrate; it would take as many years for nitrogen to equilibrate.

The phenomenon of activated diffusion in adsorption is well known to surface chemists. Maggs, for example, obtained much larger surface areas for a number of coals by butane adsorption than by nitrogen adsorption, in spite of the fact that butane has much larger molecules than nitrogen (15). The reason is that the nitrogen adsorption was measured at 77 and 90 K, whereas the butane adsorption was measured at 273 K. The nitrogen areas measured at 90 K were considerably higher than those measured at 77 K, which is also in line with the concept of activated diffusion through narrow entrances.

According to the Powers model, completely hydrated pastes of the same cement should have the same specific surface area, regardless of the initial water-cement ratio. The average of the values given in column 2 of Table 1 is 200 m^2/g. The maximum deviation from the mean is 4 percent. The nitrogen areas given in column 3 vary by almost a factor of 3. At $w_o/c = 0.35$, the nitrogen area is 27 percent of the water area; it increases systematically with increasing w_o/c ratio, and at $w_o/c = 0.70$ it becomes 70 percent of the water area. In recent and as yet unpublished work, the nitrogen area for pastes made with $w_o/c = 0.2$ was less than 1 m^2/g after 28 days of hydration, or much less than 1 percent of the water area. It was very interesting to find that the water surface area was considerably smaller after 28 days than after 7 days, even though the nonevaporable water indicated a considerable increase in the degree of hydration. The increase in hydration products resulted in the filling up of certain pores, or in making certain pores so narrow that even water could not penetrate into them.

Feldman and Sereda have cited the nuclear resonance studies of Seligmann (16) as a confirmation of their contention that most of the adsorbed water is interlayer water. The problem of interlayer water, we believe, is settled by the experiments discussed earlier, but now we will proceed to show that there is nothing in the work of Seligm that invalidates our conclusions.

Seligmann's conclusions are based on T_2, the transverse or spin-spin relaxation time, obtained from nuclear magnetic resonance measurements. Within the great insensitivity of the T_2 values to the state of binding of water, his results are not contradictory to ours.

Let us start with his ettringite samples, one equilibrated at a relative humidity of less than 1 percent (Sample 7), the other at about 50 percent (Sample 6). The T_2 values were 300 to 500 μsec for both. Seligmann concludes: "These results also demonstrate the previously mentioned lack of correlation between proton mobility and gross chemical properties; the escaping tendency of the water in Samples 6 and 7, as manifested by the equilibrium relative humidities of the samples, must be very different; yet the proton mobilities are of the same order of magnitude." The difference between the free energies of binding of water in Samples 6 and 7 is RT $\ell n\ f_6/f_7$, which is 2,300 cal/mole, if the equilibrium humidity of Sample 7 is taken as 1 percent, and considerably more if the humidity is considerably less than 1 percent. Yet Seligmann, in spite of the quoted sentence, draws conclusions about the binding energies from proton mobilities.

One of the most puzzling aspects of Seligmann's paper is that he treats physically adsorbed water as though it were a definite entity, identical for the entire adsorption isotherm (with the exception of some active centers) and identical for different adsorbents. The heat of adsorption of water on anatase gradually decreases from 24,000 cal/mole to less than half of this value within the first adsorbed layer, and the heat of adsorption in the second layer is close to the heat of liquefaction, 10,000 cal/mole (17). The heats of adsorption of water on silica gel, tobermorite gel, and anatase are very different.

Seligmann obtained a T_2 value of about 2,300 μsec for a silica gel equilibrated at a relative humidity of 36 percent. This silica gel, on which the senior author of this paper and his co-workers did much work in the past and present, has an almost completely hydroxylated surface, plus (under the experimental condition of Seligmann) a complete, adsorbed monolayer of greatly differing energies of binding, plus a considerable amount of adsorbed water in the second layer. Seligmann states: "The present data indicate that water in only a single state is being observed." If the proton mobility has any correlation at all with binding energies, the "single state" observed in this instance is that of the most weakly adsorbed part of the water. The T_2 value is then taken by Seligmann as the standard for "physically adsorbed" water and is compared with water adsorbed on tobermorite gel.

Seligmann's C_3S paste (Sample 4) was D-dried and the T_2 value was about 200 μsec. About 40 percent of hydrated C_3S is calcium hydroxide, and the T_2 value for calcium hydroxide is 7 μsec. Thus, the proton in the hydroxyl does not show up, just as in the case of silica gel. There is no interlayer water in D-dried tobermorite gel, as was shown before; the 2 molecules of water are parts of the calcium silicate hydrate in the layers and not between the layers. Bernal's structural formula may be right or wrong; this has no bearing on the subject. The fact is that the 2 molecules of water are very strongly bound as was shown earlier.

Seligmann's alite paste (Sample 3) was equilibrated at a relative humidity of 16 percent. Under this condition, there is a good deal of interlayer water present, plus at least 1 layer of adsorbed water. Thus, there is much water present that is less strongly bound than in his C_3S paste, and this is shown in his T_2 value of 300 to 500 μsec. In the C_3S paste, all the water was strongly bound; in the alite paste, there was interlayer water plus about a monolayer of adsorbed water; and in silica gel, there was considerably more adsorbed water than a monolayer and, in addition, the energy of adsorption on silica gel is considerably smaller than on tobermorite gel. The binding energies up to this point, therefore, show at least a vague qualitative correlation with proton mobilities. However, the great insensitivity to binding energies shows up again in Samples 1 and 2. These are calcium silicate hydrates equilibrated at relative humidities of 70 and 50 percent respectively, and the T_2 values are still 300 to 500 μsec. Just as in the case of ettringite, the fugacities of the water in Samples 1, 2, and 3 are very different; consequently, the free energies of binding are also very different, but the mobilities of the protons, within the large experimental errors, are the same.

Seligmann's first conclusion is as follows: "Nuclear magnetic resonance results indicate that the state of binding of evaporable water in hardened cement paste up to 70 percent relative humidity is essentially the same as that of interlayer water in swelling clays or of water of crystallization in certain lattices." This statement, in the light of the earlier discussion, is unwarranted. The correct statement would replace "state of binding" with "mobility of protons," and would point out the great insensitivity of the results.

Seligmann's second conclusion is the following: "The water in calcium silicate hydrates equilibrated at or below 70 percent relative humidity has definitely less mobility than physically adsorbed water, but is still more mobile than chemically combined water in a crystal lattice." This statement should also be revised. Physical adsorption begins at 70 percent relative humidity only on very strongly hydrophobic surfaces. On the strongly hydrophilic surface of tobermorite gel, at 70 percent relative humidity the amount of adsorbed water corresponds to almost 3 monolayers. The calcium silicate hydrates at 70 percent relative humidity contain strongly bound water within the layers, plus interlayer water, plus almost 3 layers of adsorbed water on their surfaces. It is easy to accept that the mobility of the protons in the fourth and higher adsorbed layers is greater than that of the protons of any of the rest of the water.

Although we disagree with Seligmann's conclusions, we welcome his efforts, as well as those of others, to bring a new tool to the study of the states of water in hydrated cements. Nuclear magnetic studies, especially if their accuracy is improved, may throw new light on many problems in cement chemistry.

THE EXPERIMENTS OF FELDMAN AND SEREDA

The first statement that can be made about the pastes and compacts of Feldman and Sereda is that they were nowhere near to the D-dried state. The nonevaporable water, w_n, of 0.25 g/g of cement in Feldman's paper (12) and 0.254 g/g of cement in the paper of Soroka and Sereda (18), offered as the values for complete hydration, indicates that their quick-drying was approximately equivalent to P-drying. Likewise the value of Feldman for the water area (designated by him as the "conventional" water area), 165 m^2/g for complete hydration, indicates a drying equivalent to P-drying. The D-dried surface given in Table 1, column 2, is 200 m^2/g. The fact that they used a different cement from ours does not alter our conclusion. The variation in w_n and surface area for type 1 cements at complete hydration is slight.

We have shown that D-drying and P-drying lead to very different pastes. D-drying leaves neither interlayer water nor adsorbed water in the tobermorite gel; P-drying leaves both interlayer and adsorbed water in the gel. Thus, comparing the adsorption results of Feldman and Sereda with our results for D-dried pastes has no justification.

It is of interest to compare the properties of the bottle-hydrated and the paste-hydrated cement in Feldman's Table I (12). The values of w_n are 21.5 and 23.0 respectively indicating that the degree of hydration of the former is 93.5 percent of the latter. The nitrogen surfaces are 30 and 47 m^2/g; the first of these values is 64 percent of the second. On the basis of this, it should have been concluded that the hydration products in bottle and paste hydration are different. However, the "conventional" water area comes to the author's help. The values are 142 and 152 m^2/g; the former is exactly 93.5 percent of the latter. This phenomenal agreement, not mentioned by the author, indicates that the hydration products were actually the same. Nevertheless, even though the hydration products, which determine the surface area, and the true surface areas (those measured by water) were the same, there was a difference in pore structures. The ratio of nitrogen surface to water surface was 21 percent for the bottle-hydrated compact and 31 percent for the paste, a difference of almost 50 percent. This is a clear indication of the difference in pore structure. Pore structures strongly influence the adsorption properties of solids. Feldman (12) discusses the properties of the adsorption-desorption isotherms of his bottle-hydrated compacts, draws his conclusions on the basis of the discussion, and declares the validity of the conclusions for hydrated pastes. It is not clear to us why he did not discuss his pastes instead, if he wanted to draw conclusions about the pastes.

Feldman used a water-cement ratio of 0.5 for his pastes, and at 92 percent hydration he obtained a nitrogen area of 47 m^2/g. For complete hydration, the area would be 51 m^2/g. The nitrogen area, given in Table 1, column 3, of the present paper, is almost twice as great. We have already stated that the water area obtained by Feldman was approximately what one would expect for P-dried pastes, which is about 83 percent of the area of D-dried pastes. We have not investigated the nitrogen area of P-dried pastes, but Feldman's result indicates that the discrepancy between water and nitrogen area is much greater for these than for D-dried pastes. This can possibly be explained by assuming that the adsorbed water that is on the surface of P-dried pastes blocks the entrance of nitrogen into many pores.

One additional item in Feldman's paper is worth mentioning. Soroka and Sereda (18) determined the modulus of elasticity of the solid phase in hydrated portland cement. This involves an extrapolation to zero porosity. The porosities of the samples were calculated from the weight, volume, and degree of hydration, which is unquestionably a correct way of doing it. Although the authors do not mention it, these values are in good agreement with the porosities measured by water. The modulus of elasticity obtained by them was 88×10^4 kg/cm^2, and they point out that this agrees "surprisingly well" with the results of Helmuth and Turk (19). The latter authors obtained values of 76×10^4 and 81×10^4 kg/cm^2 for 2 cements by an entirely different method. Feldman, in his paper, simultaneously submitted with that of Soroka and Sereda, rejects the value obtained by his colleagues, and on the basis of the new model proposes a value that is less than half of their value.

The proponents of the new model question the validity of the BET surface area obtained by water on the ground that some of the water was irreversibly adsorbed; consequently, there was no thermodynamic equilibrium in the relative humidity range employed, 7 to 33 percent. We have already pointed out that no conclusion can be drawn from their results about D-dried pastes, but there is more to be said on the subject.

Thermodynamic reversibility with respect to pressure means that, if there is an infinitesimal change in pressure that changes the state of the system, the system returns to its original state if the pressure is restored to its original value. Because it is impossible to produce infinitesimal changes, we test for reversibility on a macroscale. If a process is reversible with respect to a finite change in pressure, it is certainly a reversible process; but if it is not reversible within a certain time, it may still be reversible if adequate time is allowed for reversal. The adequate time may be days or months or years.

For the adsorption points in the BET region of relative humidities we allowed, on the average, about 3 weeks of equilibration for D-dried pastes. If the adsorption isotherm is determined up to saturation pressure, and a desorption isotherm is determined subsequently, much longer time is needed for equilibration. The energy of activation of desorption is equal to the energy of activation of adsorption plus the heat of adsorption. Because the heat of adsorption of water is high, the rate of desorption is much slower than the rate of adsorption. If one does not wait for weeks, one obtains an open hysteresis loop down to zero pressure. If one uses 1 day for equilibration of each point on the desorption curve, as Feldman did (12), one obtains a gigantic hysteresis loop. There is no point on his desorption isotherm (Table II) that comes anywhere near to equilibrium.

In contrast with this, Copeland waited for equilibration on the desorption side for weeks, and he obtained an isotherm in which the hysteresis loop closed around a relative humidity of 50 percent. This work was never published, but we can report here even more striking results, which will be published in the near future. Our co-worker, J. Hagymassy, determined adsorption-desorption isotherms for 9 pastes (3 C_3S, 3 C_2S, and 3 portland cement pastes). The w_o/solid ratios ranged from 0.4 to 0.7, and hydration times were several years, ranging up to 7 years. The pastes were D-dried. The desiccator method (20) was used, and different portions of the same paste were simultaneously exposed to different relative humidities, thus cutting down the time required for the isotherms from years to months. After 4½ months of equilibration of the desorption points, they joined the adsorption isotherms at a relative humidity of about 60 percent, and the hysteresis loops were considerably smaller than those of Copeland.

These results show clearly that our adsorption isotherms represent equilibrium results, regardless of whether Feldman's do or do not. He allowed much longer times for the equilibration of the adsorption points than the desorption points; consequently, the adsorption isotherms may represent equilibria, or close to it. The agreement of the w_n and water surface area values with those obtained by us for P-dried pastes indicates that equilibrium may have been attained on the adsorption side.

We are not attempting to give a detailed explanation of the "loops" of the authors of the new model, by which they try to separate reversible and irreversible water. We have already pointed out that irreversible water may become reversible if the experimenter waits long enough for equilibration. It is possible that most of the loops, if not all, would have disappeared if months would have been allowed for equilibration. It was shown in the discussion of P-dried pastes that a considerable part of the adsorbed water is more strongly bound than much of the interlayer water. The heat of adsorption of water is high; it is highest at the lowest humidities; consequently, the rate of desorption is very slow. Instead of separating reversible and irreversible water, Feldman and Sereda separated reversible and less reversible water. Hydrated cement has a variety of compounds in it, with water of hydration of different binding energies and with a spectrum of binding energies of adsorbed water; thus, their method of separation of reversible and irreversible water and their identification with adsorbed and interlayer water are unacceptable to us.

The researches of Sereda and his co-workers contain a large amount of valuable experimental work on hydrated portland cements. These results, if properly interpreted, can throw additional light on the structure of portland cement paste and concrete. We do not mean to imply that all of their own interpretations are erroneous; many of these have nothing to do with their new model or are even contradictory to it. An example of this was already cited in the paper of Soroka and Sereda (18). We do not mean to imply, either, that the Powers model is complete. We do mean to state, however, that the Powers model, as modified and extended by many of us, explains quantitatively many and semiquantitatively many other aspects of the structure of paste, and that w know of no properly interpreted experimental evidence to date that contradicts it.

Feldman and Sereda have offered an explanation of the hysteresis, which is based on the entrance and exit of interlayer water. The explanation is ingenious, and for the kind of hysteresis that is caused by interlayer water it may be correct. P-dried pastes contain interlayer water, and in the long extended adsorption runs of Feldman and Sereda additional water was likely to go between the layers, part of which probably comes out in the desorption run. However, adsorbed water itself also shows hysteresis; in fact, all adsorbates show hysteresis for practically all porous adsorbents. Nitrogen, which certainly does not enter into the interlayer spaces of hydrated cements, silicates, clay minerals, and other layer crystals, shows hysteresis for these and most other porous bodies. Examples of these for portland cements are given in a paper already cited (14), and the literature of adsorption contains hundreds of other examples for a great variety of adsorbent-adsorbate systems. The oldest theory of the hysteresis in adsorption was proposed by Zsigmondy 58 years ago (21), and several other theories have been proposed since (22). Although the theory of Feldman and Sereda can explain only a part of the hysteresis in their own adsorption-desorption data, it may be added to the other theories as a plausible explanation of a special type of hysteresis encountered in the study of layer crystals.

THE STRENGTH OF CEMENT PASTE

In the Powers model, as well as in all of its modifications and extensions, the cementing material is the cement gel, which is essentially tobermorite gel, though it probably does contain small amounts of other constituents besides the calcium silicate hydrate. One statement of our view on the cause of strength is as follows (23):

> The adhesive forces, which are responsible for strength, are primarily van der Waals forces, but there may also be some chemical binding involved. Tobermorite gel is a "limited swelling" gel–although it swells slightly in water, it is not dispersed as, for example, gelatin. A possible explanation for this is that the gel particles are bound to each other at certain points by chemical

> valence forces. The low tensile strengths of hardened paste and concrete, however, indicate that the chemically bound contact points cannot be very numerous. The tensile strength is only about one-tenth of the compressive strength, and if chemical binding would play an important role in the adhesion of the gel particles, one would expect that much greater force would be needed to pull them apart.

Sereda and his co-workers seem to disagree with these statements, though it seems to us that there is no disagreement at all. Soroka and Sereda state (18): ". . . the chemical bonds, if present in the paste, play an insignificant role." This is in agreement with our statement. Both state that there may or may not be any chemical bonds present; if they are present, they play a minor role in producing strength. For the rest, Sereda and his co-workers attribute the strength to "interparticle bonds." This is a singularly unfortunate name, because it is the interparticle bonds that are to be explained by the nature of the forces producing them. On the basis of their description of the interparticle bonds, it seems to us that they are talking about van der Waal's forces, though they refrain from using, or even seem to be opposed to, this name. If they are talking about other than van der Waal's forces, they must have some force in mind that is unknown to the present authors.

The old and the new model are in complete agreement on a point of overriding importance: that the most important cementing and strength, producing material in hardened paste and concrete is the tobermorite gel. Recently, however, an idea has been put forward by Williamson (24), which at first glance appears to be surprising, but on closer inspection it can be brought into line with our ideas.

In the abstract of his paper, Williamson states: "The originally water-filled space between the grains is partially filled with calcium hydroxide crystals that appear to be responsible for the strength of cement paste." A much weaker statement is in the text: ". . . the ultimate strength of portland cement paste is related to the $Ca(OH)_2$ that fills the originally water-filled space." We shall now examine what sort of calcium hydroxide Williamson is talking about. According to him in hydrated C_3S, ". . . the outer product can vary from an almost pure $Ca(OH)_2$ to a calcium silicate hydrate based on a two-phase structure of SiO_2 and $Ca(OH)_2$."

Williamson's arguments for the "two-phase structure" of tobermorite gel (25) have little or no bearing on the subject. It seems from his description of the structure of the calcium silicate hydrate that the $Ca(OH)_2$ and the SiO_2 form a single structure of variable composition, which is known and accepted by everybody. Nevertheless, there are 2 types of calcium hydroxide in hydrated C_3S. There are large calcium hydroxide crystals, part of them visible in an ordinary microscope, and there is calcium hydroxide in the tobermorite gel. We have already cited Brunauer's somewhat flamboyant statement that tobermorite gel is a "chemical mixture" of calcium hydroxide and hydrous silica.

The calcium hydroxide crystals may or may not have cementing or strength-producing properties. Williamson himself shows in his Figure 1 (25) that C_3S and C_2S hydrated for 1 year have the same compressive strength. Actually there are results that show greater strength for the C_2S paste than for the C_3S paste after 2 years of hydration. This is in spite of the fact that the C_2S paste contains much less calcium hydroxide than the C_3S paste. One of the present authors (Ivan Odler) made numerous experiments on the reaction of portland cement with pozzolanic materials and with sand in mortars at room temperatures. The sand was ground to have the same fineness as the pozzolanic materials. The sand did not react with the calcium hydroxide in the cement, but some of the pozzolanic materials did, and in fact removed the calcium hydroxide almost completely. These mortars had considerably higher strengths than the sand mortars because of the formation of additional calcium silicate hydrate.

The situation is very different with the lime within the tobermorite gel. Gard, Howison, and Taylor have suggested that the lime in tobermorite gel is responsible for cementing neighboring gel particles together (26). Kantro, Brunauer, and Weise went a step further, and suggested that lime cements the layers within the gel sheets to each other (20).

The cementing action by van der Waal's forces, the bonds between the surfaces, and the strength of the material depend on surface energy and specific surface area. Cal-

cium hydroxide has a high surface energy, but just because of this it has a low surface area. Silica (especially in the form of silica gel) has a very low surface energy, but just because of this it has a very high area. The function of the silica in tobermorite gel is possibly to spread out the lime, to give it a high surface. At any rate, tobermorite gel has high surface area combined with a relatively high surface energy.

None of these arguments shows that calcium hydroxide crystals have no cementing action. They only show that the calcium silicate hydrate is a better cementing agent than calcium hydroxide. It is possible that calcium hydroxide does play a role in cementing, but only future research can settle whether it plays a significant role.

ACKNOWLEDGMENT

The authors wish to express their gratitude to the New York State Department of Transportation and to the Bureau of Public Roads, Federal Highway Administration, U. S. Department of Transportation, for their support of the research on portland cement pastes conducted by the authors of this paper.

REFERENCES

1. Feldman, R. F., and Sereda, P. J. A Model for Hydrated Portland Cement as Deduced From Sorption—Length Change and Mechanical Properties. Materiaux et Constructions, Vol. 1, No. 6, 1968, pp. 509-520.
2. Powers, T. C., and Brownyard, T. L. Studies of the Physical Properties of Hardened Portland Cement Paste. ACI Jour., Proc. Vol. 43, Oct. 1946, p. 101; Nov. 1946, p. 249; Dec. 1946, p. 469; Jan. 1947, p. 549; Feb. 1947, p. 669; March 1947, p. 845; April 1947, p. 933.
3. Brunauer, S., Emmett, P. H., and Teller, E. Adsorption of Gases in Multimolecular Layers. Jour. of Am. Chem. Soc., Vol. 60, 1938, pp. 309-319.
4. Brunauer, S., Kantro, D. L., and Weise, C. H. The Surface Energy of Tobermorite. Canadian Jour. of Chem., Vol. 37, 1959, pp. 714-724.
5. Born, M., and Stern, O. Sitz. Ber. Preuss. Akad. Wiss., 1919, p. 901.
6. Brunauer, S., Kantro, D. L., and Copeland, L. E. The Stoichiometry of the Hydration of β-dicalcium Silicate and Tricalcium Silicate at Room Temperature. Jour. of Am. Chem. Soc., Vol. 80, 1958, pp. 761-767.
7. Brunauer, S., Kantro, D. L., and Weise, C. H. The Surface Energies of Calcium Oxide and Calcium Hydroxide. Canadian Jour. of Chem., Vol. 34, 1956, pp. 729-742.
8. Brunauer, S., Kantro, D. L., and Weise, C. H. The Surface Energies of Amorphous Silica and Hydrous Amorphous Silica. Canadian Jour. of Chem., Vol. 34, 1956, pp. 1483-1496.
9. Kantro, D. L., Weise, C. H., and Brunauer, S. Paste Hydration of Beta-Dicalcium Silicate, Tricalcium Silicate, and Alite. HRB Spec. Rept. 90, 1966, pp. 309-327.
10. Wittmann, F. Materiaux et Constructions, Vol. 1, 1968, p. 547.
11. Kantro, D. L., Brunauer, S., and Weise, C. H. Development of Surface in the Hydration of Calcium Silicates. II. Extensions of Investigations to Earlier and Later Stages of Hydration. Jour. of Phys. Chem., Vol. 66, No. 10, 1962, pp. 1804-1809.
12. Feldman, R. F. Sorption and Length Change Scanning Isotherms of Methanol and Water on Hydrated Portland Cement. Fifth Internat. Symposium on the Chemistry of Cement, Tokyo, Paper III-23, 1968.
13. Bernal, J. D. Proc. Third Internat. Symposium on the Chemistry of Cement. London, 1952, p. 216.
14. Mikhail, R. Sh., Copeland, L. E., and Brunauer, S. Pore Structures and Surface Areas of Hardened Portland Cement Pastes by Nitrogen Adsorption. Canadian Jour. of Chem., Vol. 42, 1964, pp. 426-438.
15. Maggs, F. A. P. Nature, Vol. 169, 1952, pp. 259, 793.
16. Seligmann, P. Nuclear Magnetic Resonance Studies of the Water in Hardened Cement Paste. Jour. of PCA Research and Dev. Laboratories, Vol. 10, No. 1, 1968, pp. 52-65.

17. Harkins, W. D., and Jura, G. Jour. of Am. Chem. Soc., Vol. 66, 1944, p. 919.
18. Soroka, I., and Sereda, P. J. The Structure of Cement-Stone and the Use of Compacts as Structural Models. Fifth Internat. Symposium on the Chemistry of Cement, Tokyo, Paper III-34, 1968.
19. Helmuth, R. A., and Turk, D. H. Elastic Moduli of Hardened Portland Cement and Tricalcium Silicate Pastes: Effect of Porosity. HRB Spec. Rept. 90, 1966, pp. 135-144.
20. Kantro, D. L., Brunauer, S., and Weise, C. H. Development of Surface in the Hydration of Calcium Silicates. In Solid Surfaces and the Gas Solid Interfaces, Advances in Chemistry Series, Vol. 33, 1961, pp. 199-219.
21. Zsigmondy, R. Z. anorg. allgem. Chem., Vol. 71, 1911, p. 356.
22. Brunauer, S., Mikhail, R. Sh., and Bodor, E. E. Jour. of Colloid and Interface Sci., Vol. 25, 1967, p. 353.
23. Brunauer, S. Proc. Eighth Conference on the Silicate Industry, Budapest, 1965, p. 205.
24. Williamson, R. B. Science, Vol. 164, 1969, p. 549.
25. Williamson, R. B. Jour. of Crystal Growth, Vol. 3-4, 1968, p. 787.
26. Gard, J. A., Howison, J. W., and Taylor, H. F. W. Synthetic Compounds Related to Tobermorite: An Electron-Microscope, X-Ray and Dehydration Study. Mag. of Concrete Research, Vol. 11, No. 33, 1959, pp. 151-158.

Discussion

R. F. FELDMAN and P. J. SEREDA, Division of Building Research, National Research Council of Canada—The authors discuss the new model at considerable length and compare it critically with the Powers model. We wish to take issue with the authors on many points. Because we are constrained by the rules on length of discussion, we can do little more than to provide a general reply in which the points in question are stated with limited supporting argument. We intend to prepare a further discussion later of the new model, with additional evidence that we hope may be acceptable as a paper in its own right.

The new model was intended to describe the average chemical, physical, and mechanical properties of hardened portland cement paste and, as such, must not be, and is not in our view, in serious conflict with available experimental evidence. We do not believe that the authors have adequately incorporated into their considerations evidence from our measurement of mechanical and physical properties (1).

We do not accept the proposition that data presented by Feldman (12) can be disregarded because they were obtained under the "wrong" conditions, i.e., that the samples were held not to have been in equilibrium as stated or they were held to have been incorrectly dried. It is our opinion that these adsorption isotherm data are valid, that they agree with other published data, and that they provide further evidence in support of the new model. We believe that the evidence adequately supports the following conclusions:

1. Interlayer water can reenter D-dried material, even at low humidities;
2. In light of this conclusion, water surface areas and densities are not correct and the respective nitrogen or methanol values are approximately correct; and
3. The fundamental physical properties of the hydrated calcium silicates, such as density, Ca-Si ratio, H_2O-Si ratio, surface area, and distance between layers, vary with conditions of preparation.

We offer further comments as follows:

The authors consider that their measurement of surface energy yields results of major importance. This technique requires that the samples used are of constant composition and are the same in every way except for the quantitative difference in surface

area. However, if C-S-H is a family of ill-defined, poorly crystallized, layered materials possessing various proportions of both internal and external area, this requirement is not met. In the experiments, the samples were prepared by vastly different methods and from different starting materials. As a result, it may be proposed that the ratio of internal and external areas changed with preparation as well as Ca-Si ratio, density, interlayer spacing, and H_2O-Si ratio.

Thus, one is led to the conclusion that measurements on a group of such samples, varying in so many ways, would not meet the requirements of the surface energy method. Thus, we suggest, apparent surface energy values must be looked upon as subject to large uncertainty and should not be regarded as adequate evidence to support the contention that water surface areas are correct.

The acceptance of the water surface area evidence (6) necessarily implies acceptance of the results of density measurements of cement paste by water immersion that yield values in the order of 2.86 g/cm^3. This is very much higher than density measurements obtained by helium pycnometry that are as low as 2.33 g/cm^3 for D-dried specimens prepared at a w-c ratio of 0.8.

If a calculation of interlayer spacing from density is meaningful, one obtains a value of 11.4 Å instead of 9.3 Å as reported by Brunauer et al. (6).

The authors devote much space to the discussion of interlayer water and conclude that water does not reenter the interlayer spaces. This conclusion is in direct conflict to much evidence of workers in the USSR (27), Mikhail (29), Powers (2), Helmuth (29), and Feldman (12). No isotherms of cement or paste-hydrated C_3S showing closed loops have been published to our knowledge. In discussing isotherms published by Feldman, the authors conclude that the samples were not adequately D-dried or were not in equilibrium, and propose that weeks, months, or even years may be required for the attainment of equilibrium. In contrast the accepted method for D-drying as developed by Copeland and Hayes (30) involves 4 to 7 days of equilibration with a vapor pressure corresponding to ice at -79 C. This drying includes removing all the strongly held first layers of adsorbed water plus removal of the more tightly held interlayer water. In point of fact, there are many pieces of evidence that favor our contention that the samples used by Feldman were in equilibrium throughout the isotherm and were D-dried.

One of the major points of conflict arises over the question of whether the interlayer water removed on D-drying can subsequently reenter the interlayer spaces. In their attempt to prove that this is so, the authors have calculated the hydraulic radius of the pores from data obtained from adsorption of water and of nitrogen. Their results show that the values of hydraulic radius were too large to be attributed to water occupying interlayer spaces. Logically, this calculation is incorrect in that $S_{H_2O} - S_{N_2}$ (Table 1, column 4), used as a measure of internal surface area, should really have been calculated from 755 - S_{N_2}, i.e., the difference between the nitrogen surface area (external) and the total surface area, including the interlayer surface, implied by the model. If the calculation is made from this premise, the average value of the calculated hydraulic radius that results is 1.32 Å, almost the same as that which could be obtained for a montmorillonite clay, 1.26 Å. Thus, the properly calculated hydraulic radius is entirely compatible with water occupying interlayer spaces.

In discussing strength of the cement paste, the authors noted the apparent agreement between the 2 models with regard to the role of chemical bonds in producing strength. We do not believe they have adequately taken into account the ideas developed by Soroka and Sereda (18) regarding the "interparticle bonds"—an expression used by Powers in developing his model. This was an attempt by both Powers and Soroka and Sereda to define the nature of the interparticle boundary.

The 2 models are actually not in agreement on this point. The Powers model postulates that interparticle distance or boundary varies and considers the existence of wedge-shaped crevices into which adsorbed water enters and alters the interparticle attraction and hence interparticle distance, thus accounting for most of the dimensional changes. We postulate that adsorbed water as such plays no part in the interparticle bond although the interlayer water may contribute where the boundary is similar to that between layers.

References

27. Luk'yanova, O. I., and Rebinder, P. A. Properties of Tobermorite-Like Hydrosilicates as a Variable Composition Phase. Doklady Akademii Nauk SSSR, Vol. 184, 1969, pp. 1144-1147.
28. Mikhail, R. Sh., Kamel, A. M., and Abo-el-enein, S. A. Surface Properties of Cement Hydration Products. I. Pore Structure of Calcium Silicate Hydrates Prepared in a Suspension Form. Jour. Appl. Chem., Vol. 19, 1969, pp. 324-328.
29. Helmuth, R. A. Private communication.
30. Copeland, L. E., and Hayes, J. C. The Determination of Nonevaporable Water in Hardened Portland Cement Paste. ASTM Bull. 194, 1953, p. 70.

PAUL SELIGMANN, Portland Cement Association—The present writer welcomes the authors' discussion of the nuclear magnetic resonance (NMR) results (16) and also the opportunity to clarify some matters that appear to have caused confusion. For this purpose it is necessary first to make some general comments on the nature of the NMR phenomenon and on the terminology used in the paper.

The major source of confusion relates to the energy of the water molecules. At no point in the original paper (16) was the use of the terms "state" or "binding" intended to refer to the energy or heat adsorption. The energies associated with nuclear resonance effects are those required to change the axis of rotation of a proton, not those required to remove a water molecule from a particular state of binding. These energies are readily calculated. At the frequency, $\mu = 7.3 \times 10^6$ Hz used in the wide line work of Blaine (31), the energy absorbed by a single proton is $h\mu$, where h is Planck's constant. This energy corresponds, in heat units, to 1.4×10^{-3} g-cal/mole of water, an exceedingly small fraction of the energy of adsorption. An observed line width then corresponds to a small range of resonance energies around this value. It must be understood that NMR measures parameters of the system other than the energy of adsorption.

The use of a magnetic field to separate different atomic or molecular states having the same energy is by no means new. This technique has, for example, been widely used in the field of atomic emission spectroscopy, where it is known as Zeeman effect, for more than half a century. A single atomic energy level is split into a number of closely spaced levels whose separation depends on the strength of the applied magnetic field. In this context, NMR is the same technique applied to nuclear absorption spectroscopy rather than atomic emission spectroscopy. In both cases, fine details of a system are determined from small energy perturbations.

NMR can be compared with a much older type of radio frequency absorption spectroscopy, the measurement of dielectric constant. In that technique, the measured absorption of radiation depends on the ability of the various dipoles to "follow" the field. In the case of NMR, the absorption measures the ability of the protons to shift their spin axes in accordance with an impressed alternating component of the local magnetic field. This local field is very complex (16). The parameter, T_2, that is measured is a relaxation time associated specifically with the local field variations caused by the rotations of spin axes of neighboring protons and has been found to vary with the state of the water, as indicated in the paper (16). T_2 thus measures the degree of restraint of the immediate environment on the spin axis of the proton. A proton that is not free to reorient its spin axis must be in a restrained or bound state; it is in this sense that the term "binding" was used in the paper.

A major result from the transient equipment, apparently overlooked by the authors, was the absence of echoes in the pulsed NMR of the pastes up to 70 percent relative humidity, as contrasted with the presence of echoes for the silica gel at a much lower relative humidity. In fact, Zimmerman and his co-workers (32) reported proton spin echoes from a silica gel covered with less than 0.05 layer of water. The absence of echoes from pastes means that even the most mobile of the protons are in a state of

restraint that is qualitatively different from that of even the protons in 0.05 layer of water adsorbed on silica gel. This difference is reflected in the "insensitivity" of the T_2 values, which stems from the poorly defined free induction decay signals obtained from pastes, as compared with the excellent echoes obtained by many workers from various silica gels and from the many other materials of high surface area discussed in the Winkler review (33). For silica gels, only those with very small pores, as studied by Tul'bovich and co-workers (34) exhibit a low proton mobility comparable with that found in cement pastes equilibrated up to 70 percent relative humidity.

Additional confusion has arisen with regard to the use of the terminology "physically adsorbed water." The classification of types of water used in the paper (16) is that of Powers and Brownyard (2). It was necessary in addition, however, to distinguish between types of physically adsorbed water as regards T_2 values and the ability to produce echoes. "Physically adsorbed water" was therefore arbitrarily used to denote the adsorbate of silica gel and similar materials, because of the wide use of water on silica gel as a classic example of physical adsorption. The interlayer water of swelling clays was used as an example of an adsorbate with low T_2 values and no capability for echo production.

It must be noted that "interlayer" refers here to a type of physical adsorption rather than chemical adsorption as is implied by the authors' model of the tobermorite formula and unit cell. The energy of adsorption for water in swelling clays is known to be in the range normally associated with physical adsorption (35). The wide difference between the surface areas measured by nitrogen and water adsorption on swelling clays has prompted some workers to speak of "external" and "internal" surface areas (36), where the latter refers to the interlayer area that can also be measured by adsorption of large organic molecules such as glycerin and ethylene glycol. All these facts, together with the unlimited swelling of the clays, indicate the water adsorption to be physical. Yet the T_2 values obtained are distinctly different from those of the water on materials like silica gel.

No model was proposed (16) to "explain" the results of the NMR measurements. Cement pastes differ from swelling clays not only in limited swelling capacity but also in the absence of X-ray diffraction lines for a definite c-spacing for the silicate phase (37), as would be characteristic of a layered structure. Any satisfactory model would have to account for the apparent surface area, the proton mobility, and also the degree of disorganization implied by the observed diffraction patterns. It is felt that this problem must be approached with great caution.

The present writer is optimistic about the improvement of experimental NMR techniques. There are now indications that new types of equipment and new ways of using presently available equipment for the study of solid materials are being developed. The absence of proton spin echoes dashed his original hopes of determining the complete proton mobility spectrum of cement paste as had been done by others for materials of high surface area. It is hoped that the new developments will still make this possible.

References

31. Blaine, R. L. Proton Magnetic Resonance in Hydrated Portland Cements. Proc. Fourth Internat. Symposium on the Chemistry of Cement, Washington, D. C., 1960, Vol. 1, Paper IV-S5, pp. 501-511; National Bureau of Standards, Monograph 43, 1962.
32. Zimmerman, J. R., Holmes, B. G., and Lasater, J. A. A Study of Adsorbed Water on Silica Gel by Nuclear Resonance Techniques. Jour. of Physical Chemistry, Vol. 60, Sept. 1956, pp. 1157-1161.
33. Winkler, H. Examination of Adsorption Phenomena by Nuclear Induction Methods. Archives des Sciences, Vol. 14, Sept. 1961, pp. 219-243.
34. Tul'bovich, B. I., Slisarenko, F. A., Klyaev, V. I., and Sorokin, S. I. Proton Magnetic Resonance of Water and Normal Hydrocarbons Sorbed by Silicate Sorbents of Various Pore Structure. Izvestiya Vysshikh Uchebnykh Zavedenii, Khimiya i Khimicheskaya Tekhnologiya, Vol. 9, No. 5, 1966, pp. 735-737.

35. Mooney, R. W., Keenan, A. G., and Wood, L. A. Adsorption of Water Vapor by Montmorillonite. I. Heat of Desorption and Application of the BET Theory. Jour. of Am. Chem. Soc., Vol. 74, 1952, pp. 1367-1371.
36. Diamond, S., and Kinter, E. B. Surface Areas of Clay Minerals as Derived From Measurements of Glyceral Retention. Proc. Fifth National Conference on Clay and Clay Minerals, 1958, pp. 318-333.
37. Copeland, L. E., and Kantro, D. L. Chemistry of Hydration of Portland Cement at Ordinary Temperature. In The Chemistry of Cements (Taylor, H. F. W., ed.), Vol. 1, New York Academic Press, 1964, p. 336.

STEPHEN BRUNAUER, IVAN ODLER, and MARVIN YUDENFREUND, Closure—First the discussion of Feldman and Sereda will be answered. The strongest argument in our paper, that based on the surface energy of tobermorite gel, is simply swept aside by the discussors. After making a wrong statement about the requirements of the technique of surface energy determinations, they point out that the samples had different lime-silica and water-silica ratios, but they fail to state that corrections were made for this. The surface energy values given in our paper refer to tobermorite gel of the composition $Ca_3Si_2O_7 \cdot 2H_2O$. They point out as an objection that "the samples were prepared by vastly different methods and from different starting materials," and they fail to see that this is an argument for and not against the correctness of the surface energy of tobermorite gel. The fact that the plot of heat of solution versus surface area fell on the same straight line for these different samples and the fact that the slope of the straight line gave the theoretically correct surface energy value are not explained by the discussors.

The tobermorite gel obtained in the hydration of C_3S and C_2S is very poorly crystallized; its X-ray diffraction pattern consists of only 3 lines. Besides the 2 determinations of the surface energy discussed in the paper, Kantro, Brunauer, and Weise (38) also determined the surface energy of completely amorphous tobermorite gel, and its value fell between the 2 values given in the paper.

The discussors point out that we have not adequately incorporated evidence from their measurements of mechanical and physical properties. This is true; the only item that we have pointed out along these lines was the rejection by Feldman of the modulus of elasticity value of Soroka and Sereda, which was in agreement with the old model, based on water vapor adsorption. Our aim in the paper was to examine the bases of the 2 models: of the old model, based on water vapor adsorption data, and of the new model, based on nitrogen adsorption data.

Because nitrogen enters a part of the pore space, it is possible that some properties of the pastes can be correlated with nitrogen adsorption. It is, therefore, not enough to show such correlations; the discussors must show that their results cannot be correlated with the old model.

We would very much prefer if the phrase "D-drying" would be used only for the method of drying first used by Copeland, and widely used by us in our research. As far as we know, this method was never used by Sereda and his co-workers; so we will call their method F-S-drying. In our paper, on the basis of w_n and the surface area measured by water, we concluded that F-S drying is about the equivalent of P-drying. On the basis of the density value of 2.33 g/cm^3, obtained by helium pycnometry, it appears that the samples of the discussors were less strongly dried than P-drying. The interlayer spacing calculated for D-dried samples was 9.3 Å, for P-dried samples 10.2 Å, and for F-S-dried samples 11.4 Å.

If we can agree on semantics, and the discussors will stop calling their samples D-dried samples, a part of the disagreement will disappear. It is pointed out in our paper that water can enter the interlayer spaces of P-dried samples; in view of the previous paragraph, water should be able to enter even more easily into the interlayer spaces of F-S-dried samples. The statement in the discussion that we "conclude that water does not reenter the interlayer spaces" is completely erroneous; we have made this

statement only about D-dried tobermorite gel, and not about P-dried or F-S-dried samples. The references cited to refute a statement we have not made have no pertinence to the subject.

Although the w_n values of Feldman and Sereda were about equal to those of our P-dried samples, this does not mean that their samples and our samples were in the same state. The quick F-S-drying, even if it removes as much water as D-drying, or more water, cannot be compared to our slow drying, in which equilibrium or near equilibrium state of the system is reached.

The reiteration of the statement that desorption equilibrium with water vapor can be established in 1 day, in spite of our paper, is beyond our understanding. The discussors point out that D-drying as developed by Copeland produces equilibration with water vapor in 4 to 7 days. They fail to point out that the equilibration is accomplished at a vapor pressure that is between 4 and 5 orders of magnitude lower than theirs. If at such low vapor pressure 4 to 7 days are needed for equilibration, how can their desorption equilibrium be established in 1 day? Furthermore, Copeland used what we later called "soft drying," i.e., drying until the water loss was 1 mg per g of paste per day. Later we adopted "hard drying," i.e., drying to a water loss of 0.1 mg per g of paste per day, and this took 2 to 3 weeks.

As far as the adsorption isotherms of the discussors are concerned, our paper states that "the adsorption isotherms may represent equilibria or close to it." But the arguments of Feldman and Sereda are based on desorption not on adsorption, and their desorption points were very far from equilibrium.

The discussors state, "No isotherms of cement or paste-hydrated C_3S showing closed loops have been published to our knowledge." We do not know of any such published work either. However, our paper cites unpublished work by Copeland and by Hagymassy. The latter work, which will be published soon, will show not only closed hysteresis loops, but very small ones; in fact, for portland cement the hysteresis loops are hardly noticeable.

The discussors state that our calculations of the hydraulic radius of the spaces into which nitrogen cannot enter is logically incorrect. Our calculations are completely correct logically, if water measures the total pore surface and total pore volume of the paste, and this is shown in the paper. However, it is of interest to point out the errors in the thinking and calculations of the discussors. In the first place, 755 m^2/g is the total geometric surface of tobermorite gel and not of hydrated portland cement. Less than half of the fully hydrated cement is tobermorite gel, so we will call the geometric surface 377 m^2/g. Let us see what results one gets on the basis of the new model. For the paste with $w_o/c = 0.35$, the surface inaccessible to nitrogen is 377 - 57 = 320 m^2/g. According to the new model, there is at least 1 layer of water between the tobermorite gel layers after D-drying. We will conservatively estimate the thickness of the water molecules as 2.1 Å, which happens to be the difference between the c-spacings of F-S-dried samples, 11.4 Å, and D-dried samples, 9.3 Å. "Logical consistency" requires that if we consider the entire geometric surface as pore surface, we should also consider the entire geometric volume as pore volume. The volume occupied by interlayer water after D-drying, according to the new model, is $0.5 \times 377 \times 10^4 \times 2.1 \times 10^{-8} = 0.0396$ ml. In addition to this, 0.1264 ml of water entered the pore system during adsorption up to saturation pressure. Thus, the total pore volume is 0.1660 ml per g of paste, and the pore volume inaccessible to nitrogen is 0.0912 ml. The hydraulic radius of the pore system inaccessible to nitrogen, thus calculated, is 2.9 Å. If the pores are visualized as parallel plates, the hydraulic radius gives an average distance of 5.8 Å between the plates; if the pores are cylindrical, the diameter of the average pore is 11.6 Å; and if the pores are spherical, the diameter of the average pore is 17.4 Å. It is pores of such sizes into which nitrogen, with a diameter of 3.5 Å, cannot penetrate, if the calculation is based on the new model. Because the dimensions given are average dimensions, many of the pores are naturally larger than the average.

In this calculation, everything was loaded in favor of the new model: The paste with smallest pores was selected; only one layer of water was assumed to be between the gel layers; and the thickness of the water molecules was assumed to be the smallest

possible thickness. Similar calculations for the paste with $w_o/c = 0.70$ give a hydraulic radius of 6.9 Å for the pores inaccessible to nitrogen; so the average distance between parallel plates is 13.8 Å, the average cylindrical diameter is 27.6 Å, and the average spherical diameter is 41.4 Å. These calculations show the logical inconsistency of the new model much better than the data given in Table 1. We should not forget, however, that these calculations are based on the wrong premises of the new model, and that the correct and logical values are those given in Table 1.

We are very grateful to Seligmann for his clear and logical discussion. It illustrates the difference between the thinking processes of physicists and chemists; when we chemists talk about "state" or "binding," we think about the energy of binding of water molecules to the surface, and the state of these molecules in the adsorbed phase. If we understand the discussion fully, our conclusion is that there is no contradiction between Seligmann's results and the old model; thus, his results cannot be cited in favor of the new model, as was done by Feldman and Sereda. We have stated in the paper that the Powers model, as modified by many of us, is not complete, and we expect that the time will come when the model will account even for such things as proton mobility.

Reference

38. Kantro, D. L., Brunauer, S., and Weise, C. H. The Ball-Mill Hydration of Tricalcium Silicate at Room Temperature. Jour. of Colloid Science, Vol. 14, 1959, pp. 363-376.

Temperature Control of Mass Concrete in Japan

TSUTOMU YANAGIDA, Public Works Research Institute, Ministry of Construction, Tokyo

•THE SCALE OF ROAD CONSTRUCTION in Japan in 1967, expressed in terms of annual expenditures for road programs, was approximately one trillion yen (about $2,780 million), and in 1969 it reached approximately one trillion two hundred billion yen (about $3,300 million) to occupy approximately 2 percent of the gross national product. However, the state of development of highways is still very far from being adequate, and it is further planned to appropriate annual budgets exceeding one trillion yen in accordance with a 5-year highway development plan.

A conspicuous feature of the numerous concrete structures that will be constructed to accompany this road development is that these structures are becoming of larger size with the marked increase in traffic, particulary in and around large cities. Specific examples include the proposed construction of large suspension bridges such as Kanmon Bridge, connecting the islands of Honshu and Kyushu, and Honshu-Shikoku Interconnection Bridge, connecting the islands of Honshu and Shikoku. The concrete structures used in long suspension bridges, of course, are also of large size.

These concrete structures are of such size that they may be called mass concrete structures. They differ from dam concrete only in that unit cement content is higher. In the design and construction of such structures, it is necessary to consider volume change of concrete due to heat generation as in the case of dams in order to prevent cracking.

TEMPERATURE STRESSES IN MASS CONCRETE

Compared to concrete of thin cross sections, concrete of large cross sections such as thick slabs have a slower rate of heat diffusion, and thus the concrete temperature of massive structures rises markedly immediately after placement. When left standing to cool in a natural state, it requires from about 2 weeks to several hundred days to return to around air temperature.

In the volume change of concrete arising from such temperature changes, it is common for free deformation to be restrained externally by outside conditions such as in the case of a foundation and internally by inside conditions such as temperature distribution within the concrete, shape of cross section, and differences in coefficients of thermal expansion and moduli of elasticity between adjoining portions. Unless suitable considerations are made in design and construction, numerous cracks will be found as temperature stresses occur.

The examples of such crack formation are many. Figure 1 shows some cases of cracks formed in concrete bridge piers (1). Cracks with widths of 0.1 to 0.3 mm and spacings of 3 to 4 m were the most numerous, with the cracks running through the full cross section. The age at which cracks appeared was between 13 and 23 days with the rate of crack-extension in one day being 25 to 40 cm. Thermocouples were embedded at the centers to measure temperature changes, and as indicated in Figure 2 it was found that cracking occurred due to extensive temperature change.

Paper sponsored by Committee on Mechanical Properties of Concrete.

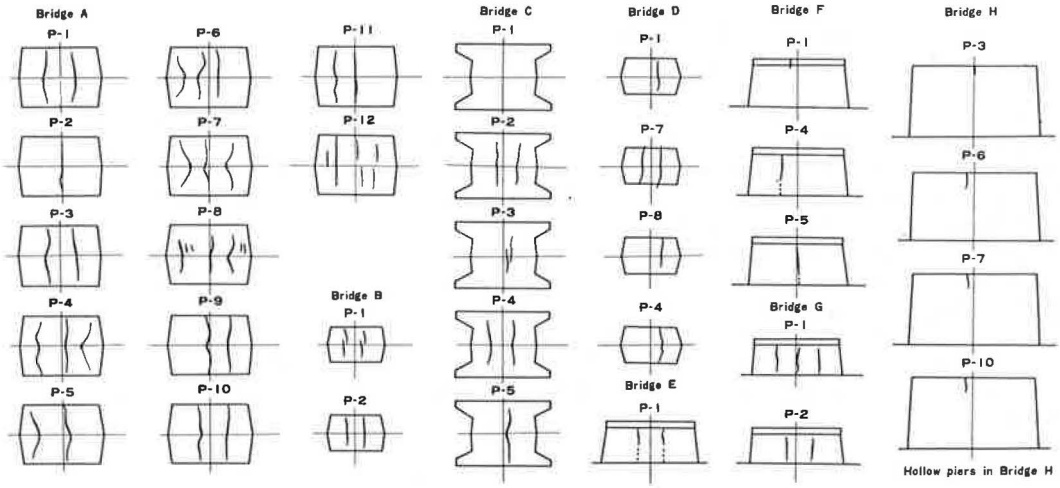

Figure 1.

Analyses of temperature stresses of members may be performed by elasticity theory; but generally, when there is foundation restraint, temperature stresses are estimated by the equation

$$\sigma_t = R \cdot E_c \cdot \alpha \cdot T \qquad (1)$$

where

σ_t = tensile stress;
R = degree of restraint;
E_e = effective modulus of elasticity of concrete, in general obtained as $E_c/1 + 0\left(4\frac{E_c}{E_f}\right)$, where E_c is modulus of elasticity of concrete and E_f is modulus of elasticity of foundation rock;

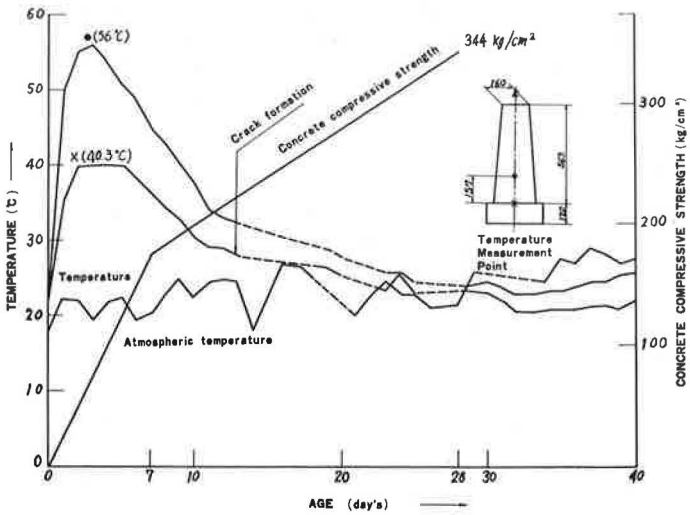

Figure 2.

α = coefficient of thermal expansion; and
T = temperature difference of concrete.

For the proper values of these constants, studies are being conducted in Japan through photoelasticity (2, 3) and by the finite element method (4) regarding degree of restraint. Investigations are also being carried on with respect to engineering properties such as modulus of elasticity and thermal characteristics. In estimating temperature difference, the Carlson method is employed with a combination of the Carlson and Glover methods used when cooling is performed.

A study of whether or not cracks will be formed confirmed either that the tensile stress sought by this method is within the range of the tensile strength or that the tensile strain is within the limits of extensibility.

In the case of a structure to be built near the sea coast or under water, reduction of cracking is of particular importance from the standpoint of durability of the structure.

TEMPERATURE CONTROL

It may be said that it is impossible to completely prevent temperature cracking. It is also difficult to predict the formation of cracks with high accuracy. Therefore, in actual practice, in order at least to reduce cracking, it is effective to limit the maximum temperature rise of the concrete by selecting suitable block dimensions and carrying out temperature control.

The measures that can be taken to limit peak temperature are reduction in heat generation through lowering of concrete temperature at the time of placement and reduction in unit cement content, facilitation of heat loss through longer intervals between concreting and reduction in lift heights, and removal of developing heat through artificial cooling.

In ordinary road construction in Japan where ready-mixed concrete is used, methc facilitating heat radiation or artificial cooling are chiefly employed. Cement generati.. less heat, other than cases of special production for the job by the manufacturer, would not be available, and normal portland cement is generally used. Therefore, although precooling may be given special consideration for large-scale projects, temperature control would ordinarily comprise calculations involving combinations of factors such as artificial cooling, time of placement (season and time of day), height of concrete lift, time interval between lifts, and concrete mix proportions. Although temperature calculations may be analyzed theoretically, at present when the hypotheses used in these calculations are not proven, emphasis is placed on simplicity rather than precision, and calculations by electronic computers are held to a minimal level.

In cases where temperature of concrete is lowered to the vicinity of final stable state temperature, such as when there is a necessity to perform grouting at an early stage, secondary cooling is performed.

Temperature Calculation Method

Not considering analysis of temperature distribution in a structure, for the purpose of comparing construction methods, it would suffice to assume a flat plane with infinite expanse and estimate the temperature rise of this plane. The method (5) of estimating maximum temperature rise described here is a combination of the Carlson and Glover methods by which temperature calculations were made for 160 cases and charted. The assumptions employed in these calculations are as follows:

1. The standard temperature is outdoor air temperature (0 C) and does not vary.
2. Concrete temperature at time of placement is equal to outdoor temperature. The concrete temperature at the surface is equal to outdoor temperature at all times.
3. The temperature of water used in pipe cooling is lower than outdoor temperature by 5 or 10 C.
4. The thermal properties of the concrete are as follows:

Thermal Diffusivity (m^2h)	Thermal Conductivity (kcal/m · h · c)
0.004	2.6
0.003	2.0
0.002	1.4

5. The adiabatic temperature rise curves are taken to be the 4 types indicated in Figure 3.

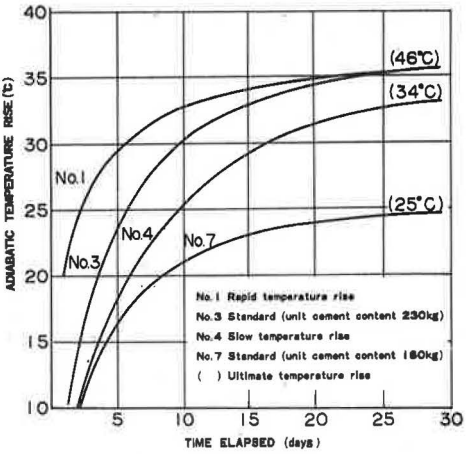

Figure 3.

Concrete Temperature Rise Under Conditions of Natural Heat Radiation—The relation between temperature rise of the third lift above either the foundation rock or the surface of old concrete and the peak temperature from adiabatic temperature rise can be expressed as a function of [thermal diffusivity/(lift height)^2], if the shape of the adiabatic temperature rise curve and the time interval between concrete placements are taken as shown in Figure 4. Selecting any rate of diffusivity and lift height and plotting the value of [thermal diffusivity/(lift height)^2] upward as a value on the x-axis and then moving laterally from the point intersecting the curve determined by the shape of the temperature rise curve and the interval of placement, one obtains the average temperature of the lift (Lift 3) on the y-axis as a ratio of the adiabatic temperature rise.

Effect of Pipe Cooling—In order to obtain the effect of pipe cooling, Figure 5 is employed. This is the ratio of temperature rise of a lift that loses heat naturally and a lift subjected to pipe cooling and is expressed as a function of the cooling constant (6). The cooling constant, X, is obtained as a function of h^2t/D^2 and $K:L/C_w \cdot \rho_w \cdot q_w$. Here, h^2 is the thermal diffusivity of concrete; t is the cooling time; D is the diameter of a cylindrical volume of concrete handled by one cooling pipe, in general taken as $D = \sqrt{(\text{lift height}) \times (\text{pipe spacing})/\pi}$; K is the coefficient of thermal conductivity of concrete; L is the length of cooling pipe; C_w is the specific heat of water; ρ is the specific gravity of water; and q_w is the discharge of cooling water. Therefore, variations in lift height, pipe spacing, thermal properties of concrete, pipe length, and discharge of cooling water may all be considered as varying the cooling constant, X.

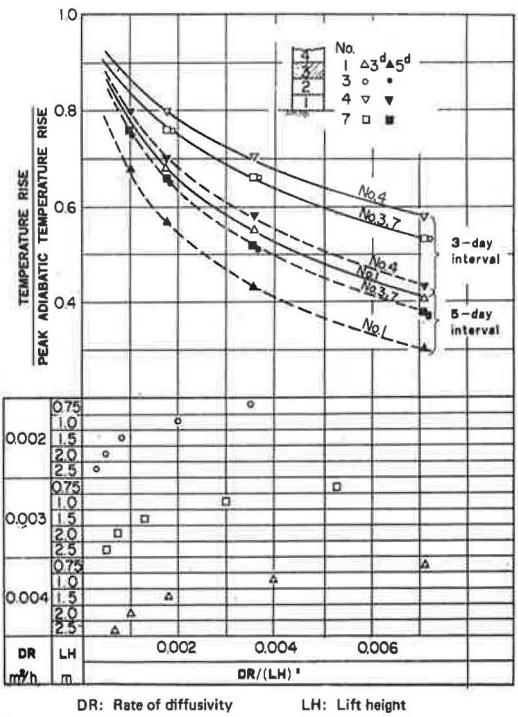

Figure 4.

To obtain the maximum temperature rise of a lift that is pipe-cooled, one first finds the temperature rise of a lift left to natural cooling in Figure 4, determines the cooling water temperature, and then employs Figure 5.

Thermal Properties of Concrete

Very seldom are proper numerical values employed in carrying out temperature calculations.

Thermal properties of concrete include items such as coefficient of thermal conductivity, specific heat, thermal diffusivity, and coefficient of thermal expansion. There are various methods of testing these properties, but in general the method used by the Bureau of Reclamation and modified in part is employed (6).

1. The coefficient of thermal conductivity is obtained by heating the center portion of a cylindrical specimen to produce a constant flow of heat in a radial direction. Measurements are made of the input required to maintain both the temperature difference between the interior and exterior of the specimen and a regular state; then calculations are carried out.

2. The specific heat is obtained from calculations on measurements of the input required to raise a concrete specimen placed in a calorimeter to a designated temperature.

3. The thermal diffusivity is obtained from calculations on measurements of temperature variation caused at the center portion by irregular heat conduction of a specimen of a designated temperature placed in a water tank of a different temperature.

4. The coefficient of thermal expansion is obtained by calculations based on the length change of a specimen embedded with a strain gage caused to vary in temperature in a range between 20 and 60 C.

Figure 6 shows the influences on thermal properties of factors such as variety of cement, water-cement ratio, aggregate content, and rock quality of aggregate. This figure shows that the factors most influencing the thermal properties of concrete are aggregate content and rock quality of aggregate.

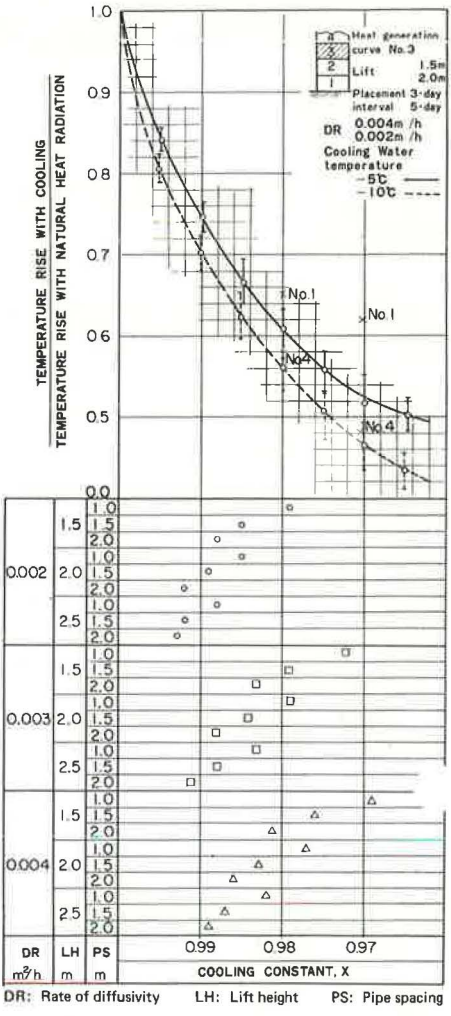

Figure 5.

A discussion follows of diffusivity, the value of which is the most needed item for carrying out temperature calculations.

Relation Between Rock Quality of Aggregate and Diffusivity—The specimens were of 20-cm diameter and 40-cm height and were embedded at the centers with thermocouple of 0.3-m diameter. The thermocouples were connected to an electron tube-type automatic equilibrium recorder for recording the temperature changes of the specimens, and calculations were made by the following equation:

$$\frac{\theta_2 - \theta_W}{\theta_1 - \theta_W} = \frac{8}{\pi}\left\{\sum_{n=1}^{n=\infty}\left[\frac{e^{-(h\cdot n\cdot \pi/H)^2 t}}{n}\right]\times\sin\frac{n\pi}{H}Z\right\}$$

$$\left\{\sum_{n=1}^{X=\infty}\left[\frac{J_0\left(\frac{X_n\cdot r}{R}\right)}{X_n\cdot J_1(X_n)}\right]\times\left[e^{-(h\cdot X_n/R)^2 t}\right]\right\} \qquad (2)$$

where

θ_1 = specimen temperature, deg C, at start of measurement;

θ_2 = temperature, deg C, of specimen center after immersion in water tank for a specified period of time;

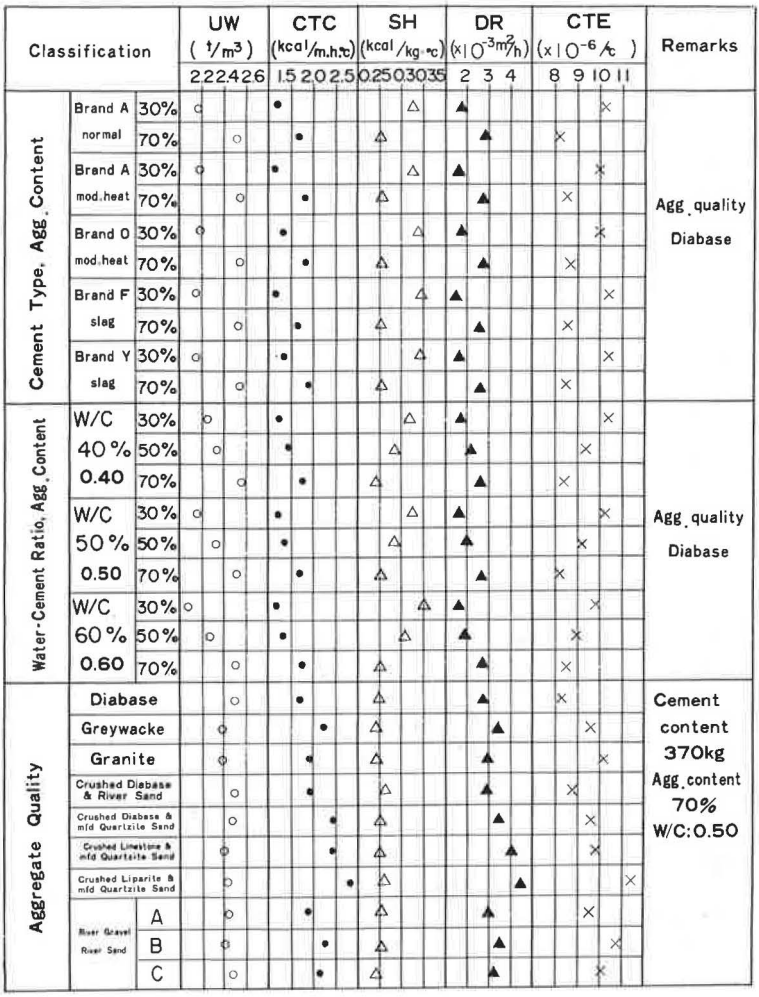

UW: Unit weight CTC: Coefficient of temperature conductivity
SH: Specific heat DR: Rate of diffusivity CTE: Coefficient of thermal expansion

Figure 6.

θw = temperature, deg C, of water tank;
h^2 = thermal diffusivity, m^2/h;
H = specimen height, m;
R = radius of specimen, m;
Z = measurement point of temperature in axial direction of specimen, in this case H/2; and
r = measurement point of temperature in radial direction, in this case 0.

The diffusivity rate can also be obtained from

$$h^2 = \frac{K}{C \cdot \rho} \tag{3}$$

For the sake of convenience the former is here called the Direct Method and the latter the Indirect Method.

Figure 7 shows the relationship between aggregate content and diffusivity when aggregates of varying rock qualities are used. Figure 8 shows the relationship between

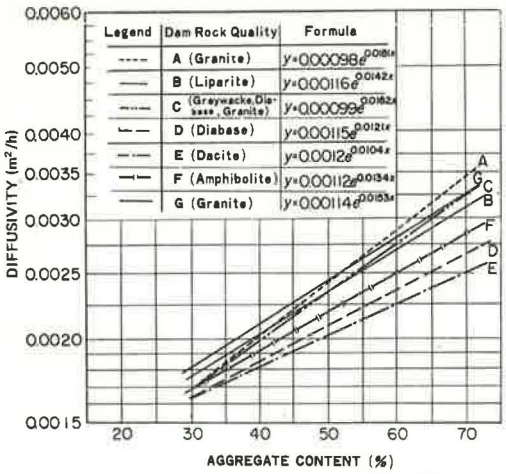

Figure 7.

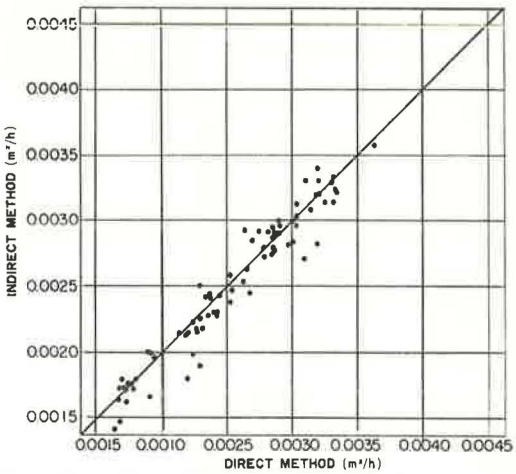

Figure 8.

the Direct Method and the Indirect Method, and it is seen that the two agree fairly well. Generally speaking, the aggregate content of mass concrete is 70 to 80 percent, and the heat diffusivity may be considered to be in the range from 0.0025 to 0.004 m^2/h.

Relations Between Temperature and Moisture Content of Specimen and Diffusivity—The relation between specimen temperature and diffusivity is shown in Figure 9; there is little variation. The relation with the specimen moisture content is shown in Figur 10. Specimens were moist-cured for 6 months and then left standing for 1 year in an atmosphere of 60 to 80 percent humidity. They were then waterproofed before measurements were made.

Relation Between Diffusivity and Coefficient of Thermal Conductivity—The relation between diffusivity and coefficient of thermal conductivity is shown in Figure 11 and may be considered to be linear.

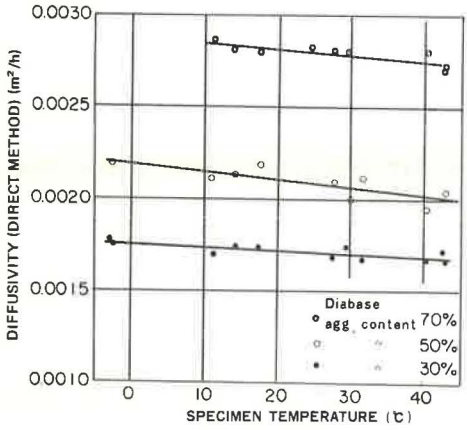

Figure 9.

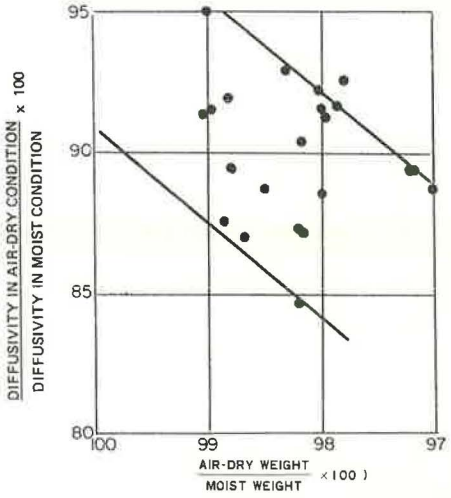

Figure 10.

Adiabatic Temperature Rise

In measurements of adiabatic temperature rise, it is difficult to maintain an insulated condition for a long period of time due to the nature of the apparatus. By employing the apparatus shown in Figure 12, which is a modification of the traditionally used apparatus, it became possible to conduct measurements for about 2 weeks.

The relationship between adiabatic temperature rise and unit cement content obtained from these measurements is shown in Figure 13. The peak temperature employed to obtain these was the results of measurements up to 14 days with the n th day and the n th + 1 day plotted on the x- and y-axes respectively in making an estimation (Fig. 14).

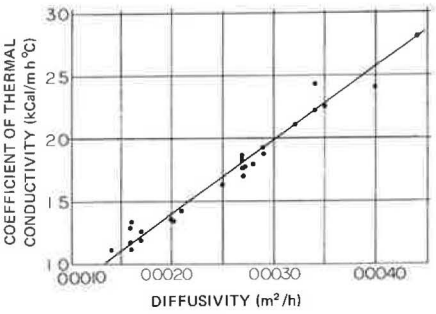

Figure 11.

The relation between concrete temperature at the time of placement and temperature rise, shown in Figure 15, indicates a difference of approximately 4 C in the case of placement temperature approximately between 10 and 30 C, but this was not very distinct.

The temperature rise history is influenced greatly by the temperature of concrete at the time of placement as shown in Figure 16.

The adiabatic temperature rise curve has heretofore been expressed by $\theta_t = \theta_0(1 - e^{-at})$ or $\theta_t = \theta_0\left(1 - e^{-at^n}\right)$, but both independently cannot very well express the temperature rise for a 2-week period. However, with today's computers, it would not be necessary to go to extremes to find a numerical expression. It is thought sufficient for information to be available for selecting the values for the various ages.

FOUNDATION RESTRAINT

When concrete placed on foundation rock or on old concrete has volume changes caused by temperature, it is subjected to foundation restraint, and temperature stresses result.

Research is being carried out in Japan on foundation restraint by various methods. In model tests employing photoelasticity, it has

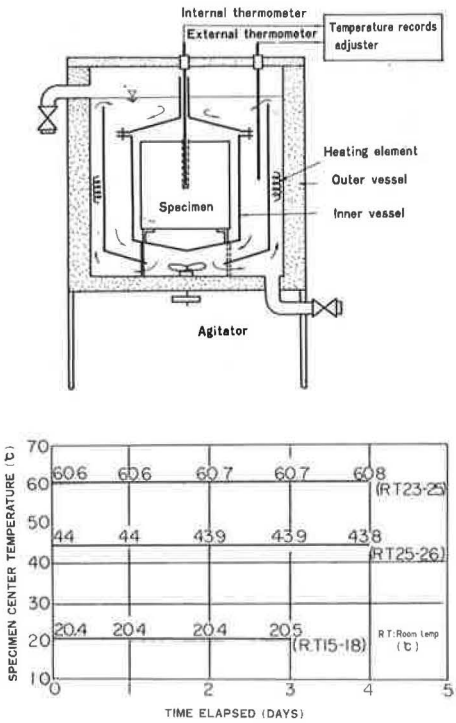

Figure 12.

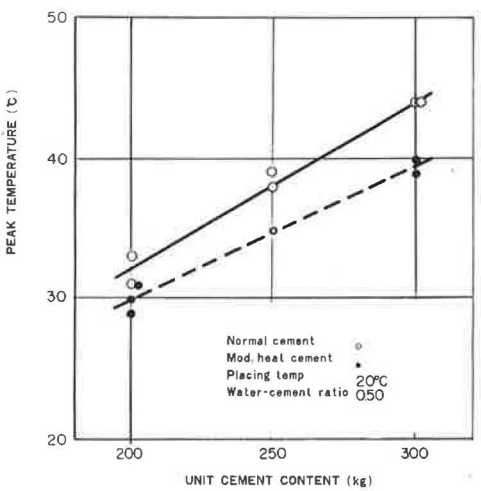

Figure 13.

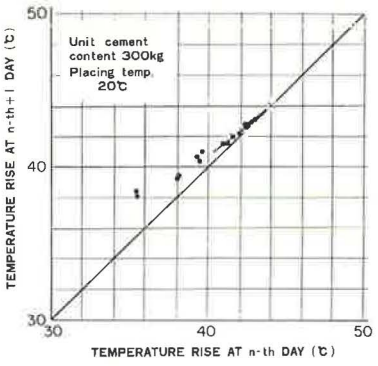

Figure 14.

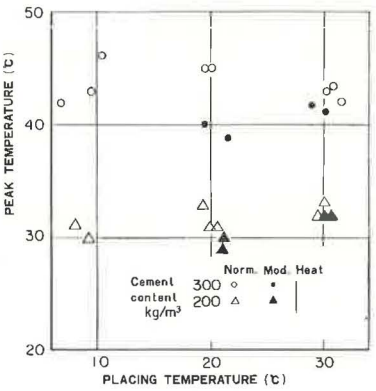

Figure 15.

been discerned that the degree of restraint (a) is a function of the ratio between the modulus of elasticity of the concrete and the modulus of elasticity of the foundation rock, (b) varies with the ratio between the length and the height of the restrained side of the concrete block placed on the surface of the foundation, and (c) varies with the shape of the concrete block. It was also learned that the foundation restraint does not extend beyond a height of 0.45 times the length of the restrained side. Further, Mori (3) has disclosed that degree of restraint, $\overline{R}$, on a semi-infinite foundation would be satisfactory at $R = 1 \Big/ \left(1 + 0.4 \frac{E_c}{E_R} \right)$, but on a foundation of identical width, it would rather be better to employ $R = 1 \Big/ \left[1 + \left(\frac{E_c}{E_R} \right)^{0.7} \right]$. Hayashi has sought the degree of restraint of a concrete block on a semi-infinite foundation by the finite element method and has secured roughly the same results as Mori.

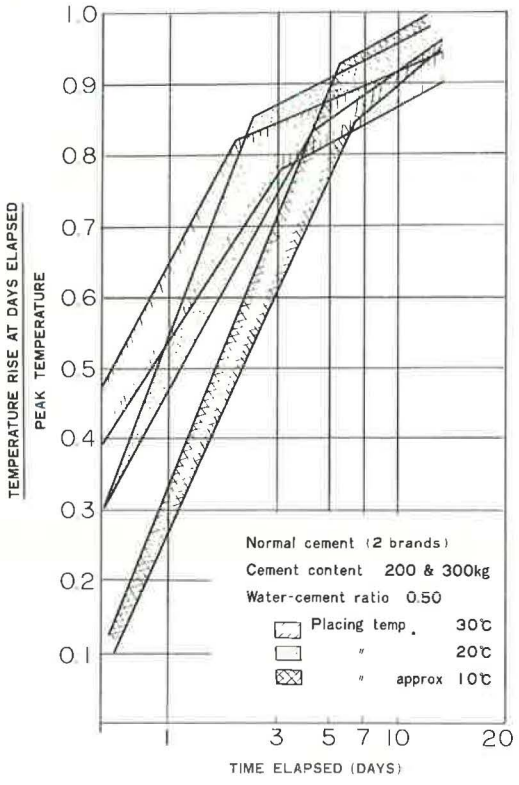

Figure 16.

CONCLUSIONS

In order to estimate temperature stresses accurately to arrive at measures for prevention of cracks, research should be continued on (a) estimation of temperature distribution, (b) calculation methods regarding restraint stresses, and (c) engineering properties of concrete at the early stage of hardening.

Each item represents a problem requiring long-term research, and all are fields in which there are relatively few researchers in Japan. However, with the continuing increase in construction of mass concrete structures there is no doubt that research in these fields will become more extensive.

REFERENCES

1. Isozaki, M., and Yanagida, T. Temperature Cracking of Piers and Crack Control. Ministry of Construction, Public Works Research Institute, Tokyo, Vol. 4-12. (In Japanese.)
2. Kawamoto, T. Fundamental Photo-Elastic Studies on the Shrinkage Stresses in Massive Structures. Trans. Japan Soc. of Civil Engineers, No. 61. (In Japanese with summary in English.)
3. Mori, C. Thermal Stress and the Factor of Restraint in Triangular and Quadrilateral Plates Restrained at an Edge. Trans. Japan Soc. of Civil Engineers, No. 89. (In Japanese with summary in English.)
4. Hayashi, M., and Kitahara, Y. Analysis of Thermal Stress in Heterogeneous Body With Arbitrary Configuration (Plane Strain)—Effect of Elastic Constraint of Foundation Rock on Thermal Stress Within Block of Mass Concrete During Temperature Drop After Placing. Central Laboratory of the Electric Power Industry, Rept. 67053. (In Japanese with summary in English.)
5. Yanagida, T. Practical Estimation of Temperature Rise in Mass Concrete. Ministry of Construction, Public Works Research Institute, Tokyo, Vol. 11-4. (In Japanese.)
6. Cooling of Dams. U. S. Bureau of Reclamation, Boulder Canyon Project Final Reports.